GEMS & GEMOLOGY

TABLE OF CONTENTS

p. 6

p. 29

p. 45

p. 48

ABOUT THE COVER: One of the most important ruby localities of the 1990s covers a broad area near the town of Mong Hsu, in northeastern Myanmar (Burma). The distinctive gemological features of these rubies are detailed in this issue's lead article. The suite of fine jewelry illustrated here contains 36 Mong Hsu rubies with a total weight of 65.90 ct; the two rubies in the ring total 5.23 ct.

Jewelry courtesy of Mouawad Jewellers. Photo by Opass Suksumboon—Opass Suksumboon Studio, Bangkok, Thailand.

Typesetting for Gems & Gemology is by Graphix Express, Santa Monica, CA. Color separations are by Effective Graphics, Compton, CA. Printing is by Cadmus Journal Services, Easton, MD.

GEMS & GEMOLOGY

LETTERS

KUDOS FOR "COLOR GRADING OF COLORED DIAMONDS"

Congratulations to the authors of the report "Colored Grading of Colored Diamonds in the GIA Gem Trade Laboratory," by King, Moses, Shigley, and Liu, which appeared in the Winter '94 issue of *Gems & Gemology* (pp. 220–242). It is a superb achievement. I am so impressed that I feel comment is appropriate.

I was very concerned when I first learned that the GIA was preparing an article on their color-grading system for colored diamonds. The measurement of color for paints and other opaque surfaces is a quite routine matter, but transparent substances present complications. There are additional problems that arise with the measurement of color in faceted gemstones, including the variations of color with orientation, across the stone, face up versus face down, and so on. Much nonsense has been written on this subject.

I need not have worried; publication of this article has put all my concerns to rest. The authors (as well as the many others within GIA who helped) are to be congratulated on an excellent solution to a difficult task. They appear to have covered all the problems that could arise in normal practice. I believe the terminology grid, which they based on the time-tested Munsell and ISCC-NCS approaches, is also likely to survive the test of time. Their technique is extremely well presented in the article; no doubt the editors also deserve some credit for this.

I hope that the GIA will continue to publish details on their grading system as more information becomes available in the future.

So again: Congratulations!

KURT NASSAU, Ph.D.
Nassau Consultants
Lebanon, New Jersey

SAPPHIRE-BEARING ALKALI BASALTS IN NIGERIA

With great interest I read the article "Gem Corundum in Alkali Basalt: Origin and Occurrence," by Drs. Levinson and Cook, in the Winter 1994 issue (pp. 253–262). However, I would like to update the information in one remark, on page 256: "Significantly, all reported economic, and potentially economic, secondary occurrences of basaltic corundum are spatially associated with the alkali type of basalt. (Coenraads et al., 1990, mention two possible exceptions, in Nigeria and Southern China, but these are not well documented.)"

In the *Journal of Gemmology*, 1990, Vol. 22, No. 4 (pp. 195–202), J. Kanis and R. R. Harding published an article titled "Gemstone Prospects in Central Nigeria," in which we described the occurrence of sapphires and zircons of the Jemaa district, in central Nigeria. We compared the Jemaa alkali basalts with the occurrences in Australia, Thailand, and Kampuchea.

From our description, it is evident that the vast sapphire deposits in central Nigeria are not "a possible exception," but definitely belong to the alkali type of corundum occurrence.

JAN KANIS, Ph.D.
Veitsrodt, Germany

Reply and Erratum

We regret that we missed the paper by Kanis and Harding in our literature search, and we thank Dr. Kanis for bringing this to our attention.

We would like to take this opportunity to correct an error in the caption to figure 6 (p. 260) in our paper: the longest corundum crystal is 1.3 cm (about 0.5 inches), not 13 cm (about 5 inches).

A. A. Levinson, Ph.D. and Fred Cook, Ph.D.
Calgary, Alberta, Canada

RUBIES FROM MONG HSU

By Adolf Peretti, Karl Schmetzer, Heinz-Jürgen Bernhardt, and Fred Mouawad

Large quantities of rubies—both rough and faceted—from a commercially important new source in Myanmar (Burma) have been available on the Bangkok market since 1992. The ruby crystals from the Mong Hsu marble deposit have dipyramidal to barrel-shaped habits and reveal dark violet to almost black "cores" and red "rims." With heat treatment, which removes their blue color component, the cores become intense red. The rubies grew under varying conditions in complex growth sequences. The color distribution between cores and rims is related to a different incorporation of chromium and/or titanium during crystal growth. Gemological, microscopic, chemical, and spectroscopic properties presented here permit the separation of faceted Mong Hsu rubies from their synthetic and other natural counterparts. Problems arising from artificial fracture fillings are also addressed.

ABOUT THE AUTHORS

Dr. Peretti, formerly director of the Gübelin Gemological Laboratory, is an independent gemological consultant residing in Adligenswil, near Lucerne, Switzerland. Dr. Schmetzer is a research scientist residing in Petershausen, near Munich, Germany. Dr. Bernhardt is a research scientist at the Insititut für Mineralogie of Ruhr-Universität, Bochum, Germany. Mr. Mouawad is a Graduate Gemologist and vice-president of the Mouawad Group of Companies, Geneva, Switzerland, currently at Harvard University Business School, Cambridge, Massachusetts.

Since 1992, Mong Hsu has been a primary source of ruby available in Thailand (figure 1). Mong Hsu is a small town situated in northeastern Myanmar (formerly Burma) in Shan State, which borders Thailand, Laos, and China. Untreated samples from this new source typically consist of bicolored corundum, with dark violet to almost black sapphire cores and ruby rims (figure 2). With heat treatment, the violet cores can be converted to red. Large quantities of untreated corundum crystals are brought into Thailand at Mae Sai and, to a lesser extent, at Mae Hong Son (see figure 3). In 1993, about 200 buyers from Chantaburi (Thailand) were spending several million U.S. dollars a month on Mong Hsu rough in Mae Sai ("Special report: Mong Hsu . . .," 1993). Thus, the Mong Hsu ruby has become an important source of supply to the world market.

In September 1992, one of the authors (AP) joined a group of gemologists who traveled to Myanmar and Vietnam at the invitation of the Asian Institute of Gemmological Sciences (AIGS), Bangkok, to learn about the occurrences of rubies and sapphires in these countries (see Jobbins, 1992; Kammerling et al., 1994). During this trip, at the mid-year Emporium in Yangon (Rangoon), Myanmar, the Myanma Gems Enterprise (MGE) announced a new ruby deposit in the region of Mong Hsu, and showed the group a series of rough samples with violet cores and red outer layers (called rims here for simplicity). Six samples were submitted for further study to one of the authors (AP), who also took the opportunity to test some cut stones (including heat-treated samples without violet cores) from this new source. The untreated rough and heat-treated cut rubies examined during that visit were essentially identical to the material examined later for this study. According to information subsequently obtained in Bangkok, many Thai dealers were already buying Mong Hsu rubies (see "Burma's Mong Hsu mine rediscovered . . .," 1993).

By October 1992, large quantities of faceted material approximately 0.5–1 ct in size and of high-quality color saturation and transparency had also begun to appear on the European market. One of the first lots of this material (obtained from a dealer in Munich) was studied in detail by

Figure 1. Since 1991, the Mong Hsu area in northeastern Myanmar has produced large quantities of superb rubies. This suite contains 58.22 ct of Mong Hsu rubies (the largest is 2.62 ct). Courtesy of Mouawad Jewellers; photo by Wicky Tjerk.

one of the authors (KS). Seventy of the 74 cut stones in this lot were almost identical with respect to their gemological characteristics, and unlike material from any other known locality; of the remaining four stones, two had typical Mogok features and two were typical of Thai ruby. When it was determined that the features of this new material were very similar to those of the Mong Hsu stones acquired in Yangon (notwithstanding any potential change of color and other properties that might be caused by heat treatment), the decision was made to carry out a complete study of these rubies.

Preliminary reports about some of the properties of Mong Hsu rubies have appeared in trade journals (Clark, 1993; Laughter, 1993a and b; Peretti, 1993; Milisenda and Henn, 1994), and an initial research study was published by Smith and Surdez (1994).

LOCATION

Although, because of security concerns, the authors were not able to visit the Mong Hsu deposit, first-hand information and photographs were obtained from miners in the summer of 1993. Reports on the local geology and mining operations have been published by Hlaing (1991, 1993, 1994) and are summarized below.

Mong Hsu is located about 250 km (150 miles) southeast of Mogok (figure 3), at an elevation of 700 m above sea level. It can be reached from Taung Gyi, the capital of Shan State, by traveling over a rough road for about 14 hours (Hlaing, 1994). Secondary (alluvial) corundum deposits are found in the terraces of Nam Hsu River, southeast of Mong Hsu township. These river terraces, where the first rubies were discovered and where mining and prospecting started, are 4 km long and 0.8 km wide, trending from northwest to southeast, and 80–160 m deep. In 1992, about 2,000 miners were working these alluvial deposits.

Additional secondary deposits have been found 16 km (10 miles) farther southeast. These extend over an area more than 100 km² between the two mountains Hsan Tao and Loi Paning. The "government

Figure 2. A distinctive feature of Mong Hsu ruby crystals is their deep violet (sapphire) core, which is surrounded by a red (ruby) rim. With heat treatment, the violet core becomes a deep red. This Mong Hsu ruby "thin section" is 5.3 mm wide; photo courtesy of John Emmett.

prospecting area" is restricted to a central 0.8 km² portion (figure 3). By 1994, about 500 joint ventures between private individuals and the Myanmar government were operating in the region (Hlaing,

1994), literally chewing up the surrounding hills (figure 4). Alluvial ruby is also found at Loi Khan and Mong Sang, which lie southwest and south (respectively) of Mong Hsu (again, see figure 3).

GEOLOGY AND MINERAL ASSEMBLAGES

According to the geologic map of Myanmar (Earth Sciences Research Division, 1977), the Mong Hsu ruby deposits are situated at the contact of upper Paleozoic marbles and other Paleozoic rocks, including various types of metamorphosed sediments. Hlaing (1991, 1993, 1994) reports that the major rock types in the region of the primary ruby occurrences are mica schist, phyllite, and calcsilicate rocks; the rubies occur in a marble belonging to this Paleozoic series.

Additional information on the different rock types in the vicinity of the Mong Hsu mines was obtained from the study of minerals that appear mixed with the ruby rough from the market at Mae Sai and on the surface of the corundum crystals themselves. These were identified by means of X-ray powder diffraction analysis, quantitative electron microprobe analysis, and a scanning electron microscope with energy-dispersive X-ray detector.

Figure 3. This map of the Mong Hsu region in northeastern Myanmar (see inset) shows the areas of current mining activity. The alluvial deposits (stippled areas), where the first rubies were found, are in river terraces southeast of the town of Mong Hsu. Primary occurrences of ruby with adjacent secondary deposits were discovered around Loi Hsan Tao. The pink region represents the area of gem potential suggested by prospecting in 1993. Adapted from Hlaing, 1993; courtesy of the Australian Gemmologist.
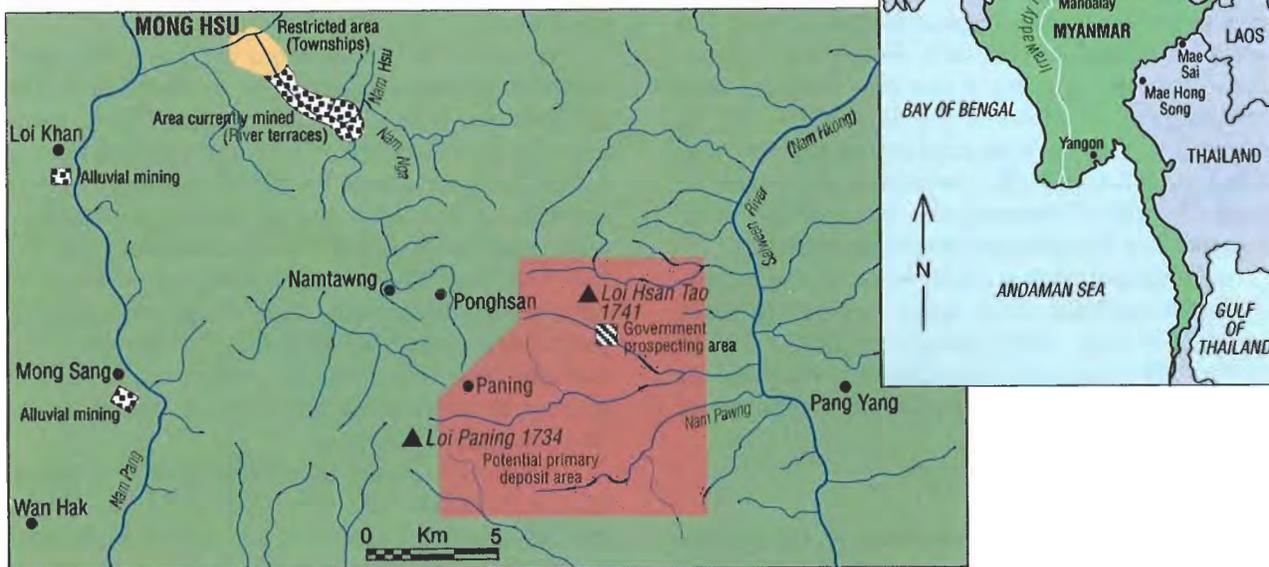
They include green and brown chromium-bearing dravite (tourmaline), andalusite, almandine, quartz, and green, chromium- and vanadium-bearing tremolite. One of the almandine crystals was overgrown with white mica. Overgrowths on the ruby crystals were identified as fuchsite (green mica), white mica, and light green Mg-chlorite.

Garnet, green tourmaline, tremolite, white mica, and quartz were also described by Hlaing (1993), with staurolite and pyrite mentioned as accessory minerals. The overgrowth of green tourmaline on Mong Hsu rubies noted by Hlaing (1993) was not found in this study; rather, all light green to green overgrowths on rubies available to us were identified as either fuchsite or Mg-chlorite.

From these mineral assemblages, it is evident that, although both the Mong Hsu and Mogok occurrences are metamorphic, they differ in the specific environment in which the rubies formed (Earth Sciences Research Division, 1977; Hlaing, 1981; Keller, 1983; Hunstiger, 1990; Kane and Kammerling, 1992; Kammerling et al., 1994). At Mogok, ruby occurs *in situ* in amphibolite-to-granulite facies metamorphosed marbles and calcsilicate marbles. In contrast, the mineral assemblages of Mong Hsu indicate marbles and metapelitic rocks metamorphosed to (lower temperature) amphibolite facies. Thus, Mogok represents a higher degree of metamorphism than does the Mong Hsu mining area.

MINING

Mining of the secondary deposits is by the classic methods used in Mogok (as described by, e.g., Kane and Kammerling, 1992) and elsewhere in Southeast Asia. In fact, a Mogok miner is believed to have been the first to discover rubies in Nam Nga Stream at Mong Hsu (Hlaing 1994), and many miners have traveled from Mogok to work at the new locality. In and along the waterways, the gravels are removed and washed in simple baskets. Ruby-bearing gravel layers (known as *byon*) in the surrounding area are reached by: (1) digging holes from the surface into which the miner is lowered (and the gravels removed) by a simple rope and pulley system; (2) excavating horizontal tunnels into the hill itself, at the level of the gravel layer; and (3) open-pit mining, with the gravels sorted and recovered by sometimes elaborate sluicing systems (figure 5). At some mining sites, mechanized sieves are used to work the gravels (Hlaing, 1994).

Figure 4. Holes and shafts dug to mine the gem-bearing gravels penetrate the hillsides at Mong Hsu in this 1993 photo by V. Yothavut.

CUT STONES AVAILABLE IN THE MARKET

The vast majority of faceted Mong Hsu rubies found on the world market are heat treated, and there is a wide range of qualities. Large quantities of transparent stones with fine red color were available in 1993 and 1994 in sizes up to 0.7 ct (see, e.g., figure 6). Stones of good to very good color and clarity were found in the 1–2 ct range. Stones between 3 and 5 ct were found to be mostly of medium to good quality. These observations are consistent with those reported recently in the trade press ("Rains wash out Mong Hsu supply," 1994). Clarity may be reduced in samples of all sizes by translucent zones of dense white clouds or by the presence

Figure 5. At the Mong Hsu ruby occurrence, an elaborate sluicing system brings the gravels down this hillside for processing. Photo by V. Yothavut.
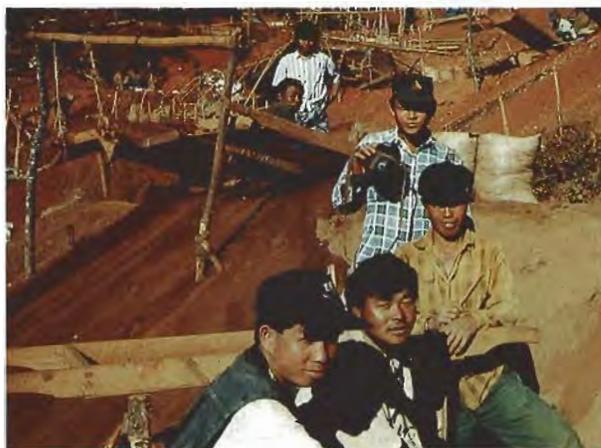
Figure 6. Mong Hsu rubies are typically heat treated, to produce a well-saturated red hue as shown here. Like most of the faceted stones produced to date, these Mong Hsu rubies, from the study sample, are small, 0.348 to 0.683 ct. Photo by Shane F. McClure.

of fingerprint-like inclusions and cracks (see "Microscopic Features" below).

In many of the faceted rubies examined for this study, foreign fillings—such as glass-like substances—were found in fissures and surface cavities (again, see "Microscopic Features" below). Gem laboratories in Asia have reported seeing glass fillings in more than 50% (and, one Thai laboratory, in as much as 90%) of the Mong Hsu rubies examined to date ("Glass filled rubies increasing," 1994). Stones above 5 ct with excellent color and clarity, and no evidence of foreign fillings, appear to be extremely rare.

Fillings in large fissures and cracks improve the apparent clarity of the stones considerably (Peretti, 1993; Milisenda and Henn, 1994). They result from heat treatment in borax or a similar substance, but heat treatment in chemicals is not necessary to alter the violet cores of color-zoned stones to red, as shown by heat-treatment experiments performed in Germany (see figures 7 and 8). According to information obtained in Bangkok, some commercial Thai laboratories use a two-step procedure to heat treat Mong Hsu rubies. First, the samples are heated, without the use of borax, to remove the violet color. Then, the rubies are heated in a borax container to fill fissures and thus enhance apparent clarity. Consequently, some Mong Hsu rubies that have fractures filled with a foreign substance have been treated for both clarity and color enhancement. In these cases, glass or other foreign fracture fillings are not simply an "inadvertent" by-product of heat treatment conducted to remove the blue color component in the samples, as some in the trade have claimed.

Because rubies with artificially filled fractures must be sold as treated, large lots of Mong Hsu rubies containing many stones with such fillings were rejected by European dealers and returned to Bangkok in 1993. In addition, some fracture-filled Mong Hsu rubies have been misidentified as flux-grown synthetic rubies. Some Thai companies have tried to remove the fillings through acid treatment or by recutting the stones. These problems—and others, such as the high volume of production—caused a steep drop in the price of Mong Hsu rough

Figure 7. Heat treatment (in Germany) produced the dramatic color change (right) in this Mong Hsu crystal, which was originally almost black (left). Total length, about 6 mm.

Figure 8. This 8-mm-long Mong Hsu crystal has been cut to show the effect of heat treatment on the core area. The right half is the original (untreated) control sample; with heat treatment, the left half is now a solid red.

at Mae Sai and Bangkok in 1993, to nearly half of its peak (see, e.g., Koivula et al., 1993b; Kammerling et al., 1994; Hlaing, 1994).

CHARACTERISTICS OF MONG HSU RUBIES

Materials and Methods. In addition to the six rough samples provided by MGE in September 1992 and the 74 faceted stones obtained in October 1992 from a Munich dealer, we subsequently saw and examined several parcels of untreated and heat-treated rough and faceted Mong Hsu rubies in both the Bangkok and European markets. Using as our guide the unusual gemological properties (e.g., growth features) of Mong Hsu rubies that we had determined by late 1992, we were able to select parcels of stones that we were confident were free of rubies from other localities for further examination. As of summer 1993, we had selected approximately 50 rough samples and 100 faceted stones—most less than 1 ct (again, see figure 6), with a few up to 2.5 ct—for this research project. In addition, during separate visits to northern Thailand in mid-1993, two of the authors (AP and FM) saw large quantities of untreated Mong Hsu rubies that had entered Thailand at Mae Sai. We purchased several parcels of selected samples for this study. After preliminary examination of about 1,000 carats (in sizes up to 5 ct) of the material obtained at Mae Sai, which was top-quality rough, we selected a parcel of 23 rough, untreated pieces for further study (see, e.g., figure 9). In addition, we examined a great number of the samples selected at Mae Sai after they had been heat treated in Chantaburi, Thailand; from these, we selected nine for further study in Europe. One of the authors (KS) also heat treated about 15 Mong Hsu samples in Germany.

In summary, we had access to more than 200 cut and about 100 rough gem-quality rubies, which we were confident were of Mong Hsu origin, for detailed gemological and mineralogic studies.

We performed standard gemological testing on about 50 of these samples (faceted stones and rough with polished windows). To characterize the internal and external growth planes, we studied approximately 200 samples total (about 60% of which were faceted) using a Schneider horizontal (immersion) microscope with a specially designed sample holder and with specially designed (to measure angles) eyepieces (Schmetzer, 1986a; Kiefert and Schmetzer, 1991; see box A); an additional 12 rough crystals were examined with a standard goniometer. We studied and photographed the inclusions using the

Figure 9. We selected these untreated pieces of Mong Hsu ruby rough from our study sample to illustrate some of the many different forms in which this material occurs. The first two rows are typical barrel-shaped, well-terminated crystals; the third row shows flat samples that are sometimes seen, which possibly formed in narrow veins; the waterworn crystals in the fourth row represent a minor proportion of the ruby lots. For an idea of size, note that the crystal on the far left in the upper row is approximately 8 mm long.

Schneider microscope with Zeiss optics as well as an Eickhorst vertical microscope with Nikon optics (the latter with fiber-optic illumination).

Solid inclusions were identified by Raman microprobe spectroscopy, using an X-Y Dilor instrument, as well as by a Philips scanning electron microscope with a Tracor energy-dispersive X-ray spectrometer (SEM-EDS).

Bulk chemical analyses of five untreated rough and five heat-treated cut stones of variable color saturation were performed by energy-dispersive X-ray fluorescence (EDXRF) using a Tracor Northern TN 5000 system. The analyses yield the mean chemical

BOX A:
Determination of Growth Structures

The determination of a gem's structural properties, such as straight growth planes that parallel the external faces of the original crystal, or twin planes, is becoming increasingly important as an additional, easily performed method to characterize natural and synthetic gemstones. It requires a microscope, an immersion cell, and immersion liquids (see, e.g., Kiefert and Schmetzer, 1991, for a detailed discussion of the apparatus used for this report). Also useful for the determinative procedures in a horizontal microscope are (1) a biaxial or triaxial sample holder with a dial attached to its vertical axis, and (2) a rotary measuring eyepiece with cross hairs attached to the lens and a dial attached to the ocular tube.

The basic habit of corundum consists of a small number of significant crystal forms: the basal pinacoid, the hexagonal prism, the positive rhombohedron, and the negative rhombohedron, as well as different hexagonal dipyramids. The angles formed by one crystal face and the c-axis, as well as those formed by two distinct crystal faces, are fixed and well known. The biaxial sample holder is used to determine crystal faces by measuring the angle between the optic axis of the ruby crystal and families of straight, parallel growth planes. The measuring eyepiece is used to determine the angles between two different families of straight, parallel growth planes independent of the orientation of the crystal's optic axis.

The first step in examining a faceted ruby is to locate the stone's optic axis and orient it so that it is parallel to the axis of the horizontal microscope. With the stone in this orientation, which is easily accomplished by interference figures seen with crossed polarizers, the gemologist can determine the growth planes by tilting the gem in the direction the optic axis is inclined *vis á vis* the microscope axis. The angle between the optic axis and a family of straight parallel growth planes can be read on the sample-holder dial.

For Mong Hsu rubies, traces of the hexagonal dipyramid ω are sharply outlined with the optic axis inclined about 5° from the microscope axis (as illustrated in figure A-1, right). When Mong Hsu rubies are examined in a direction about 30° inclined to the c-axis, traces of growth planes parallel to the positive rhombohedron r and the hexagonal dipyramid n can be seen (figure A-1, left).

As a second step, the gemstone should be rotated through 90° toward an orientation in which the optic axis is parallel to the vertical axis of the sample holder. In this orientation, the growth structures parallel to the basal pinacoid c are easily recognized. As the gem is rotated about the vertical axis of the sample holder, growth structures parallel to rhombohedral faces and to different hexagonal dipyramids can also be seen. After each rotation through 30°, another series of growth planes becomes visible, and identical planes are repeated after each rotation through 60°.

For Mong Hsu rubies, this second step reveals characteristic growth planes that typically consist of c, ω, and n (figure A-2, left). After rotation through 30°, a characteristic pattern formed by r and c usually becomes visible (figure A-2, right).

---

composition of a surface exposed to the X-ray beam (approximately 2 mm in diameter). Sixteen elements (Al, Mg, Si, P, K, Ca, Ti, V, Cr, Mn, Fe, Ni, Cu, Ga, Zr, Nb) were analyzed with software provided by the manufacturer, which normalizes the resulting oxide percentages to 100 wt.% totals.

Five faceted and three rough samples were analyzed by electron microprobe (CAMECA Camebax SX 50), using an acceleration voltage of 20 kV; standard materials of corundum (Al_2O_3), rutile (TiO_2), eskolaite (Cr_2O_3), hematite (Fe_2O_3), and Mn and V metals; and counting times of 60 seconds for each element (necessary to detect traces of, e.g., iron). To evaluate the inhomogeneous chemical compositions of the samples, between two and seven traverses of 30 to 50 point analyses each were measured across the cores and outer areas of the five faceted and two of the rough samples. A more detailed examination, with four scans of 600 to 800 point analyses each, was performed on the third rough sample (figure B-1), which was extraordinary. We had the samples oriented so that the visible color zoning between the core and the rim could be traversed.

Spectral data of 25 representative samples, including untreated rough and heat-treated cut stones, were obtained with a Leitz-Unicam SP 800 UV-VIS spectrophotometer. Infrared spectroscopy was carried out on 15 heat-treated samples using a Pye-Unicam 9600 FTIR spectrometer and a diffuse-reflection unit.

Crystallography. Facet-quality Mong Hsu rubies are typically well-terminated, barrel-shaped crystals
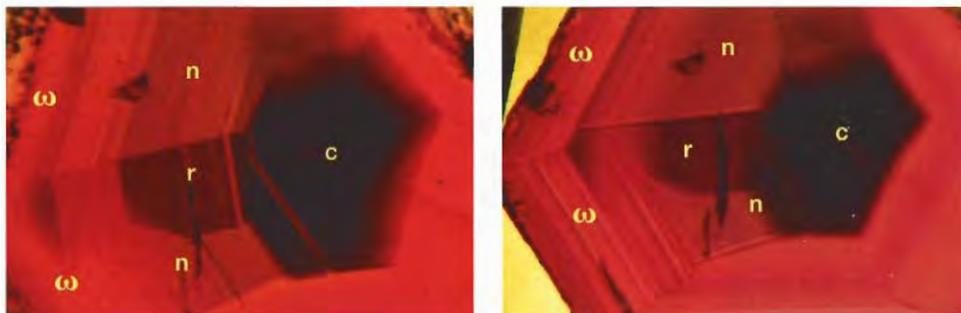
Figure A-1. Mong Hsu ruby slice (about 4.5 mm wide), cut perpendicular to the c-axis: inclined about 5° to the c-axis (right), ω planes are sharp; inclined about 30° (left), r and n planes are sharp. Immersion.
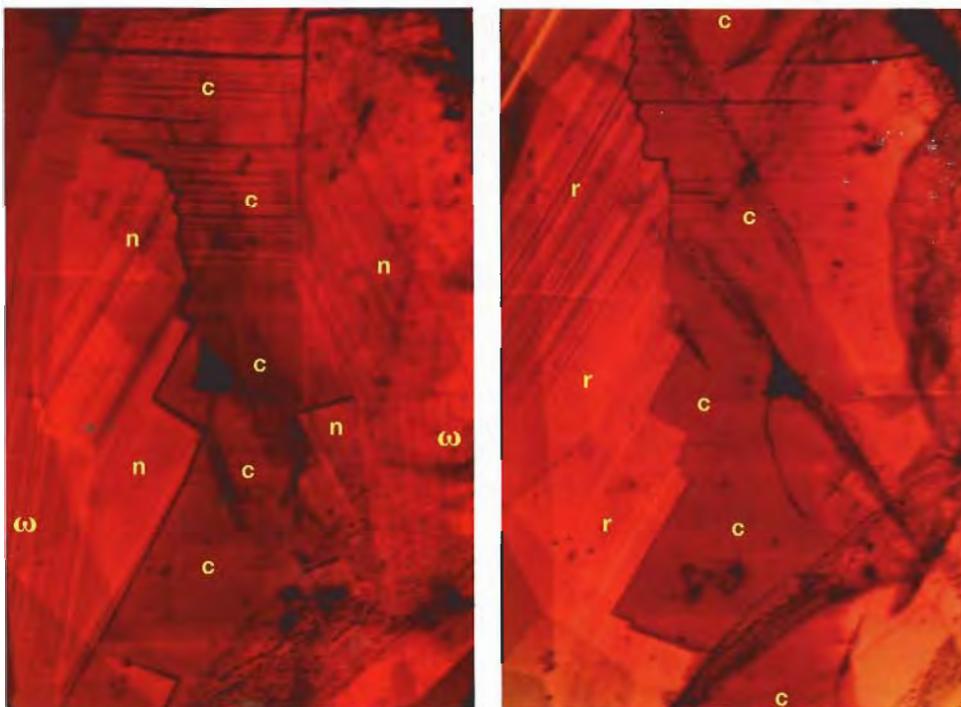
Figure A-2. In this heat-treated and faceted Mong Hsu ruby, the intense red "core" is confined to growth faces parallel to the basal pinacoid c; lighter red areas are confined to two hexagonal dipyramids n and ω (left) and to the positive rhombohedron r (right). View perpendicular to the c-axis; during a rotation of the stones through 30° about the c-axis, two different sharp outlines of growth structures are visible. Immersion, magnified 50×.

(figure 10). Two major habits were observed (figure 11): The first is dominated by the hexagonal dipyramid ω (14 14 $\overline{28}$ 3) and by the basal pinacoid c (0001), with a subordinate positive rhombohedron r (10$\overline{1}$1). The other habit shows additional hexagonal dipyramids n (22$\overline{4}$3). Only minor amounts of water-worn crystals were found in the lots examined.

Another form of Mong Hsu ruby is extremely flat, possibly due to growth in narrow veins (again see figure 9). Crystals with this morphology, in general, are not useful for jewelry purposes and were therefore not included in this report.

Visual Appearance. Less than 5% of the rough Mong Hsu samples we examined were a uniform red or violet to almost black. Most stones from this locality show a distinct color zoning, with transparent red outer zones ("rims") and violet to almost black centers (commonly called "cores") that appear opaque to translucent (again, see figures 9 and 10). In thin section, a core that originally looked almost black and opaque will undoubtedly appear violet and transparent (see, e.g., figure 2). Depending on what part of the original crystal a fragment represents, great variability in color and color zoning is observed in lots of the rough. A more detailed description of this extraordinary color zoning is presented in "Microscopic Features" below.

Heat treatment removes the violet component of the cores to produce stones that are uniformly red, as confirmed by experiments carried out in Germany (see figures 7 and 8). There is, however, some variation in the shades of red seen in the heat-treated samples. In addition, in some of the rough

Figure 10. A well-formed Mong Hsu crystal consists of two hexagonal dipyramids, ω and n, the positive rhombohedron r, and the basal pinacoid c, as illustrated by this 5-mm sample. Note the violet core.

Figure 11. The crystal habit of Mong Hsu rubies consists of two hexagonal dipyramids, n (22$\bar{4}$3) and ω (14 14 $\overline{28}$ 3), the basal pinacoid c (0001), and the positive rhombohedron r (10$\bar{1}$1). The crystal drawn on the left is dominated by ω and c faces, with a subordinate r plane; the crystal shown on the right is dominated by ω and c faces, with subordinate r and n planes.

heat treated commercially, we observed translucent, highly reflecting, whitish zones that made the stones unsuitable for faceting. As a result of these whitish zones, a percentage of the material is rejected after heat treatment. Although distinct color zoning is usually not visible with the unaided eye, microscopic examination reveals a highly characteristic type of color zoning related to specific growth structures in most of the heat-treated samples—with intense red related to core zones and lighter red related to rims.

Gemological Properties. The distinctive color distribution in Mong Hsu rubies is also reflected in some of their gemological properties (table 1).

UV Fluorescence. The differences between cores and rim areas are well illustrated by their reactions to long- and short-wave ultraviolet radiation. In untreated samples, the cores are inert or fluoresce light orange to light red, whereas the rims fluoresce intense orange-red to red. This difference is less obvious after heat treatment: The cores of heat-treated samples fluoresce orange-red to red, whereas the rims remain intense orange-red to intense red.

Optical Properties. We found the variations in refractive index among the different samples to be unusually high for both the ordinary and extraordinary rays, with a slightly variable birefringence between 0.008 and 0.010 (see table 1). A similar large variation in R.I.'s was reported by Smith and Surdez (1994) for rubies from Mong Hsu, and was recently described for rubies from Malawi that revealed highly variable amounts of trace elements, especially chromium (Bank et al., 1988).

We also found differences in R.I. between cores and rims of both heat-treated and untreated Mong Hsu samples. For example, one rough sample that was sawn and polished revealed R.I.'s of n_o = 1.774 for the core and 1.770 for the rim, n_e = 1.765 for the core and 1.762 for the rim (birefringence = 0.009 and 0.008, respectively).

Therefore, depending on the orientation of the table facet with respect to the optical axis and the portion of the original crystal the table encompasses, different refractive indices are possible. If the table facet is largely confined to one single growth zone (see "Microscopic Features" below and boxes A and B), sharp shadow edges are observed for the ordinary and the extraordinary rays on the refrac-

TABLE 1. Gemological characteristics of Mong Hsu rubies.[a]

Property	Untreated samples		Heat-treated samples	
	Core	Rim	Core	Rim
Color	Violet to black	Red	Intense red	Red
Pleochroic colors				
Parallel to c	Light bluish violet to reddish violet	Orange-red	Orange-red	Orange-red
Perpendicular to c	Intense bluish violet to reddish violet	Purplish red	Purplish red	Purplish red
Fluorescence				
Long-wave UV	Inert or light orange	Intense orange red	Orange red	Intense orange-red
Short-wave UV	Inert or light red	Intense red	Red	Intense red
Specific gravity (range)	3.990 - 4.010			
Refractive indices (range)				
n_o	1.768 - 1.780			
n_e	1.760 - 1.770			
Birefringence	0.008 - 0.010			

[a] For the ordinary type of samples with violet to black cores and red rims.

tometer (table 1). This is often the case for samples with table facets cut parallel to the c-axis or for samples with small cores. If the table facet encompasses a "mixed" area—that is, part is from the core and part is from the rim, the shadow edges are often less distinct and in extreme cases no readings are visible on the refractometer. Typically, this is the case with a stone on which the table facet is oriented perpendicular to the c-axis, with an intense red central core and a lighter red rim. All intermediate situations are observed for faceted samples with random orientation.

This unusual variation in refractive indices within one crystal is usually caused by the chemical zoning between cores and rims, but it also may occur between different zones within cores and outer areas (see "Chemical Properties" and box B).

Other gemological properties of the Mong Hsu rubies tested, such as pleochroism and specific gravity (table 1), were consistent with those of natural rubies from other localities. Note that the color of the untreated cores appeared intense violet perpendicular to the c-axis and somewhat lighter violet parallel to the c-axis.

Microscopic Features. *Growth Structures and Color Zoning in Untreated Mong Hsu Rubies.* By determining the internal growth structures in a cut stone, the gemologist can reconstruct the habit of the original ruby crystal. (Again, see box A for the procedures used in this study.) Changes in the habit during growth and color zoning characteristics also can be studied (see, e.g., box B.)

Well-preserved Mong Hsu corundum crystals are defined by c, r, n, and ω faces. These growth features can also be observed in faceted stones or in fragments of rough stones as thin traces of growth planes parallel to the former external faces of the ruby.

Because of the complex growth sequence established for Mong Hsu rubies (see box B), crystals and crystal fragments also reveal distinctive color zoning. Samples that are homogeneous in color (suggesting crystal growth in a single phase) occur only rarely. These are, for example, red with c, r, n, and ω faces (again, see figure 9) or dark violet to almost black with c, r, and ω faces (again, see figure 7). The most common pattern in Mong Hsu rubies, however, consists of a dark, nontransparent core and a red outer zone (see again Figure 2).

An even more complex pattern is formed in samples that contain two dark violet "cores" that are separated by a red layer along the c-axis (figure 12). In a view parallel to the c-axis, a dark core in the center is followed by a light red zone, a second lighter violet zone (representing the second "core"), and an outer red rim. In a very few instances, we observed Mong Hsu rubies with a thin, intense red rim confined to n or ω faces (figure 13). The thin red rims represent the latest stage of growth for these samples in which an enrichment of chromium took place.

A modification of the typical habit and color zoning in Mong Hsu rubies is shown in figure 14. The violet-to-black color in this extraordinary ruby forms only in growth zones parallel to basal planes,

BOX B: Color Zoning and Habit Changes in Untreated Mong Hsu Rubies

The most distinctive, characteristic feature of untreated Mong Hsu rubies is their color zoning. Although two zones are usually evident—violet "cores" and red "rims"—the zoning in Mong Hsu rubies is actually somewhat more complicated than this.

Most Mong Hsu ruby crystals consist of one (or, rarely, two) violet to almost black cores with intense red rims. An extraordinary sample with two dark violet "cores" separated by an intense red zone (figure B-1) best reveals this general scheme for color zoning related to growth history. The duplicate sequence identified in this stone (table B-1) confirms the "single" characteristic sequence observed in most Mong Hsu rubies (an exception is the stone illustrated in figure 14).

Red growth zones (R) consist of red (ruby) layers parallel to the basal pinacoid c, to the positive rhombohedron r, and to two hexagonal dipyramids, n and ω. Because all four faces (c, r, n, and ω) have growth rates greater than zero, red layers form parallel to all four.

Violet (V) growth zones consist of violet (sapphire) layers parallel to c, r, and n. In V growth zones, only these three faces reveal growth rates greater than zero; ω growth rates are not observed. This indicates that ω dominates the external crystal form, although no violet layers grow parallel to ω.

Along the c-axis of the ruby shown in figure B-1, which is schematically drawn in figure B-2, the V zones in the center of the crystal abruptly convert to R zones. The R zones then gradually convert to intermediate (I) zones, which subsequently convert to violet (V') zones. The I zones consist of alternating thin red layers parallel to c, r, n, and ω, and small violet layers parallel to c, r, and n (again, see table B-1; also see figure B-3), but not ω.

In summary, along the c-axis of the crystal described, the following cyclic sequence of growth zones is observed:
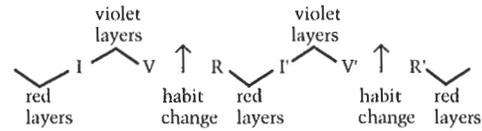
Each of the two violet "cores" in this crystal consists of violet layers parallel to c, r, and n faces, which form in subsequent I and V growth zones. Over the two violet cores are red layers parallel to c, r, n, and ω, which grow in subsequent R and I zones. Those parts of the "cores" that formed during V are usually dark violet and translucent to almost opaque black; those that formed during I are lighter violet and translucent to transparent.

We have found the growth sequence R I V to apply to most of the Mong Hsu rubies examined. Note that in some crystals, stage R is very small. Others

Figure B-1. This 10.5-mm-long untreated crystal, with two violet cores surrounded by red areas, illustrates the relationship between growth conditions and habit change typical of Mong Hsu rubies.

Figure B-2. This schematic representation of habit change and color zoning in the center of the Mong Hsu ruby in figure B-1 shows the R (red), V (violet) and I (intermediate) growth phases seen in the following growth sequence (from bottom): I V R I' V' R'. The arrow indicates the position of a microprobe scan.
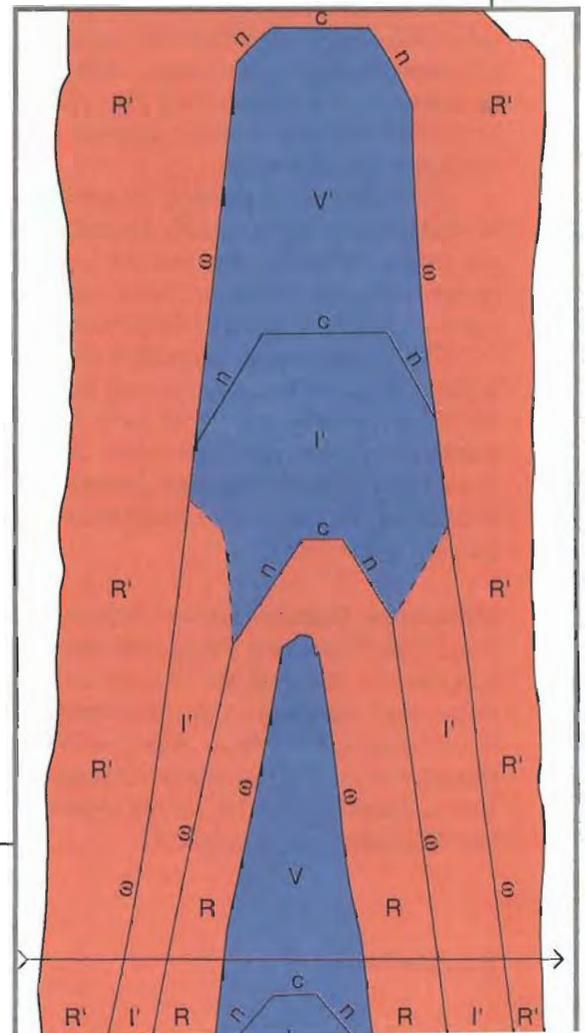
were grown during a period that did not cover the full R I V growth sequence; such a crystal may consist only of a dark violet, nontransparent core grown in stage V, and a red rim grown in stage R.

Also notable in Mong Hsu rubies with the R I V growth sequence is the decreasing size of the hexagonal dipyramid n. During growth phase R, relatively large n faces form (see, e.g., figure 11B). In the subsequent zones I and V, n is progressively smaller; in the end stage of phase V, n is absent (figure 11A). Consequently, with an abrupt change of growth conditions from stage V to stage R, there is also a distinct habit change.

In summary, at the beginning of growth stage R, the crystal habit consists of c, r, n, and ω faces (figures 10 and 11B). In the growth sequence R I V, the growth rate of n strongly increases until, at the end of stage V, it disappears completely. Concurrently, the growth rate of face ω reaches zero, so ω dominates the external crystal form (figures 11A and 7). To date, we have seen no systematic change in the r and c faces over the sequence R I V in the samples available.

The complex growth structure of Mong Hsu rubies is reflected by a complex chemical zoning. For the sample pictured in figure B-1, four microprobe traverses, with 600 to 800 point analyses each, were performed. The position of one of these scans across the sample (including 700 equidistant analysis points) is shown in figure B-2. It twice crossed three red ω growth zones R', I', and R, as well as violet n and c growth layers belonging to the V area. The profile revealed that chromium values are symmetrical in both areas right and left of the center of the crystal; in general, chromium contents are higher in the violet core of growth zone V than in the R', I', and R growth zones. Again, in the violet core, differences between areas related to the basal pinacoid c (1.20–1.35 wt.% Cr_2O_3) and areas related to dipyramidal n growth faces (0.90–0.95 wt.% Cr_2O_3) were also measured. Chromium contents in the red R and I' zones of the rim (0.63–0.75 wt.%) are generally lower than in the violet core.

In the small area between two adjacent ω growth zones in the red rim (i.e., between I' and R'), the scan reveals a distinct decrease from about 0.63 to 0.38 wt.% Cr_2O_3, correlated to an increase from 0.05 to
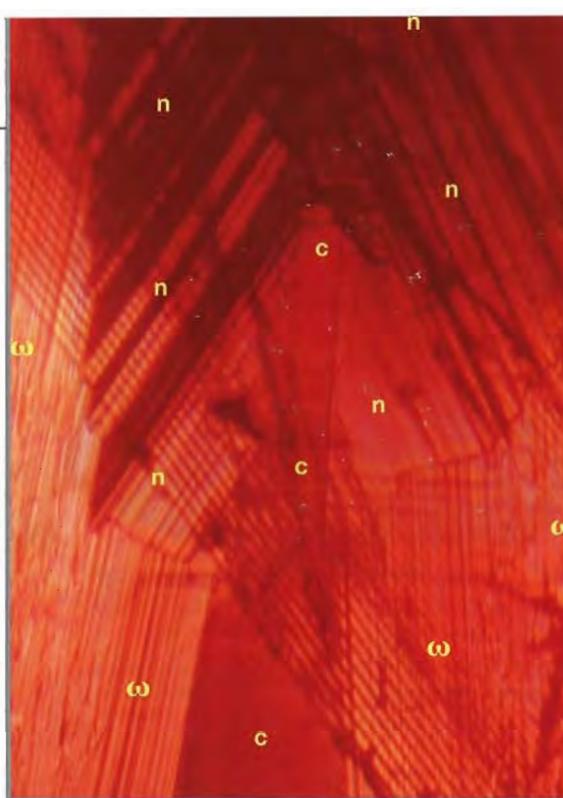
Figure B-3. An enlarged portion of the Mong Hsu ruby in figures B-1 and B-2 shows part of the I' growth zone, with alternating violet and red layers parallel to n, and red layers parallel to ω. Immersion, magnified 50×.

about 0.40 wt.% TiO_2. This represents a growth zone that was present during the formation of the second violet core V'. In the outer ω growth zone of R', we recorded a continuous increase (from 0.63 to 0.97 wt.%) in Cr_2O_3, which reaches values in the outermost layers that are similar to the concentration in the core area that is related to n faces (see also figure 13).

Average vanadium and titanium contents in the violet core are about twice those measured in the red rim. No distinct zoning of iron was observed in this traverse. The other three scans show even more complex results, but these details are beyond the scope of this article. In summary, the complex color zoning seen with the microscope is reflected by a complex chemical zoning in the sample.

TABLE B-1. General outline of habit change in different growth phases (R, I, V) of Mong Hsu rubies.[a]

Variables	R (red)				I (intermediate)				V (violet)			
	c	r	n	ω	c	r	n	ω	c	r	n	ω
Growth rate	Mod.	Mod.	Slow	Slow	Mod.	Mod.	Mod.	Alternating slow/none	Mod.	Mod.	Very fast	None
Layers formed	Yes	Yes	Yes	Yes	Yes	Yes	Yes	Alternating yes/no	Yes	Yes	Yes	No
Relative sizes of faces	Mod.	Mod.	Large	Very large	Mod.	Mod.	Mod.	Very large	Mod.	Mod.	Very small or absent	Very large
Variety	Ruby				Alternating ruby/violet sapphire				Violet sapphire			
Habit	c, r, n, ω (figure 11) n is large				c, r, n, ω n becomes smaller				c, r, ω (figure 11) n is very small or absent			

[a]Habit changes from R to I and from I to V are continuous; the habit change from V to R is abrupt.
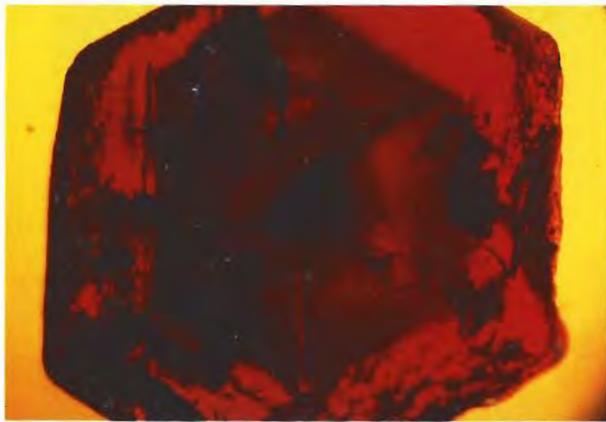
Figure 12. This untreated piece of Mong Hsu rough revealed a complex growth history: A small black core in the center is surrounded by a first red layer, over which is a second violet zone that, in turn, is surrounded by a red layer. View parallel to the c-axis, immersion, magnified 40×.
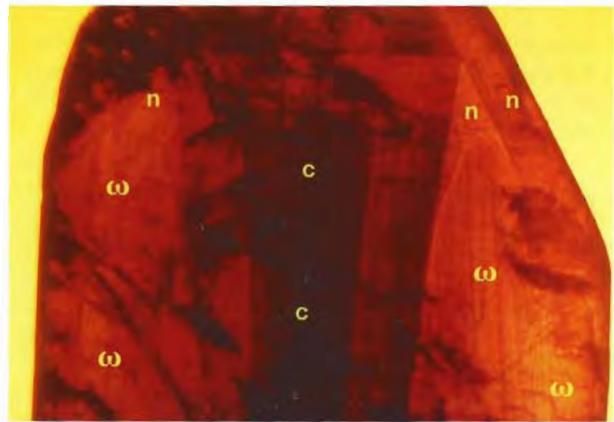
Figure 14. Unlike most of the other Mong Hsu rubies examined for this study, the violet core in this untreated rough sample is confined only to the basal c face, while n and ω growth planes are red. The size of the basal plane increases toward the outer zone of the crystal, in a wedge-shaped pattern. View perpendicular to the c-axis, immersion, magnified 30×.

Figure 13. In this untreated Mong Hsu fragment with n and ω growth planes, an intense red stripe confined to a natural n face represents the latest growth stage. View perpendicular to the c-axis, immersion, magnified 30×.
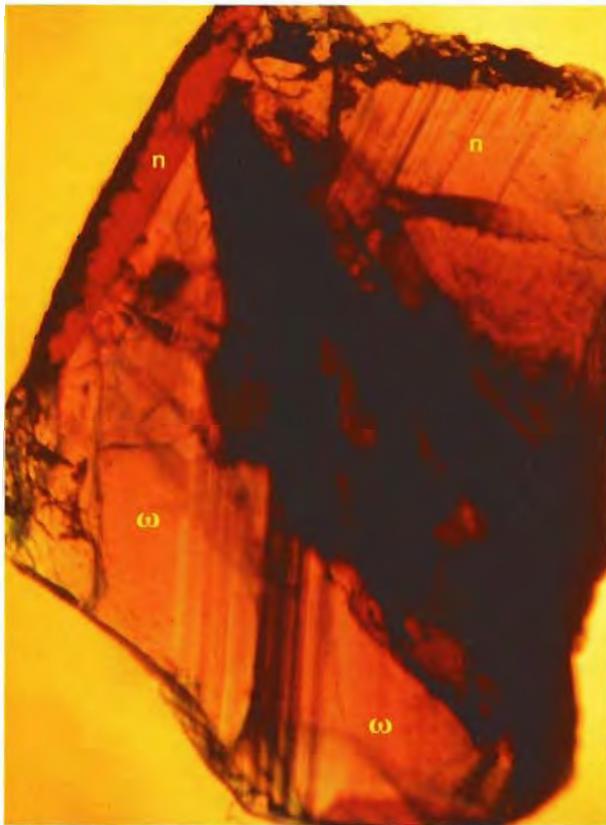
whereas growth planes parallel to n and ω are red. We also observed that the c-plane increased in size during growth, in a direction toward the outer faces of the crystal. Thus, the violet portion in the stone appeared as a wedge-shaped pattern in the rough crystal, with the base of the wedge confined to the latest growth area. In another sample, which also had a wedge-shaped growth pattern confined to the basal plane, dark violet areas were developed as small stripes parallel to ω, and lighter violet stripes were observed parallel to n, but areas confined to c and r growth zones were red.

Growth Structures in Heat-Treated Rubies. Some of the growth characteristics related to natural color zoning are not observed in cut Mong Hsu rubies, because part of the growth history of a crystal is lost during cutting and heat treatment turns the violet cores red. However, neither cutting nor heat treatment alters the characteristic internal growth planes, which we were able to identify in most of the faceted Mong Hsu rubies examined.

Due to the fact that these same patterns and combinations of patterns have never, to the best of our knowledge, been observed in natural rubies before, we feel they are useful to distinguish Mong Hsu rubies from rubies from other localities. In other words: The individual crystal faces observed in Mong Hsu rubies have been identified in rubies from other sources, but the overall pattern of color zoning and habit—that is, the combination of faces
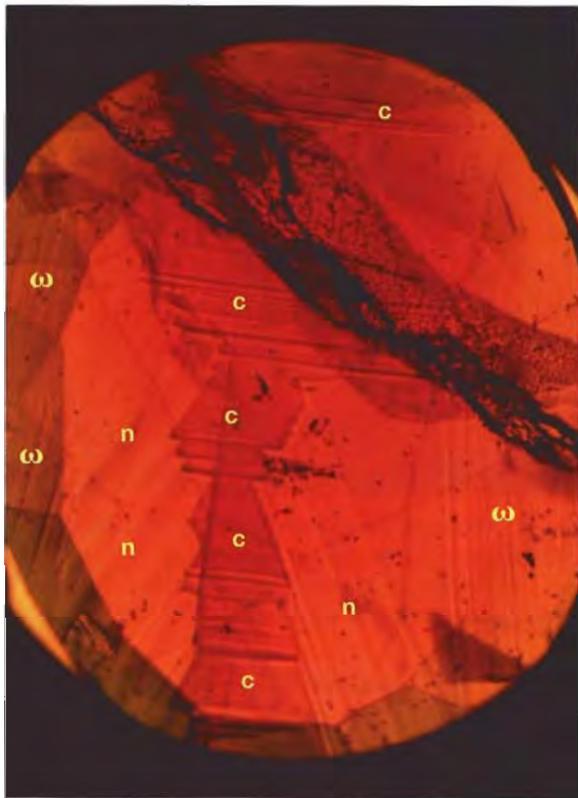
Figure 15. This faceted, heat-treated Mong Hsu ruby is typical of most of the cut Mong Hsu rubies we examined. An intense red core is confined to faces parallel to the basal c plane, the size of the basal plane varies irregularly along the c-axis, and the lighter red areas are confined to n and ω growth zones. View perpendicular to the c-axis, immersion, crossed polarizers, magnified 40×.

Figure 16. In this faceted, heat-treated Mong Hsu ruby, with dominant growth parallel to c in the core and ω planes in the rim (as is typical for rubies from this locality), only subordinate and small n faces are observed in the core. View perpendicular to the c-axis, immersion, magnified 50×.

and the color zoning related to certain growth zones—has not. In addition, because of their distinctive growth patterns, Mong Hsu rubies can be easily separated from their synthetic counterparts.

Typical examples of growth structures that can be found in heat-treated Mong Hsu rubies are shown in figures A-2, 15, and 16. In most of our samples, dark red color zones were confined to basal c growth planes of variable size (figure 15). These dark red zones are surrounded by lighter red areas with growth planes parallel to r, n, and ω (figure A-2). Because faceted stones represent only one area within the original crystal, in the complex growth sequence of Mong Hsu rubies (see box B) the growth zones confined to n faces may be extremely small or absent (figure 16).

Twinning. Twinning is encountered only infrequently in Mong Hsu rubies. The most common type appears to be a repeated rhombohedral twin-

ning, predominantly in one direction parallel to one rhombohedral r face. We observed particles confined to intersection lines of twin planes in only two of our samples, which confirms that rubies with two directions of rhombohedral twinning parallel to two r faces are extremely rare from this locality.

Solid Inclusions. Only rarely did we observe solid inclusions other than whitish particles (see below) in the Mong Hsu rubies examined. These include rutile and fluorite (figure 17; both identified by Raman spectroscopy and SEM-EDS), as well as spinel, which was identified by Raman spectroscopy. Dolomite was identified by SEM-EDS analysis in one crystal; it occurred as a series of rounded, transparent inclusions throughout the red portion. Dolomite was also identified by Smith and
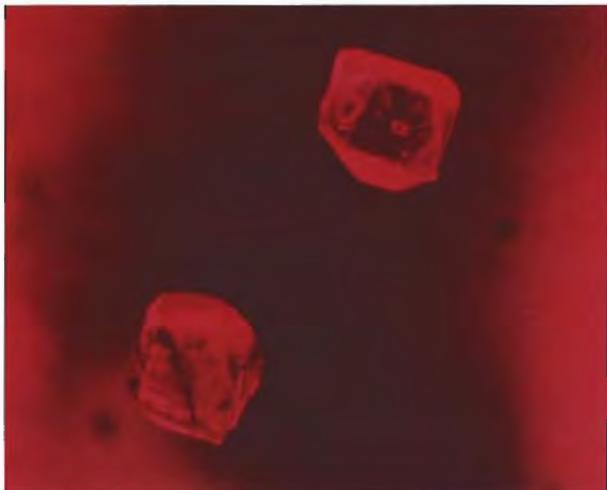
Figure 17. Fluorite (left) and spinel (right) are among the few solid inclusions observed in Mong Hsu rubies. Fiber-optic illumination, transmitted and reflected light; diameter of the solid inclusions is approximately 0.2 mm.
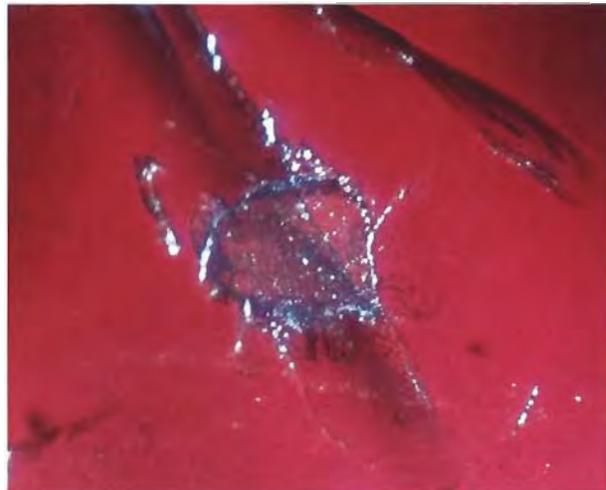
Figure 18. White Mg-chlorite was identified in the outermost parts of some untreated Mong Hsu rubies. Fiber-optic illumination, reflected and transmitted light, magnified 90×.

Surdez (1994) in Mong Hsu rubies; they found apatite as well.

As noted earlier, white mica, fuchsite, and Mg-chlorite were found as overgrowths on some rough Mong Hsu specimens. Mg-chlorite and white mica also were identified by Raman spectroscopy (based on the reference work of Prieto et al., 1991) as inclusions in the outermost parts of some rough crystals (figure 18). It appears that they are, in most cases, removed during preforming of the rough before heat treatment.

Whitish Particles. Various types of small particles ("whitish dust") also are found in both the untreated rough and heat-treated cut Mong Hsu rubies. These particles represent one of the most characteristic inclusion features compared to rubies from other natural sources, and so they are useful in separating Mong Hsu rubies from those from other sources or from synthetic rubies (see also Laughter, 1993a and b; Smith and Surdez, 1994). These inclusions are best resolved using fiber-optic illumination. Two types are:

- Whitish streamers that are oriented perpendicular to growth planes (figures 19–21). They usually extend from the outermost edge of the violet core or lie in close proximity to that area. They

Figure 20. A whitish streamer (left) emerges from the end of a pseudosecondary feather of fluid inclusions along the black core of this untreated Mong Hsu. View almost parallel to the c-axis, fiber-optic illumination, transmitted and reflected light, magnified 60×; photomicrograph by E. Gübelin.

Figure 19. This whitish streamer in an untreated Mong Hsu ruby appears to originate from a solid inclusion located at the boundary between the violet core and red rim. Fiber-optic illumination, reflected light, magnified 100×.
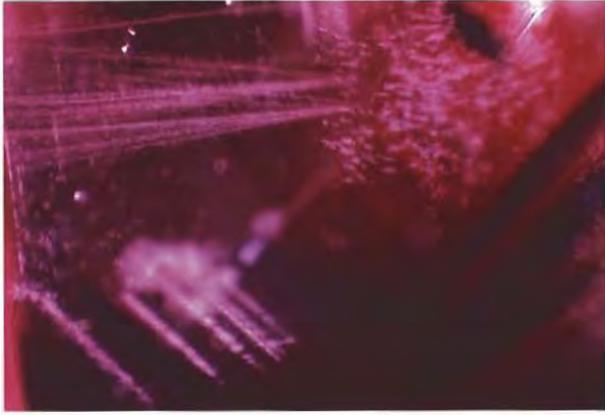
Figure 21. Clouds of snowflake-like particles appear in the upper right of this untreated Mong Hsu ruby, together with a streamer that runs perpendicular to growth structures (top left) and particles confined to ω growth areas (bottom left). View almost parallel to the c-axis, fiber-optic illumination, reflected light, magnified 80×.

Figure 22. Often the whitish dust-like particles seen in untreated Mong Hsu rubies occurred in zones confined to growth planes. This type of inclusion was not removed by heat treatment. View almost parallel to the c-axis, fiber-optic illumination, reflected light, magnified 60×.

appear to be initiated by the trapping of solid (figure 19) or fluid (figure 20) inclusions, which tend to be concentrated in the boundary zone between core and rim. These initial crystal defects do not completely heal during subsequent growth, and new defects—which also act as traps for fluids—are continuously formed. Ultimately, they appear as a series of lines consisting of small reflecting particles, which are oriented perpendicular to the growth planes of that particular zone.

- Whitish dust, resembling clouds of snowflakes (figure 21), frequently can be seen irregularly dispersed in large zones of a crystal. This type of inclusion is often confined to certain growth zones (figure 22), usually related to the ω plane (figure 21).

Whitish particles of a completely different type are formed by heat treatment. These particles form dense areas, in some cases in ω zones that grew after the originally violet core (figure 23), and occa-

sionally in growth zones confined to the basal face. Note that dense zones of whitish particles were also observed in areas confined to the violet or almost black core. In extreme cases, the whitish particles are so dense that the stone appears semi-translucent, with large whitish reflecting areas, which makes it unsuitable for the jewelry market. In one heat-treated sample, we observed dense, oriented, needle-like particles. We also observed the formation of such needles in another sample heat treated in Germany; they appeared in an area, confined to the rim of the stone, that had originally been transparent red, as well as in violet zones. We do not yet know the exact nature of these needles.

Fluid Inclusions. In contrast to solid inclusions, fluid inclusions were frequently seen in both untreated and heat-treated Mong Hsu rubies, in cores as well as rims. For the most part, they represent various primary fluids trapped in single cavities as well as in pseudosecondary (figure 20) and secondary "feathers" or "fingerprints." They are

Figure 23. Violet to almost black zones in the center of this Mong Hsu crystal in its natural state (right) were completely gone after heat treatment (left), but whitish particles had formed in ω growth zones outside the center. View almost parallel to the c-axis, fiber-optic illumination, reflected and transmitted light, magnified 60×.
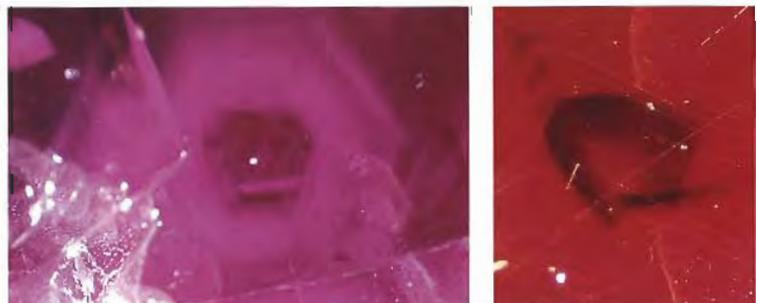
Figure 24. Healing feathers ("fingerprints")—actually interconnecting tubes and isolated dots of fluid inclusions—were commonly seen in both heat-treated (as here) and untreated Mong Hsu rubies. Immersion, magnified 60×.

related to the cracking of the ruby and subsequent healing by fluids.

If this type of inclusion forms early in crystal growth close to the core, the outline of the core is sometimes seen parallel to the border of the "feather" (figure 20). Another "feather" in a heat-treated Mong Hsu ruby (figure 24) consists of isolated droplets and interconnecting tubes. It formed later than the example illustrated in figure 20.

Fracture Fillings Produced by Heat Treatment. Heat treatment may create additional fractures in the ruby because of the decrepitation of solid matter or fluids trapped in small cavities. This reduces

the transparency of the stone. As demonstrated by heat-treatment experiments in Germany, no chemicals are needed to remove the blue color component completely from the Mong Hsu stones. As noted earlier, though, commercial treaters often use various chemicals, such as borax, during a second heating process to fill cracks and fissures exposed at the surface and thus enhance apparent clarity (Hughes, 1988; Peretti, 1993; Henn and Bank, 1993). Borax or similar substances can act as a flux to dissolve alumina and can cause, at least partly, a recrystallization or healing of open fracture planes (Hänni, 1992; Koivula et al., 1993a; Milisenda and Henn, 1994). Mica or chlorite present in these open cavities or fissures will dissolve in the presence of borax and form borosilicates that are then trapped as artificial glassy fillings. The formation of a crystalline phase in fractures of treated Mong Hsu rubies has also been observed, and the compound was identified by means of X-ray powder diffraction as aluminum borate (H. A. Hänni, pers. comm., 1994).

We observed fissures and cavities containing these foreign fillers in many Mong Hsu samples obtained from the trade. In some treated rubies, we saw flow structures in the glassy fillers of heavily included samples, which easily identified them as foreign material (figure 25). In contrast, only careful microscopic examination revealed the presence of foreign substances in other, partly recrystallized fractures (figure 26). The exact composition of various filling materials, however, cannot be identified by microscopic examination. In areas in which the filling material reaches the surface of the ruby, the filled fissure can be recognized by its reduced luster

Figure 25. Flow structures can be seen in this fissure, which has been partially filled with a solid foreign material. During heat treatment for clarity enhancement, the host Mong Hsu ruby was placed in contact with borax or a similar substance. Immersion, magnified 60×.

Figure 26. In some partly recrystallized fractures, it is difficult to locate the foreign substance (possibly borax or an aluminum borate) to which the ruby was exposed during heat treatment. Immersion, magnified 60×.

Oxide/R.I.	Untreated rough					Heat-treated faceted				
	A	B	C	D	E	F	G	H	I	J
Oxide										
Al_2O_3	99.300	98.600	98.400	99.200	98.800	99.000	98.400	98.400	98.900	99.500
Cr_2O_3	0.460	0.914	1.216	0.572	0.594	0.654	1.166	1.391	0.718	0.354
FeO	0.006	0.060	0.031	0.003	0.035	0.003	0.017	0.008	0.007	0.005
TiO_2	0.107	0.194	0.168	0.134	0.338	0.145	0.233	0.046	0.210	0.045
V_2O_3	0.038	0.050	0.057	0.045	0.100	0.090	0.023	0.035	0.090	0.014
Ga_2O_3	0.010	0.010	0.014	0.013	0.017	0.009	0.006	0.011	0.010	0.004
Refractive indices										
n_o	—[b]	1.773	1.774	1.771	1.772	1.771	1.775	1.775	—[b]	1.770
n_e	—[b]	1.765	1.765	1.762	1.763	1.763	1.766	1.766	—[b]	1.762

[a] *The columns do not total 100 wt.% due to traces of MnO, K_2O, MgO, CaO, and SiO_2. No traces of CuO, NiO, ZrO_2, P_2O_5, or Nb_2O_5 were detected.*
[b] *No sharp shadow edges observed on the refractometer.*

compared to that of the polished ruby when viewed with reflected light (see, e.g., Kane, 1984; Scarratt and Harding, 1984; Scarratt et al., 1986; Hänni, 1986).

Chemical Properties. The methods applied to determine the rubies' chemical properties provide analytical data that represent different-size areas within the samples. X-ray fluorescence analysis reveals an average composition of that part of the ruby (in an area that can be measured in millimeters) that was exposed to the X-ray beam, such as part of the table of a faceted stone. The electron microprobe analyzes areas with diameters in the micrometer range. Thus, traverses with several point analyses across the polished surface of a ruby indicate the chemical variability of a sample. For certain trace elements, such as gallium, the more sensitive X-ray fluorescence analysis is required to obtain quantitative data.

The reliability of the data obtained for this study by X-ray fluorescence and electron microprobe analyses is supported by the similarity in average trace-element concentrations reported by both methods.

X-ray Fluorescence Analysis. The results of X-ray fluorescence analyses of various rubies (five untreated and five heat treated) are shown in table 2. The untreated rubies were composed of rough fragments of crystals with plane polished faces. As can be seen from table 2, the rubies contain significant trace-element concentrations of Cr_2O_3, FeO, TiO_2, V_2O_3, and Ga_2O_3. Large differences in the trace-element concentrations among the various samples were measured, but we saw no significant differences in trace-element amounts between treated and untreated stones.

For the eight samples analyzed for which refractive indices could be measured on the refractometer (again, see table 2), a reasonable correlation was found between R.I.'s and chromium concentrations, and a good coincidence was obtained in a plot with the sum of trace-element concentrations (calculated as $Cr_2O_3 + Ti_2O_3 + V_2O_3 + Fe_2O_3 + Ga_2O_3$) versus refractive indices (figure 27). Consequently,

Figure 27. Refractive indices were correlated with chemical composition in the eight Mong Hsu rubies analyzed by X-ray fluorescence for which refractive indices could be measured (see table 2). The correlations are expressed here as the sum of trace-element concentrations; red squares = ordinary ray (n_o), black squares = extraordinary ray (n_e). A distinct increase in refractive indices is caused by increasing trace-element contents.
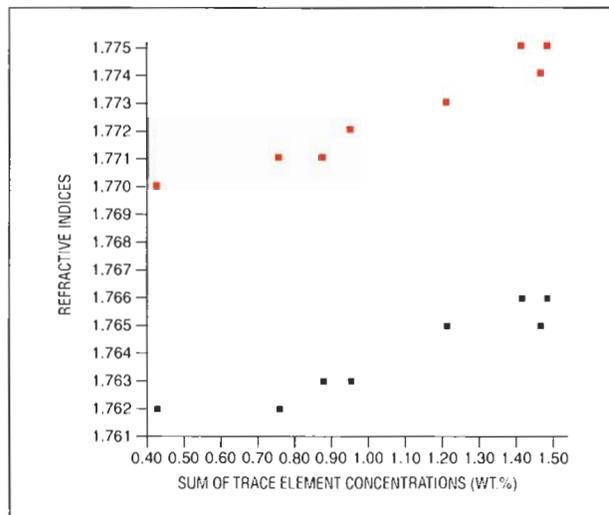
variations in refractive index are related to variations in trace-element contents.

Electron Microprobe Analysis. As the results shown in table 3 indicate, systematic variations within the samples were observed for TiO_2 and Cr_2O_3 and, in some samples, for V_2O_3; only the statistical variations of the analytical instrument were found for FeO and MnO.

On the basis of the relationships between Cr_2O_3 and TiO_2 (in combination with FeO), we have identified three basic types of chemical zoning in Mong Hsu rubies to date (see also box B):

- *Type A:* A distinct variation in Cr_2O_3 that is not correlated to titanium was found for samples 1, 3, and 4 (figure 28A). These rubies had high Cr_2O_3 concentrations in the intense red zone (that represents the core of the original crystal) and lesser quantities of Cr_2O_3 in the lighter red "rim" (samples 1 and 3). In sample 4, we found a

less extreme microscopic red color zoning, although the sample was faceted with its table perpendicular to the c-axis. Accordingly, the chemical variations were less pronounced than in other samples with a strong visual color zoning.

- *Type B:* A distinct variation in Cr_2O_3 was found to correlate with a distinct TiO_2 zoning in heat-treated samples 2 and 5 (figure 28B). High concentrations of Cr_2O_3 and TiO_2 were restricted to the relatively intense red core.

- *Type C:* A distinct zoning of TiO_2 perpendicular to the c-axis, inversely correlated to Cr_2O_3 in the outer zones of the rim, was found in untreated sample 6 (figure 28C), which had a homogeneous violet core and a light red rim. TiO_2 concentrations were higher in the core than in the rim. Cr_2O_3 was higher in the outermost part of the rim. No systematic variations

TABLE 3. Electron microprobe analyses of Mong Hsu rubies.

Variable	Faceted sample number[a]					Rough sample number[a]		
	1	2[b]	3[c]	4	5	6[d]		7[e]
Orientation	Table parallel c-axis	Table perp. c-axis	Table perp. c-axis	Table perp. c-axis	Table parallel c-axis	Cut parallel c-axis		Cut perp. c-axis
Visual appearance	Dark red core, lighter red rim	Dark red core, lighter red rim	Dark red core, lighter red rim	Red core, lighter red rim	Dark red core, lighter red rim	Dark violet core, lighter red rim		Complex zoning dark violet core, light red rim
Number of scans	3	4	4	4	2	5	3	7
Number of analyses	109	138	138	138	78	208	108	288
Direction of scans	Perp. c-axis	Perp. c-axis	Perp. c-axis	Perp. c-axis	Perp. c-axis	Perp. c-axis	Parallel c-axis	Perp. c-axis
Analyses in wt.% (range)								
Al_2O_3	98.42–99.44	98.17–99.72	96.53–98.97	98.15–99.60	98.15–99.66	98.33–99.78	98.40–99.90	98.45–99.91
Cr_2O_3	0.26– 0.89	0.42– 1.05	0.90– 2.86	0.60– 0.89	0.39– 0.98	0.40– 1.03	0.42– 0.69	0.40– 1.34
V_2O_3	0.00– 0.13	0.00– 0.11	0.00– 0.12	0.00– 0.07	0.00– 0.10	0.00– 0.08	0.00– 0.07	0.00– 0.08
TiO_2	0.09– 0.28	0.05– 0.23	0.00– 0.14	0.06– 0.27	0.04– 0.31	0.00– 0.38	0.04– 0.34	0.03– 0.51
FeO	0.00– 0.03	0.00– 0.02	0.00– 0.04	0.00– 0.03	0.00– 0.02	0.00– 0.04	0.00– 0.03	0.00– 0.04
MnO	0.00– 0.03	0.00– 0.03	0.00– 0.02	0.00– 0.02	0.00– 0.04	0.00– 0.03	0.00– 0.02	0.00– 0.03
Chemical zoning	Cr	Cr and Ti	Cr	Cr	Cr and Ti	Ti/ Cr	No distinct zoning	Complex zoning of Cr and Ti
Area of high concentration	Core	Core	Core	Core	Core	Core/outer rim		
Correlation between Ti and Cr	No	Yes	No	No	Yes	No	No	No

a All faceted samples had been heat treated; both rough samples were untreated. Perp. = perpendicular.
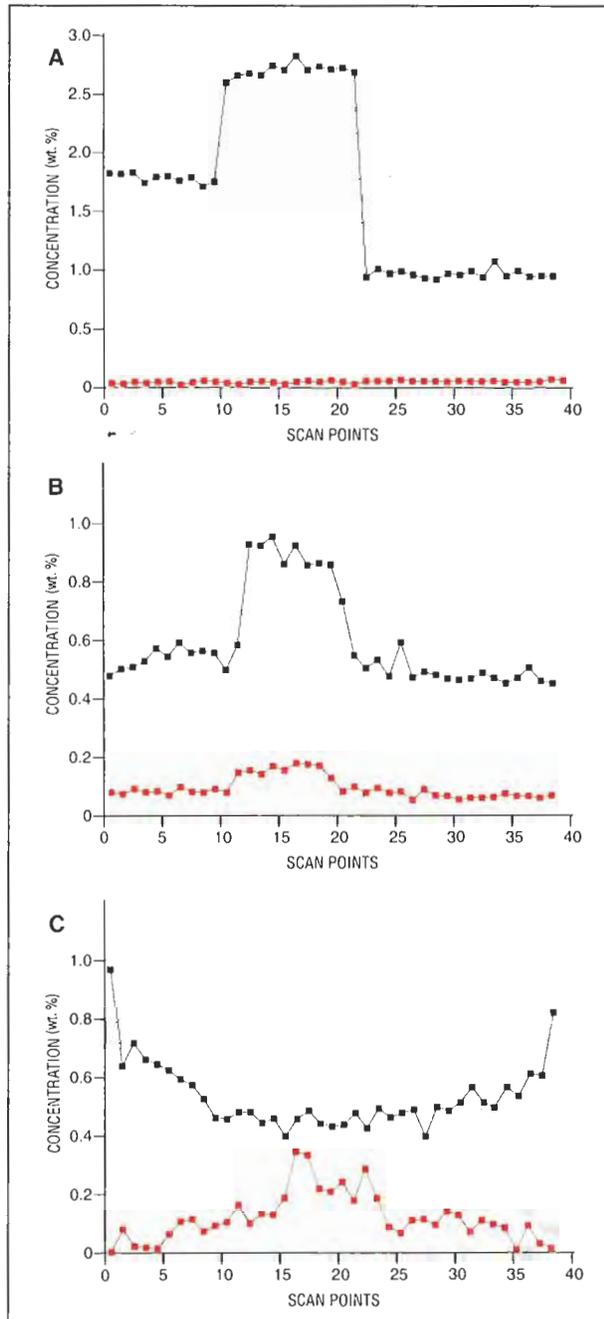*b See figure 28B.*
c See figure 28A.
d See figure 28C.
e see figure A-1.

were found in this sample in a direction parallel to the c-axis.

In sample 7 (table 3), the complex growth and color zoning involving c, n, r, and ω faces (figure A-1) revealed an extremely complex zoning of both Cr_2O_3 and TiO_2 that does not fit any of the simple types described above.

Figure 28. These three electron microprobe traverses reveal the differences in Cr_2O_3 contents (black squares) and TiO_2 contents (red squares) between core and rim areas of three Mong Hsu rubies. Samples A (no. 3, table 3) and B (no. 2, table 3) are both faceted and heat-treated; sample C (no. 6, table 3) is an untreated polished platelet. Sample A shows higher Cr_2O_3 in the core than the rim, and no TiO_2 zoning. Sample B shows Cr_2O_3 concentrations correlated with a distinct TiO_2 zoning, with higher Cr_2O_3 and TiO_2 contents in the core and lower values in the rim. Sample C reveals increased TiO_2 in the core, increasing Cr_2O_3 toward the outer zones of the rim, and an inverse correlation between Cr_2O_3 zoning and variations in TiO_2. All scans were performed in a direction perpendicular to the c-axis.

In some samples, we found a correlation between V_2O_3 and Cr_2O_3; that is, high chromium and relatively high vanadium in the intense red cores, with lower chromium and vanadium in the lighter red rims. No correlation was seen between iron and titanium or between iron and chromium.

Thus, it can be concluded that the color zoning correlates with a systematic variation in Cr_2O_3 and/or TiO_2 (see also box B): The violet (untreated) and intense red (heat-treated) cores of Mong Hsu rubies have significantly higher Cr_2O_3 concentrations than the lighter red "rim" layers around them. We also identified zones with high TiO_2 concentrations (relative to the rim portion) in the violet (untreated) and red (heat-treated) cores of some Mong Hsu rubies (type C). In some samples, we found both high Cr_2O_3 and high TiO_2 concentrations in the core.

In summary, it appears that the main chemical zoning of Mong Hsu rubies, between crystal core and rim zones, is due to greater amounts of chromium and/or titanium in the areas confined to the intense red or violet cores. Between distinct zones within the rims, chromium and/or titanium values also may vary (see box B, as well as figures 13 and 28C).

The trace-element concentrations of Mong Hsu rubies can be compared to those of natural rubies from other deposits of commercial importance, including Luc Yen (Vietnam), Morogoro (Tanzania), Mogok (Myanmar), Kenya, Sri Lanka, Malawi, and Thailand (Harder, 1969; Schmetzer, 1986b; Bank et al., 1988; Tang et al., 1988, 1989; Hänni and Schmetzer, 1991; Kane et al., 1991; Delé-Dubois et
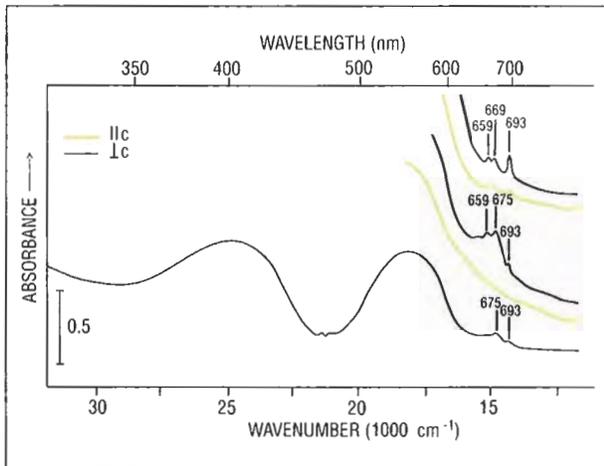
Figure 29. These absorption spectra were recorded in three Mong Hsu rubies. The top is from a heat-treated faceted stone with its table oriented parallel to the c-axis, 2.3 mm thick (sample 1, table 3). The middle is from the violet core of an untreated slice (about 2.5 mm thick) cut parallel to the c-axis (sample 6, table 3). The bottom is from an untreated slice (about 1 mm thick) cut perpendicular to the c-axis with violet core and red rim (see sample 7, table 3, figure A-1). In the red to yellow spectral range of untreated samples, a broad absorption without distinct maximum and an absorption band at 675 nm are superimposed on the chromium (ruby) spectrum.

al., 1993). The Cr_2O_3 concentrations in Mong Hsu rubies can be extremely high. The FeO concentrations are relatively low compared to those of rubies from other marble-type deposits such as Morogoro or Luc Yen. The upper end of the TiO_2 range is much higher than the values found in rubies from these same occurrences. The V_2O_3 concentrations are similar to those reported for rubies from Mogok, but can be much higher than those published for rubies from some other marble-type deposits, such as Morogoro and Luc Yen. The range of FeO, TiO_2 and V_2O_3 concentrations found in Mong Hsu rubies is different from those of rubies from basaltic rocks (e.g., Thailand).

The combination of relatively high Cr_2O_3, TiO_2, and V_2O_3 along with relatively low concentrations of FeO has so far not been reported for any of the various types of synthetic rubies (Tang et al., 1989; Muhlmeister and Devouard, 1991; Peretti and Smith, 1993; Hänni et al., 1994).

In summary, the trace-element patterns of Mong Hsu rubies are useful to distinguish faceted samples from their synthetic counterparts.

Although there may be some overlaps with other natural rubies originating from marble deposits, trace-element contents of individual samples, in combination with other characteristics, can also be helpful for locality determination.

Spectroscopic Features. *Visible and Ultraviolet Spectroscopy.* Absorption spectra of heat-treated Mong Hsu rubies and of the outer rims of untreated specimens were typical of those seen in low-iron rubies, with no iron-related absorption at 450 nm. Absorption characteristics in the ultraviolet were similar to those of iron-poor rubies from marble-type deposits (Bosshart, 1982; Smith and Surdez, 1994).

The spectra of untreated samples with violet cores revealed additional absorption features in the red and yellow area, between about 800 nm and the broad chromium absorption band in the green range, which are superimposed on the ruby absorptions (figure 29). These absorption features are described as:

- a broad absorption in the spectrum parallel and perpendicular to the c-axis, ranging from about 800 nm to about 550 nm without a distinct absorption maximum, and

- a polarized absorption band in the spectrum perpendicular to the c-axis, with a maximum at 675 nm, that is, in the range of the well-known chromium lines at 693, 669, and 659 nm.

In different violet samples measured, the relative intensities of the bands in the red to yellow area vary. In some, the 675-nm band was weaker than the 693-nm Cr^{3+} absorption line; in others, the 675-nm absorption, which is strongly polarized, exceeded this well-known chromium absorption in intensity (figure 29).

These additional absorption features in the red, particularly the broad absorption, are responsible for the color in the cores, that is, light violet parallel to the c-axis and intense violet perpendicular to c. Thus, the violet color in Mong Hsu rubies is caused by the superimposition of a red (ruby) component caused by chromium and a blue component that is removed by heat treatment. The blue component consists of two different absorption features, which are more intense in the spectrum perpendicular to the c-axis.

Violet sapphires and purplish red rubies are known from various localities, such as Ratnapura, Sri Lanka, and Umba, Tanzania. In all types of violet samples from various occurrences, the blue

component of the violet color is due to a broad absorption band in the red area, which can be at least partially removed by heat treatment, even at relatively low temperatures such as 1000° or 1200°C, which have been used historically for the heat-treatment of corundum (Bauer and Schlossmacher, 1932).

An extremely broad absorption band in the red-to-green spectral region (between 800 and 500 nm) has been seen in blue sapphires from various localities and is generally assigned to an Fe^{2+}/Ti^{4+} charge-transfer absorption. The blue color in this type of low-iron sapphire (i.e., without a specific Fe^{2+}/Fe^{3+} absorption band in the near infrared) can also be partially removed by heat treatment at low temperatures; some of these sapphires turn colorless when heated (Schmetzer and Bank, 1980). If the iron-titanium charge-transfer absorption is superimposed on a ruby spectrum, the color of the sample is altered from red to purplish red, purple, or violet, according to the relative intensity of the two color-causing components in the spectrum (Schmetzer and Bank, 1981).

Given the spectral characteristics of Mong Hsu rubies and their titanium zoning, the additional broad absorption in the red and the resulting violet color of the cores of these rubies is consistent with the presence of such a blue sapphire component.

In the absorption spectrum of untreated Mong Hsu samples with violet cores, however, we also observed an additional polarized absorption band at 675 nm (figure 29), which is not fully understood at present. In some of the samples, this absorption band exceeded the 693-nm chromium line in intensity. The only correlation found in the literature for this band is an absorption in the spectrum of Mn^{4+} in corundum (Geschwind et al., 1962; Crozier, 1965; Potnau and Adde, 1976). Mn^{4+} appears in synthetic flux-grown and Verneuil-grown corundum crystals, which are doped by manganese, with MgO added for charge compensation. Mn^{4+} is isoelectronic with Cr^{3+} and has three d electrons. It reveals, in addition to the sharp 675-nm band, a broad absorption at about 470 nm and an absorption edge in the ultraviolet range, the low-energy tail of which extends to the visible area, causing an almost continuously increasing absorption from about 500 nm toward smaller wavelengths. If a broad absorption band of Mn^{4+} at 470 nm is present in the spectrum of chromium-bearing corundum, this absorption is, most probably, hidden between the two dominant color-causing chromium absorption bands. Thus, in a sample of Mong Hsu ruby with high amounts of

chromium and relatively low manganese concentrations (see tables 2 and 3), it is conceivable that only the small 675-nm absorption band close to the small chromium fluorescence line at 693 nm will be observed. This assignment, however, needs further experimental research for confirmation, especially for the explanation of a possible stabilization mechanism by charge compensation and its reaction to heat-treatment.

In summary, the spectra of the violet cores in Mong Hsu rubies consist of the well-known absorption lines and absorption bands of Cr^{3+} in corundum, on which are superimposed a broad Fe^{2+}/Ti^{4+} charge-transfer absorption and an additional line at 675 nm, the nature of which is not yet known. The influence of one or both additional absorption features in the red on the violet color of different cores varies, and additional research is necessary (for example, by a combination of microscope absorption spectroscopy and microprobe analyses) to understand the cause of color in these highly zoned samples.

Infrared Spectroscopy. IR spectroscopy of transparent, heat-treated samples revealed spectra with sharp absorption lines in the 3000 to 3500 cm^{-1} range—either with two maxima, at 3233 and 3310 cm^{-1} (figure 30), or with one maximum at 3310 cm^{-1}— or spectra with a complete absence of infrared absorptions in the range mentioned. Smith and

Figure 30. This infrared spectrum of a heat-treated Mong Hsu ruby reveals sharp absorption lines at 3233 and 3310 cm^{-1}, which are assigned to OH-stretching vibrations. These lines are characteristic for OH groups in rubies, which are related to structural defects. Such lines are not found in flux-grown synthetic rubies.
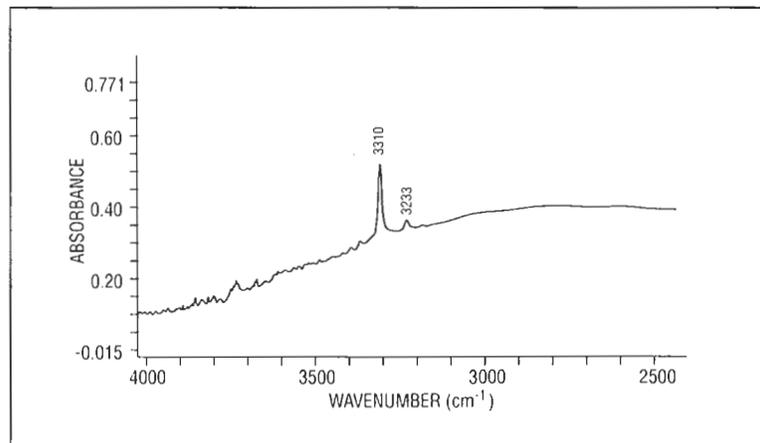
Surdez (1994) reported seven sharp bands of varying intensity at 3189 (weak), 3233 (medium), 3299 (very weak), 3310 (strong), 3368 (very weak), 3380 (very weak), and 3393 cm^{-1} (very weak) in the absorption spectra of Mong Hsu rubies. Similar features have been found in the infrared spectra of Verneuil-grown synthetic rubies and sapphires that were doped with various trace elements in different concentrations and, at least partly, annealed in a hydrogen atmosphere at high temperatures (Borer et al., 1970; Eigenmann and Günthard, 1971; Eigenmann et al., 1972; Blum et al., 1973; Volynets et al., 1972, 1974; Beran, 1991; Moon and Phillips, 1994). Consequently, the sharp absorption bands in the infrared spectra of Mong Hsu rubies are assigned to OH-stretching vibrations and indicate that hydroxyl groups have been incorporated in the crystal structure of some heat-treated samples.

Smith (1995) recorded an absorption spectrum in some untreated samples that consisted of several broad absorption bands. He assigned this spectrum to microscopic or submicroscopic inclusions of diaspore, AlO(OH).

OH-stretching vibrations were also measured previously in the infrared spectra of a few untreated ruby and sapphire samples from Sri Lanka (Schmetzer, unpublished), in a ruby from Sri Lanka and a blue sapphire from Montana (Beran, 1991), and in untreated blue Australian sapphires (Moon and Phillips, 1994). They were not found in the spectra of flux-grown synthetic rubies (Belt, 1967; Volynets et al., 1972; Peretti and Smith, 1994).

For practical gemology, the presence of OH-related absorption lines in the infrared spectrum of an unknown ruby indicates that the sample is not a flux-grown synthetic ruby, although it may be a Verneuil-grown or hydrothermally grown synthetic sample (either of which is more readily identifiable from natural rubies than the flux-grown material) or a natural stone. For discussion of the difference between Verneuil- and hydrothermally grown synthetic ruby, see Belt (1967), Beran (1991), and Peretti and Smith (1993, 1994).

SUMMARY AND CONCLUSION

Large quantities of rubies from the new deposit at Mong Hsu have been widely available since 1992. Most are heat-treated before they enter the jewelry trade. Mong Hsu rubies are easily recognized by their distinctive microscopic properties. They have a number of features that thus far have not been reported for rubies from other occurrences. These include:

- A distinct color zoning confined to specific growth structures, with one or two violet "cores" surrounded by a red "rim."
- Spectroscopic features in the red to yellow portion of the visible spectrum, with absorption bands that are removed during heat treatment to change the cores from violet to red.
- The presence of whitish particles in certain growth zones, formed as a result of heat treatment.

We found that the color zoning in our samples is closely related to a complex chemical zoning confined to growth layers formed parallel to the basal pinacoid, to the positive rhombohedron, and to two hexagonal dipyramids. We observed a distinct growth sequence whereby red and violet areas formed in various growth cycles, with a specific habit change between different growth zones. The variation in physical properties, such as refractive indices, is closely related to the chemical composition of the samples. Although those properties of the crystals that are related to different growth conditions during the formation of the rubies—that is, growth zoning, color zoning, and chemical zoning related to temperature and/or pressure and/or chemical composition of the environment—are well understood. Only preliminary models are presently available to provide a detailed explanation of the cause of successive growth cycles (Peretti and Mouawad, 1994).

Nor is there a comprehensive explanation for those properties of Mong Hsu rubies that change with heat treatment. Likewise, no model is available that can explain all features related to the change in UV-visible and IR spectroscopic properties, which are closely related to the color change and possibly also to the formation of the whitish particles.

The distinctive properties of Mong Hsu rubies are useful in separating faceted samples from their synthetic counterparts and also in establishing the locality of origin. The most prominent diagnostic properties of faceted, heat-treated Mong Hsu rubies require careful microscopic examination, using immersion techniques in conjunction with fiber-optic illumination. Key features include growth structures confined to a distinct color zoning between cores and rims; different types of whitish particles and whitish streamers are also of diagnostic value. Specialized laboratory techniques, such as XRF analysis and IR spectroscopy, provide additional diagnostic information. Problems for the trade

arise, however, from the large numbers of stones with fractures that appear to have been filled with a foreign material, especially partially healed fractures with glassy and/or crystalline fillers.

REFERENCES

Bank H., Henn U., Lind Th. (1988) Rubine aus Malawi. *Zeitschrift der Deutschen Gemmologischen Gesellschaft*, Vol. 37, No. 3/4, pp. 113–119.

Bauer M., Schlossmacher K. (1932) *Edelsteinkunde. 3. Aufl.*, Bernhard Tauchnitz, Leipzig, p. 209, 498.

Belt R.F. (1967) Hydrothermal ruby: Infrared spectra and X-ray topography. *Journal of Applied Physics*, Vol. 38, No. 6, pp. 2688–2689.

Beran A. (1991) Trace hydrogen in Verneuil-grown corundum and its color varieties—An IR spectroscopic study. *European Journal of Mineralogy*, Vol. 3, pp. 971–975.

Blum H., Frey R., Günthard Hs.H., Ha Tae-Kyu (1973) Ab initio scf study of OHO^{3-} system and its relation to the structure of alpha-Al_2O_3:OHO^{3-}(Me^{2+}). *Chemical Physics*, Vol. 2, pp. 262–270.

Borer W.J., Günthard Hs.H., Ballmer P. (1970) Solid state reactions and defects in Verneuil laser rubies. *Helvetica Physica Acta*, Vol. 43, pp. 74–92.

Bosshart G. (1982) Distinction of natural and synthetic rubies by ultraviolet spectrophotometry. *Journal of Gemmology*, Vol. 18, No. 2, pp. 145–160.

Burma's Mongshu mine rediscovered, heat-treated rubies comparable to Mogok quality (1993). *Jewelry Newsline*, Vol. 1, No. 2, p. 1, 8.

Clark C. (1993) Thai cooking class. *JewelSiam*, Vol. 4, No. 5, p. 57.

Crozier M.H. (1965) Optical Zeeman effect in the R_1 and R_2 lines of Mn^{4+} in Al_2O_3. *Physics Letters*, Vol. 18, No. 3, pp. 219–220.

Delé-Dubois M.L., Fournier J., Peretti A. (1993) Rubis du Vietnam—Etude comparative avec les rubis de Birmanie et d'autres provenances. *Revue de Gemmologie a.f.g.*, No. 114, March 1993, pp. 7–10.

Earth Sciences Research Division (1977) Geological Map of the Socialist Republic of the Union of Myanmar 1:1'000'000, with brochure, 22 pp.

Eigenmann K., Günthard Hs.H. (1971) Hydrogen incorporation in doped alpha-Al_2O_3 by high temperature redox reactions. *Chemical Physics Letters*, Vol. 12, No. 1, pp. 12–15.

Eigenmann K., Kurtz K., Günthard Hs.H. (1972) Solid state reactions and defects in doped Verneuil sapphire. *Helvetica Physica Acta*, Vol. 45, pp. 452–480.

Geschwind S., Kisliuk P., Klein M.P., Remeika J.P., Wood D.L. (1962) Sharp-line fluorescence, electron paramagnetic resonance, and thermoluminescence of Mn^{4+} in alpha-Al_2O_3. *Physical Review*, Vol. 126, No. 5, pp. 1684–1686.

Glass filled rubies increasing (1994). *Jewellery News Asia*, No. 119, July, pp. 66, 68, 70.

Hänni H.A. (1986) Behandelte Korunde mit glasartigen Füllungen. *Zeitschrift der Deutschen Gemmologischen Gesellschaft*, Vol. 35, No. 3/4, pp. 87–96.

Hänni H.A. (1992) Identification of fissure-treated gemstones. *Journal of Gemmology*, Vol. 23, No. 4, pp. 201–205.

Hänni H.A., Schmetzer K. (1991) New rubies from the Morogoro area, Tanzania. *Gems & Gemology*, Vol. 27, No. 3, pp. 156–167.

Hänni H.A., Schmetzer K., Bernhardt H.-J. (1994) Synthetic rubies by Douros: A new challenge for gemologists. *Gems & Gemology*, Vol. 30, No. 2, pp. 72–86.

Harder H. (1969) Farbgebende Spurenelemente in natürlichen Korunden. *Neues Jahrbuch für Mineralogie Abhandlungen*, Vol. 110, pp. 128–141.

Henn U., Bank H. (1993) Neues Rubinvorkommen in Myanmar (Burma). *Zeitschrift der Deutschen Gemmologischen Gesellschaft*, Vol. 42, No. 2/3, pp. 63–65.

Hlaing U Tin (1981) Mineralogical studies and minor element analyses of corundum and associated minerals of the Mogok gemstone tract. M.S. thesis, University of Rangoon, Myanmar, 217 pp.

Hlaing U Tin (1991) A new Myanmar ruby deposit. *Australian Gemmologist*, Vol. 17, No. 12, pp. 509–510.

Hlaing U Tin (1993) Mong Hsu ruby update. *Australian Gemmologist*, Vol. 18, No. 5, pp. 157–160.

Hlaing U Tin (1994) A trip to Mong Hsu. *JewelSiam*, Vol. 5, No. 1, pp. 54–57.

Hughes R.W. (1988) Surface repaired corundum—Two unusual variations. *Journal of Gemmology*, Vol. 21, No. 1, pp. 8–10.

Hunstiger C. (1990) Darstellung und Vergleich primärer Rubinvorkommen in metamorphen Muttergesteinen. Petrographie und Phasenpetrologie. Teil III. *Zeitschrift der Deutschen Gemmologischen Gesellschaft*, Vol. 39, No. 2/3, pp. 121–145.

Jobbins E.A. (1992) A taste of new gem deposits in South East Asia. *Gems and Jewellery News*, Vol. 2, No. 1, p. 12.

Kammerling R.C., Scarratt K., Bosshart G., Jobbins E.A., Kane R.E., Gübelin E.J., Levinson A.A. (1994) Myanmar and its gems—An update. *Journal of Gemmology*, Vol. 24, No. 1, pp. 3–40.

Kane R.E. (1984) Natural rubies with glass-filled cavities. *Gems & Gemology*, Vol. 20, No. 4, pp. 187–199.

Kane R.E., Kammerling R.C. (1992) Status of ruby and sapphire mining in the Mogok stone tract. *Gems & Gemology*, Vol. 28, No. 3, pp. 152–174.

Kane R.E., McClure S.F., Kammerling R.C., Nguyen Dang Khoa, Mora C., Repetto S., Nguyen Duc Khai, Koivula J.I. (1991): Rubies and fancy sapphires from Vietnam. *Gems & Gemology*, Vol. 27, No. 3, pp. 136–155.

Keller P.C. (1983) The rubies of Burma: A review of the Mogok stone tract. *Gems & Gemology*, Vol. 19, No. 4, pp. 209–219.

Kiefert L., Schmetzer K. (1991) The microscopic determination of structural properties for the characterization of optical uniaxial natural and synthetic gemstones, part 1: General considerations and description of the methods. *Journal of Gemmology*, Vol. 22, No. 6, pp. 344–354.

Koivula J.I., Kammerling R.C., Fritsch E. (1993a) Gem news: Update on ruby enhancement. *Gems & Gemology*, Vol. 29, No. 3, pp. 214–215.

Koivula J.I., Kammerling R.C., Fritsch E. (1993b) Gem news: Update on Monghsu ruby. *Gems & Gemology*, Vol. 29, No. 4, pp. 286–287.

Laughter T.L. (1993a) Mong Hsu mix-up. *JewelSiam*, Vol. 4, No. 5, pp. 34–37.

Laughter T.L. (1993b) How do you do? I am from Mong Hsu. *JewelSiam*, Vol. 4, No. 5, pp. 38–41.

Milisenda C.C., Henn U. (1994) Neues Rubinvorkommen in Myanmar (Burma). *Goldschmiede und Uhrmacher Zeitung*, Vol. 92, No. 4, pp. 147–148.

Moon A.R., Phillips M.R. (1994) Defect clustering and color in Fe,Ti:alpha-Al_2O_3. *Journal of the American Ceramic Society*, Vol. 77, No. 2, pp. 356–367.

Muhlmeister S., Devouard B. (1991) Determining the natural or synthetic origin of rubies using energy-dispersive X-ray fluorescence (EDXRF). In A.S. Keller, Ed., *Proceedings of the International Gemological Symposium 1991*, Gemological Institute of America, Santa Monica, CA, pp. 139–140.

Peretti A. (1993) Foreign substances in Mong Hsu rubies. *JewelSiam*, Vol. 4, No. 5, p. 42.

Peretti A., Smith C.P. (1993) A new type of synthetic ruby on the market: offered as hydrothermal rubies from Novosibirsk. *Australian Gemmologist*, Vol. 18, No. 5, pp. 149–157.

Peretti A., Smith C.P. (1994) Letter to the editor. *Journal of Gemmology*, Vol. 24, No. 1, pp. 61–63.

Peretti A., Mouawad F. (1994) Fluorite inclusions in Mong Hsu ruby. *JewelSiam*, Vol. 5, No. 4, pp. 136–137.

Potnau J., Adde R. (1976) Crystalline field parameters of Cr^{2+} and Cr^{4+} in corundum. *Journal de Physique*, Vol. 37, pp. 603–610.

Prieto A.C., Dubessy J., Cathelineau M. (1991) Structure-composition relationships in trioctahedral chlorites: A vibrational spectroscopy study. *Clays and Clay Minerals*, Vol. 39, No. 5, pp. 531–539.

Rains wash out Mong Hsu supply (1994). *JewelSiam*, Vol. 5, No. 5, p. 78.

Scarratt K., Harding R.R. (1984) Glass infilling of cavities in natural ruby. *Journal of Gemmology*, Vol. 19, No. 4, pp. 293–297.

Scarratt K., Harding R.R., Din V.K. (1986) Glass fillings in sapphire. *Journal of Gemmology*, Vol. 20, No. 4, pp. 203–207.

Schmetzer K. (1986a) An improved sample holder and its use in the distinction of natural and synthetic ruby as well as natural and synthetic amethyst. *Journal of Gemmology*, Vol. 20, No. 1, pp. 20–33.

Schmetzer K. (1986b) *Natürliche und synthetische Rubine— Eigenschaften und Bestimmung.* Stuttgart, Schweizerbart.

Schmetzer K., Bank H. (1980) Explanations of the absorption spectra of natural and synthetic Fe- and Ti-containing corundums. *Neues Jahrbuch für Mineralogie Abhandlungen*, Vol. 139, No. 2, pp. 216–225.

Schmetzer K., Bank H. (1981) The color of natural corundum. *Neues Jahrbuch für Mineralogie Monatshefte*, Vol. 1981, No. 2, pp. 59–68.

Smith C.P. (1995) A contribution to understanding the infrared spectra of Mong Hsu rubies. *Journal of Gemmology*, Vol. 24, No. 5, pp. 321–335.

Smith C.P., Surdez N. (1994) The Mong Hsu ruby: a new type of Burmese ruby. *JewelSiam*, Vol. 4, No. 6, pp. 82–98.

Special report: Mong Hsu ruby fact sheet (1993). *JewelSiam*, Vol. 4, No. 5, p. 33.

Tang S.M., Tang S.H., Tang, T.S., Retty A.T. (1988) Analysis of Burmese and Thai rubies by PIXE. *Applied Spectroscopy*, Vol. 42, No. 1, pp. 44–48.

Tang S.M., Tang S.H., Mok K.F., Retty A.T., Tay T.S. (1989) A study of natural and synthetic rubies by PIXE. *Applied Spectroscopy*, Vol. 43, No. 2, pp. 219–223.

Volynets F.K., Sidorova E.A., Stsepuro N.A. (1974) OH groups in corundum crystals which were grown with the Verneille technique. *Journal of Applied Spectroscopy*, Vol. 17, pp. 1626–1628.

Volynets F.K., Vorob'ev V.G., Sidorova E.A. (1972) Infrared absorption bands in corundum crystals. *Journal of Applied Spectroscopy*, Vol. 10, pp. 665–667.

Spring 1987
"Modern" Jewelry: Retro to Abstract
Infrared Spectroscopy in Gem Identification
A Study of the General Electric Synthetic Jadeite
Iridescent Orthoamphibole from Greenland

Summer 1987
Gemstone Durability: Design to Display
Wessels Mine Sugilite
Three Notable Fancy-Color Diamonds
The Separation of Natural from Synthetic
Emeralds by Infrared Spectroscopy
The Rutilated Topaz Misnomer

Fall 1987
An Update on Color in Gems. Part I
The Lennix Synthetic Emerald
Kyocera Corp. Products that Show Play-of-Color
Man-Made Jewelry Malachite
Inamori Synthetic Cat's-Eye Alexandrite

Winter 1987
The De Beers Gem-Quality Synthetic Diamonds
Queen Conch "Pearls"
The Seven Types of Yellow Sapphire and Their
Stability to Light

Summer 1988
The Diamond Deposits of Kalimantan, Borneo
An Update on Color in Gems. Part 3
Pastel Pyropes
Three-Phase Inclusions in Sapphires from Sri Lanka

Fall 1988
An Economic Review of Diamonds
The Sapphires of Penglai, Hainan Island, China
Iridescent Orthoamphibole from Wyoming
Detection of Treatment in Two Green Diamonds

Winter 1988
Gemstone Irradiation and Radioactivity
Amethyst from Brazil
Opal from Opal Butte, Oregon
Kyocera's Synthetic Star Ruby

Spring 1989
The Sinkankas Library
The Gujar Killi Emerald Deposit
Beryl Gem Nodules from the Bananal Mine
"Opalite:" Plastic Imitation Opal

Summer 1989
Filled Diamonds
Synthetic Diamond Thin Films
Grading the Hope Diamond
Diamonds with Color-Zoned Pavilions

Fall 1989
Polynesian Black Pearls
The Capoeirana Emerald Deposit
Brazil-Twinned Synthetic Quartz
Thermal Alteration of Inclusions in Rutilated Topaz
Chicken-Blood Stone from China

Winter 1989
Emerald and Gold Treasures of the Atocha
Zircon from the Harts Range, Australia
Blue Pectolite
Reflectance Infrared Spectroscopy in Gemology
Mildly Radioactive Rhinestones

Spring 1990
Gem Localities of the 1980s
Gemstone Enhancement and Its Detection
Synthetic Gem Materials of the 1980s
New Technologies of the 80s

Winter 1990
The Dresden Green Diamond
Identification of Kashmir Sapphires
A Suite of Black Diamond Jewelry
Emeraldolite

Spring 1991
Age, Origin, and Emplacement of Diamonds
Emeralds of Panjshir Valley, Afghanistan

Summer 1991
Fracture Filling of Emeralds: Opticon and "Oils"
Emeralds from the Ural Mountains, USSR
Treated Andamooka Matrix Opal

Fall 1991
Rubies and Fancy Sapphires from Vietnam
New Rubies from Morogoro, Tanzania
Bohemian Garnet—Today

Winter 1991
Marine Mining of Diamonds off Southern Africa
Sunstone Labradorite from the Ponderosa Mine
Nontraditional Gemstone Cutting
Nontransparent "CZ" from Russia

Spring 1992
Gem-Quality Green Zoisite
Kilbourne Hole Peridot
Fluid Inclusion Study of Querétaro Opal
Natural-Color Nonconductive Gray-to-Blue Diamonds
Peridot as an Interplanetary Gemstone

Summer 1992
Gem Wealth of Tanzania
Gamma-Ray Spectroscopy and Radioactivity
Dyed Natural Corundum as a Ruby Imitation
An Update on Sumitomo Synthetic Diamonds

Fall 1992
Ruby and Sapphire Mining in Mogok
Bleached and Polymer-Impregnated Jadeite
Radiation-Induced Yellow-Green in Garnet

Winter 1992
Determining the Gold Content of Jewelry Metals
Diamond Sources and Production
Sapphires from Changle, China

Spring 1993
Queensland Boulder Opal
Update on Diffusion-Treated Corundum:
Red and Other Colors
A New Gem Beryl Locality: Luumäki, Finland
De Beers Near Colorless-to-Blue Experimental
Gem-Quality Synthetic Diamonds

Summer 1993
Flux-Grown Synthetic Red and Blue Spinels
from Russia
Emeralds and Green Beryls of Upper Egypt
Reactor-Irradiated Green Topaz

Fall 1993
Jewels of the Edwardians
A Guide Map to the Gem Deposits of Sri Lanka
Two Treated-Color Synthetic Red Diamonds
Two Near-Colorless General Electric Type IIa
Synthetic Diamond Crystals

Winter 1993
Russian Gem-Quality Synthetic Yellow Diamonds
Heat Treating Rock Creek (Montana) Sapphires
Garnets from Altay, China

Spring 1994
The Anahí Ametrine Mine, Bolivia
Indaia Sapphire Deposits of Minas Gerais, Brazil
Flux-Induced Fingerprints in Synthetic Ruby

Summer 1994
Synthetic Rubies by Douros
Emeralds from the Mananjary Region,
Madagascar: Internal Features
Synthetic Forsterite and Synthetic Peridot
Update on Mining Rubies and Fancy Sapphires in
Northern Vietnam

Fall 1994
Filled Diamonds: Identification and Durability
Inclusions of Native Copper and Tenorite in
Cuprian-Elbaite Tourmaline, Paraíba, Brazil

Winter 1994
Color Grading of Colored Diamonds in the GIA
Gem Trade Laboratory
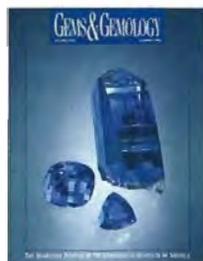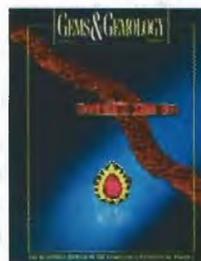Ruby and Sapphire from the Ural Mountains, Russia
Gem Corundum in Alkali Basalt

Some issues from the 1984–1986
volume years are also available. Please call the
Subscriptions Office for details.

ORDER NOW!

THE YOGO SAPPHIRE DEPOSIT

By Keith A. Mychaluk

Yogo Gulch, discovered more than 100 years ago, is one of four major sapphire-producing areas in Montana, United States. Yogo sapphires are known for their uniform, well-saturated blue color; relative absence of inclusions and zonation; and high luster and brilliance in both artificial and natural light; they do not require heat treatment. Rough crystals, usually flat with low cutting retention, generally weigh less than one carat (but have been reported up to 19 ct). Unlike the other Montana deposits, which are secondary, Yogo sapphires are mined directly from a lamprophyre host rock. There are at least six known dikes, five sapphire-bearing, at Yogo. From 1895 to 1994, the Yogo deposit produced an estimated 18.2 million carats of rough that are believed to have yielded more than 500,000 carats of cut stones. Considerable reserves remain.

*T*he state of Montana, in the western United States, hosts several large and economically important sapphire deposits. The four major deposits—at Yogo Gulch, Missouri River, Rock Creek, and Dry Cottonwood Creek—were all discovered in the late 1800s by gold prospectors. Three of the deposits are large secondary (placer) occurrences for which the original source rocks have not been conclusively identified. At Yogo Gulch (henceforth referred to as Yogo), however, the sapphires are found *in situ* in a lamprophyre dike system, with only minor related placer deposits. Yogo is one of the few major sapphire mines worldwide where sapphires are extracted directly from their host rock.

Not only are Yogo sapphires unique among Montana sapphires in terms of deposit type, but they also exhibit distinctive gemological features. The vast majority of Yogo sapphires are naturally the same uniformly saturated blue (figure 1), whereas sapphires from the placer deposits of western Montana are predominantly pale green, blue, or yellow before heat treatment. The relative absence of inclusions, fractures, and color zoning also distinguishes Yogo sapphires from other Montana sapphires.

Unlike sapphire-producing areas elsewhere in the state, which have received little geologic investigation since the significant contribution made by Clabaugh (1952), Yogo Gulch has been studied since the late 1970s by various geologists (see, e.g., Meyer and Mitchell, 1988; Brownlow and Komorowski, 1988; Dahy, 1988, 1991; and Baker, 1994).

The author was the first geologist to study the Vortex mine, an extension of the Yogo sapphire deposit developed in 1987 (Mychaluk, 1992). Between 1990 and 1992, the author collected and studied 200 rock and 100 rough sapphire samples from the Vortex mine and tailings from the nearby English and American mines. Representative samples of various rock types, and the minerals separated from them, were examined by thin-section microscopy and X-ray diffraction analysis. The author also analyzed core-drilling logs and samples from drill holes made by Vortex Mining Company in 1993. Further, the author visited the Vortex mine many times between 1990 and 1995, and was the first

Figure 1. The sapphires from the historic deposit at Yogo Gulch, Montana, are noted for their deep, uniform color and their brilliance when cut. Unlike most sapphires on the market today, they are not heat treated. Typically, though, they are small (the rough averages less than 1 ct). The loose Yogo sapphires illustrated here weigh 0.93—1.34 ct; they and the pin set with Yogo sapphires are courtesy of Mac Mader and American Gem Corp. The Yogo sapphire in the ring weighs 1.04 ct; it is courtesy of Robert E. Kane. Photo © Harold & Erica Van Pelt.

geologist to view the lowest workings of the 61-m-deep mine in 1994 .

This article reviews the history of the sapphire deposit at Yogo Gulch and the distinctive gemological properties of the sapphires. The geology and occurrence of the sapphires is discussed, including examination of various theories as to how they were formed and emplaced. Attention is also given to historical production and ore-grade variability of the entire Yogo deposit.

LOCATION AND ACCESS

The Yogo Gulch sapphire deposit is located about 25 km (15 miles) southwest of Utica, Montana, in Judith Basin County (figure 2). The deposit lies within the legal land description of T.13.N, R.11.E, sections 20 through 24, on the northeastern flanks of the Little Belt Mountains; it is about 33 km (20 miles) from the historic lead-zinc-silver mining camps of Neihart and Hughesville. The mine is accessible all year by U.S. Forest Service gravel roads leading south from Utica. Utica itself is located on Montana Route 239, approximately 28 km (17 miles) southeast of Stanford, the county seat, and roughly 125 km (78 miles) southeast of Great Falls.

The eastern portion of the deposit is located in grass-covered rolling hills, whereas the western portion is situated in rugged and heavily forested terrain. Yogo Creek, in Yogo Gulch, flows across the deposit in the west and has carved a canyon through ancient limestone formations. Yogo Creek is a tributary of the Judith River, which in turn flows into the Missouri River.

Figure 2. This map of Montana shows the locations of the state's four major sapphire-producing localities: (1) Yogo Gulch, (2) Missouri River (Eldorado, Spokane, French, Gruell's, Cheyenne, Dana's, and American bars), (3) Rock Creek, (4) Dry Cottonwood Creek. Modified from Zeihen, 1987.

HISTORY OF MINING AT YOGO GULCH

Sapphires were first discovered in Montana—in the Missouri River near Helena—on May 5, 1865, by Ed Collins. Gold prospectors later found sapphires in Dry Cottonwood Creek north of Butte in 1889, and in Rock Creek near Philipsburg in 1892 (Clabaugh, 1952; again, see figure 2). In general, the sapphires from these three deposits proved to be of low-saturated colors; natural, deep blue stones were rare. However, the last significant sapphire discovery in Montana, at Yogo Gulch in 1895, yielded superb blue stones. The history and general geology of Yogo are discussed in detail by Clabaugh (1952) and Voynick (1987a). Except as noted, the author has drawn the following account from these two authors.

Placer gold was discovered by prospectors in the upper end of Yogo Creek in 1866, but the area was not given serious attention until 1878. Several more years passed before, in 1895 gold prospector Jake Hoover began to collect the translucent blue stones that were being trapped in his sluices in lower Yogo Creek. He sent samples to an assay office, which then forwarded them to Dr. George F. Kunz, at Tiffany & Co. in New York City (Clabaugh, 1952). The stones were identified as sapphires of unusual quality, and Kunz sent Hoover and his partners a check in the amount of $3,750 (about twice what his gold operation had paid). This figure was based on the current London prices paid for rough sapphires from Southeast Asia: $6 per

carat for first-quality stones, $1.25 per carat for second quality, and $0.25 per carat for everything else (Voynick, 1987a). Tiffany & Co. eventually became an important buyer of Yogo sapphires and manufactured some important pieces of reportedly Yogo sapphire jewelry, including the famous Iris Brooch (figure 3).

In 1896, Jim Ettien, a local sheep herder, discovered several hundred carats of sapphires around badger and gopher burrows aligned along a linear depression that marked the surface exposure of an igneous dike (now called the "A" dike; see figure 4) on the flatlands above Yogo Creek (Weed, 1899). He staked the first claims to the dike that year. Soon others, notably John Burke and Pat Sweeney, staked more claims to the dike. By 1897, Hoover and his partners had bought out Ettien's claims and formed the New Mine Sapphire Syndicate.

In 1898, London gem merchants Johnson, Walker and Tolhurst Ltd., acquired the majority interest in the New Mine Sapphire Syndicate and began an intensive mining and marketing effort. They initially concentrated on removing sapphire-bearing ore from surface outcrops of the middle section of the A dike by means of hydraulic mining; this area is now referred to as the English Cut (figure 5). By 1902, the syndicate had two underground operations, the English (or British) mine and the Middle mine, working the dike.

The American Sapphire Company of New York began operations on the western third of the A dike

by purchasing Burke and Sweeney's claims in 1904; it opened the American mine—also underground—in 1905 (Clabaugh, 1952). In 1909, its capital exhausted, the firm reorganized as the Yogo American Sapphire Company. The New Mine Sapphire Syndicate acquired Yogo American in 1914. Although the syndicate never reopened the American mine, they recovered the $80,000 purchase price under the supervision of the company's renowned mine manager, Englishman Charles Gadsden, by reworking the mine's tailings.

The New Mine Sapphire Syndicate continued underground mining at the English and Middle mines until 1923, when a severe storm destroyed equipment and infrastructure alike. The operation continued by processing stockpiled ore until 1929, when economic factors (including the loss of the market for industrial-quality corundum to synthetics, and taxation by both the U.S. and British governments) finally forced it to close. After more than 25 years of inactivity, the New Mine Sapphire Syndicate sold the property to American interests in 1955. Total production from 1895 to 1929 amounted to 16 million carats of sapphires, of which about 2.25 million carats were gem quality—with an estimated value between $20 million and $30 million (in 1952 dollars; Clabaugh, 1952).

Various groups attempted to reopen Yogo between 1955 and 1968, but met with little success; the geology of the deposit was not well understood, mining costs were high, and marketing was limited. In 1968, Sapphire Village Inc. purchased the property. The firm raised capital by subdividing agricultural land near the mine and selling the residential lots with the right to dig limited quantities of sapphire-bearing ore from the eastern portion of the A dike (Voynick, 1987a). In 1972, Chikara Kunisaki bought out the other shareholders of Sapphire Village and formed Sapphire International Corp. The Kunisaki Tunnel, which reportedly cost $5 million to construct, was driven eastward into the A dike at the old American mine site. The operation proved uneconomic and in 1978 was leased to a new venture, Sapphire-Yogo Mines. Full-scale mining never materialized, and the property was returned to Sapphire International the following year (Voynick, 1987a).

Colorado-based Intergem Inc. leased the property from Sapphire International from 1980 to 1986. Intergem's mining effort focused on the eastern portion of the A dike, now known as the Intergem Cut (figure 4; Dahy, 1988). Intergem also expanded into jewelry manufacturing and made a serious attempt

Figure 3. One of the most famous pieces of Yogo sapphire jewelry is this "Iris Brooch," a corsage ornament containing 120 Yogo sapphires (as well as diamonds, demantoid garnets, and topaz) that was manufactured by Tiffany & Co. at the turn of the century. Photo courtesy of the Walters Art Gallery, Baltimore, Maryland.

to reestablish Yogo sapphires in the U.S. market. As a result of an aggressive promotional campaign, which guaranteed that their sapphires were not heat treated, Intergem sold 4,000 carats of cut sapphires and $3 million of finished jewelry in 1984 (Voynick, 1987a). However, higher taxes, greater regulation by the state government, and persistent financial problems forced Intergem into insolvency in 1986 (Voynick, 1987a). Ownership of the property again returned to Sapphire International, now called Roncor, in 1987.

Since 1987, Roncor has been reworking tailings and unprocessed ore left over from the Intergem era. Roncor, like Intergem, is vertically integrated: It not only mines Yogo sapphires, but it also manufactures jewelry. It, too, guarantees that the sapphires are not heat treated. In 1993, Roncor signed a two-year, $2 million agreement with AMAX Inc. (now Cyprus-AMAX Inc.) to help evaluate the potential of the Yogo deposit (Verbin, 1993). Cyprus-AMAX has since removed an 8,000-ton bulk sample from two inclines driven into the A dike—one at the Middle mine and the other along the Intergem Cut (L. Perry, pers. comm., 1995). The
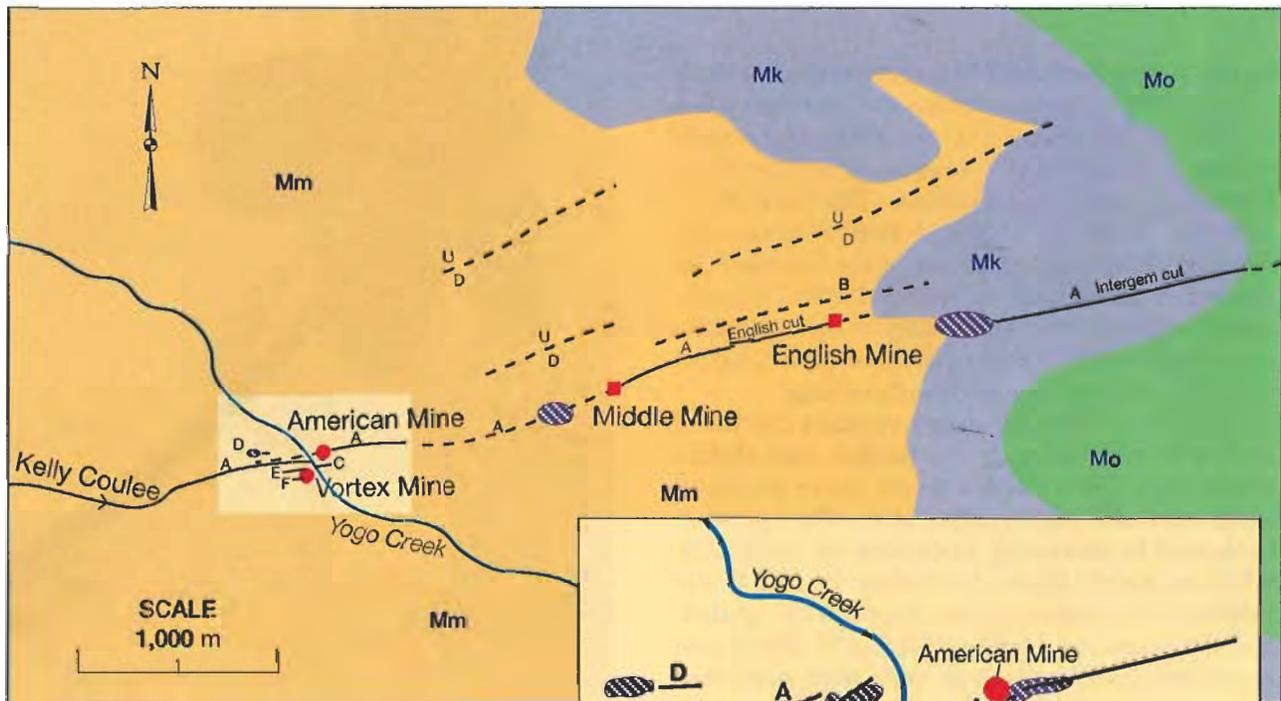
Figure 4. The Yogo sapphire deposit consists of at least six subparallel lamprophyre dikes, labeled by the author as "A", "B", "C", etc. All but the "B" (commonly called the "barren" dike) are known to be sapphire bearing. The vast majority of sapphire production at Yogo has been derived from the main A dike; it is this dike that is commonly referred to when the Yogo sapphire deposit is discussed. The inset provides detail on the area that is currently active. The dike system has intruded into limestone of the Mission Canyon formation (Mm) and shales of the younger Kibbey (Mk) and Otter (Mo) formations, probably along a pre-existing fault or fracture. Dahy (1988) mapped several faults paralleling the dike system to both the north and south (where upthrown side = U and downthrown side = D). Map modified from Dahy (1991).
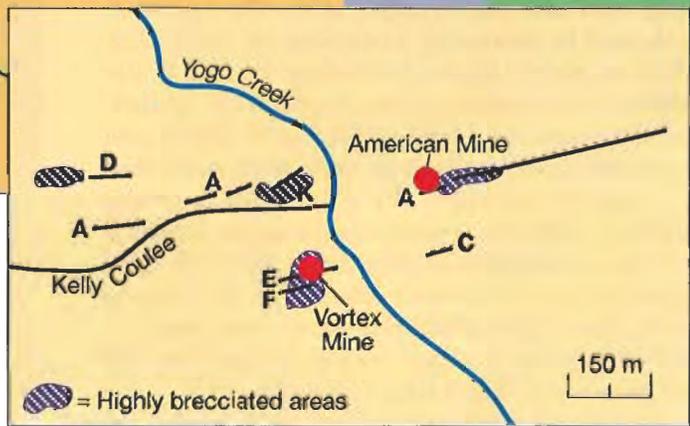
sample was partially processed during the summer of 1994 at Roncor's on-site plant (P. Ecker, pers. comm., 1994), but the results are confidential. Cyprus-AMAX was unable to negotiate a new lease arrangement with Roncor; their lease expired on January 31, 1995. (P. Ecker, pers. comm., 1995).

Figure 5. The sapphire-bearing A dike, which has produced the bulk of Yogo sapphires, averages 2.4 m wide and has a known length of 5 km (not continuous). The upper portions have weathered to a soft clay-like material. The A-dike section shown here was hydraulically mined by the British New Mine Sapphire Syndicate at the turn of the century; it is now referred to as the English Cut. Photo by the author.

Figure 6. Yogo blue sapphires are known for their well-saturated color and brilliance when faceted. These three stones, which range from 0.50 to 1.69 ct, were cut from Vortex mine material. Courtesy of Vortex Mining Co.; photo © GIA and Tino Hammid.

Figure 7. A small portion of Yogo sapphires are violet to purple, like the 1.27-ct stone shown here with two blue Yogo counterparts (2.22 and 2.77 ct). Note that all three stones are rounded, without distinct crystal faces. This is typical of the Yogo rough. Courtesy of Vortex Mining Co.; photo © GIA and Tino Hammid.

The Vortex Mining Company was formed in 1984 by a group of local Utica, Montana, prospectors. Vortex's exploration effort resulted in significant discoveries on the west end of the deposit, including several new sapphire-bearing dikes and associated brecciation zones (Voynick, 1987a and b; Dahy, 1988, 1991; Mychaluk, 1992). The Vortex mine began operations in 1987, and it is currently the only active underground mine at Yogo. Vortex Mining is also involved in jewelry manufacturing as well as mining. Both Roncor and Vortex Mining continue to market Yogo sapphires as the world's only sapphire that is guaranteed not to be heat treated.

GEMOLOGICAL CHARACTERISTICS

Color. Yogo sapphires are famous for their uniform blue color, general absence of inclusions and zonation, as well as for their vivid luster and brilliance in both artificial and natural light (see, e.g., figures 1, 3, and 6). Approximately 97% of all Yogo sapphires are "cornflower blue" and 3% are various shades of violet or purple (D. Brown, pers. comm., 1995; figure 7). George F. Kunz used the term *cornflower blue* to describe the color of Yogo sapphires, referring to the common garden flower of that name (*Centaurea cyanus*). Stones with distinct red, pink, or green hues are extremely rare and are usually too small for faceting (M. Ridgeway, pers. comm., 1993). Hughes (1990) stated that Intergem recovered only two "true" rubies and 10 green sapphires from 300,000 carats of Yogo rough, none of which were suitable for faceting. New Mine Sapphire Syndicate mine manager Charles Gadsden found only three or four rubies between 1895 and 1929 (Clabaugh, 1952).

Because Yogo sapphires are typically a well-saturated, uniform blue—rather than pale or zoned—it has not been necessary to heat treat the stones for the commercial market (Voynick, 1987a; L. Perry, pers. comm., 1994). Hughes (1990, p. 305) stated, "More amazing than the color itself is the great consistency of color from one stone to the next. Virtually all are of the same even-blue hue." It is

Figure 8. Some Yogo sapphires show a distinct alexandrite effect, like the approximately 1-ct stone in the center of this photo. It changes from purple (similar to the stone on the right) in incandescent light to blue (similar to that of the stone on the left) in day or fluorescent light. Photo by John I. Koivula.

this blue color that has been likened to that of sapphires from Kashmir (Sinkankas, 1976), although other gemologists find that the color appearance of Yogo sapphires is very distinctive (R. E. Kane, pers. comm., 1993).

Dichroism in Yogo sapphires can be quite pronounced (Clabaugh, 1952; Allen, 1991): light green perpendicular to the c-axis, blue parallel to the c-axis. Some chromium-bearing Yogo sapphires exhibit an alexandrite effect, appearing blue in day or fluorescent light and red (Baker, 1994) or purple (figure 8; J. I. Koivula, pers. comm., 1995) under incandescent light.

Inclusions. Yogo sapphires also have few detracting inclusions (Zeihen, 1987; Brownlow and

Figure 9. Although most Yogo sapphires are relatively clean, inclusions of analcime have been seen in many stones. Photomicrograph by John I. Koivula; magnified 40×
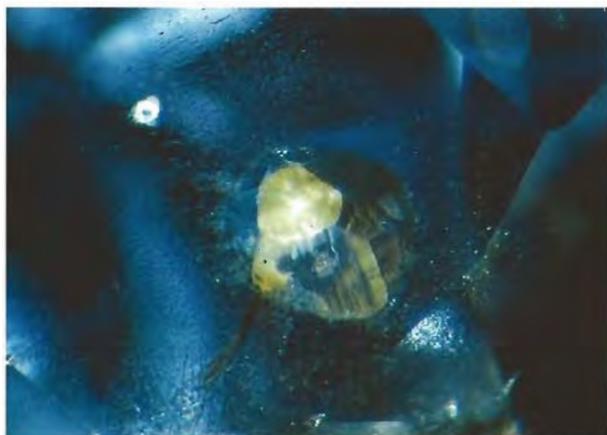
Komorowski, 1988; Hughes, 1990). Gübelin and Koivula (1986) did note small inclusions of pyrite, dark mica, calcite, analcime (figure 9), and rutile (figure 10). Dunn (1976) also identified inclusions of spinel. Gübelin and Koivula (1986) reported that many Yogo inclusions appear similar to those found in Thai rubies, a conclusion later supported by Hughes (1990).

Crystal Shape and Size. Dominant crystal forms are short rhombohedral prisms terminated by the basal pinacoid (Clabaugh, 1952; Hughes, 1990; DelRe, 1994), although Yogo sapphires typically show little evidence of their original crystal shapes (again, see figures 7 and 8). Most of the stones recovered are rounded (figure 11), chipped, abraded, pitted, or broken into shards and wafers. The apparent modification of the original crystal shapes has been explained by partial dissolution (resorption) by the host magma (Clabaugh, 1952; Dahy, 1988), mechanical abrasion during dike emplacement and brecciation (Mychaluk, 1992), and to some extent by mining and recovery methods (e.g., blasting and crushing of the ore). It should be noted, though, that most Yogo sapphires also have "flat" shapes, as indicated by the crystal faces that can still be seen. Intergem consulting geologist Delmer Brown (pers. comm., 1995) has hypothesized that, because the specific gravity of the sapphires is greater than that of the host rock, only crystals of this shape (i.e., lower mass) wafted to the top; possibly, mining deeper in the dike will reveal more euhedral and fewer flat crystals. Chemical reactions between the sapphires and iron in the magma have also created dark green hercynite ($FeAl_2O_4$) reaction rims around some of the sapphires (Clabaugh, 1952).

Figure 10. Another inclusion seen in some Yogo sapphires is rutile. Photomicrograph by John I. Koivula; magnified 30×
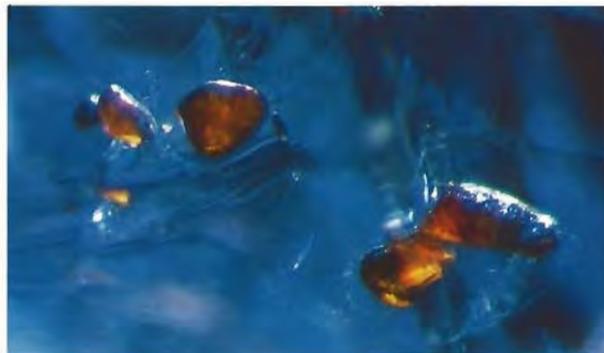
Figure 11. Rough Yogo sapphire crystals often appear rounded, broken, or flattened. The Vortex mine specimen shown here is a classic example of a Yogo sapphire that was chemically rounded (actually, partially resorbed) during transportation in the host magma. The faceting-quality sapphire measures 5 mm long × 2 mm deep. Photo by Maha DeMaggio.

Most rough Yogo sapphires weigh less than one carat, although stones up to 19 ct have been found. Clabaugh's list of some larger rough Yogo sapphires included individual stones weighing 10 and 12 ct. Nevertheless, Hughes (1990) stated that only 10% of the rough stones recovered from Yogo exceed one carat.

The flat shapes of most of the Yogo crystals recovered thus far is a major drawback for gem cutters. Cutting retention for a standard brilliant cut averages 20%. The largest rough Yogo sapphire, 19 ct (found in 1910), was reportedly cut into four stones, one of which weighed 8.5 carats (Clabaugh, 1952). According to Voynick (1987a), the largest known cut Yogo sapphire weighs 10.2 carats and is presently in the collection of the Smithsonian Institution. However, some gemologists feel—because of its inclusions—that the source of this stone has been wrongly identified. It has exsolution needles of rutile in a hexagonal zoned pattern, and large liquid-and-gas CO_2 fluid inclusions, both of which are not found in Yogo sapphires (J. I. Koivula, pers. comm., 1995).

GEOLOGY
Overview. The Yogo Gulch deposit has traditionally been described, for simplicity, as a single sapphire-bearing igneous dike (Clabaugh, 1952; Meyer and Mitchell, 1988; Dahy, 1988; Brownlow and Komorowski, 1988). However, the deposit actually consists of a complex set of subparallel lamprophyre dikes (a lamprophyre is a group of dark, porphyritic igneous rocks that usually contain phenocrysts of dark mica, pyroxene, or olivine in a fine-grained, crystalline groundmass and associated breccia zones. It appears that the emplacement of these dikes has been influenced by faulting and the development of karst in the host limestone (karst is a type of topography formed on or within limestone by dissolution; it is characterized by sinkholes, caves, and underground drainage). Six of the dikes, labeled "A" through "F" for the purpose of this article, are shown in figure 4 and discussed below.

Main (A) Dike. The A dike has produced the bulk of Yogo sapphires to date. Hence, before the author's research, it is the only dike that was studied in any detail. The A dike is about 5 km long and <1 to 6 m (average 2.4 m) wide (Clabaugh, 1952). The dike has intruded limestone (Mission Canyon formation) and shales (Kibbey and Otter formations), probably along a pre-existing fault or fracture. Only very limited contact-metamorphic effects are seen in the host rocks, indicating relatively quick emplacement and cooling. According to Dahy (1991), the dike may be separated into three *en echelon* (overlapping or step-like) segments in a zone oriented S75°W; each segment has been significantly mined, both on the surface and underground. The three original underground mines at Yogo—the English, Middle, and American—are all located on the A dike. They have provided the vast majority of geologic and mineralogic data available to date on the Yogo deposit.

"Barren" (B) Dike. The B dike lies approximately 183 m to the north of the A dike and runs parallel to it for about 1.6 km. The apparent absence of sapphires in this dike has been explained by the fact that it is a mafic lamprophyre (specifically, a minette), whereas thus far sapphires have been found only in ultramafic lamprophyre (Dahy, 1988). Given the limited sampling that has taken place to date, though, further research is needed to verify this theory.

C Dike. Approximately 46 m south of the A dike, near the American mine, is the sapphire-bearing C dike (Dahy, 1988). Discovered at the same time as the A dike, the C dike was not developed because it
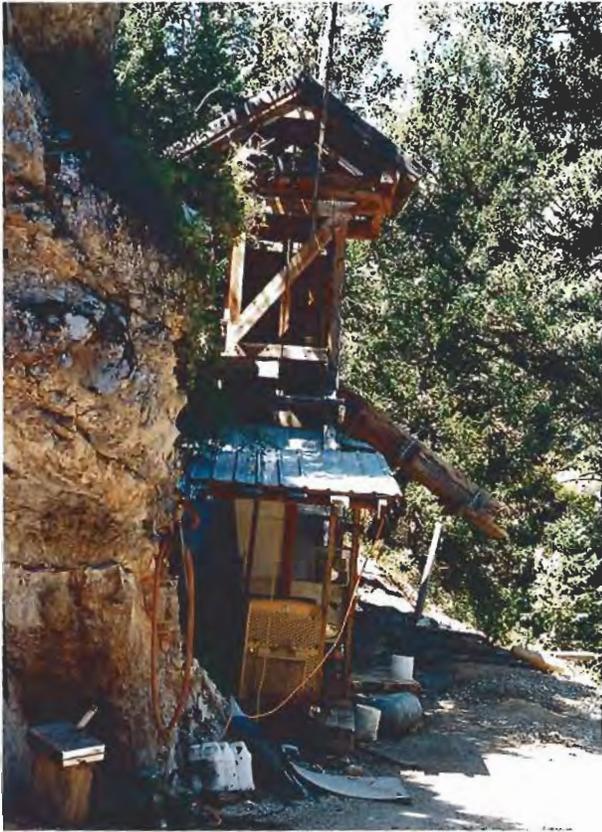
Figure 12. The Vortex mine was first discovered around 1924, when a group of miners, related to the old Yogo American Sapphire Company, sank several prospect pits into this cliff. Vortex Mining Co. began development of the long-abandoned site in 1987. The main shaft, pictured here, has now reached a depth of 61 m. Sapphires are being recovered from at least one dike. Photo by the author.

found it to be approximately 0.6–1.2 m wide and proved a length of 152 m (P. Ecker, pers. comm., 1994). Like the C dike, all D-dike material has been altered to yellowish clay minerals; no original, unweathered dike rock has been found. As of 1987, the largest rough stone recovered from the D dike was 6 ct, whereas the largest cut stone weighed 2.4 ct (Zeihen, 1987). Currently, there is no mining activity at this dike.

E Dike. Across Yogo Creek from the American mine is the new Vortex mine (figure 12). This thin, highly weathered dike was initially discovered from a set of prospect pits made in 1924. Vortex Mining began development in 1987 (L. Perry, pers. comm., 1994). Subsequent work determined that the dike within the Vortex mine is not an extension of the main A dike, but rather is a separate dike, labeled "E" here (again, see figure 4). In the upper levels of the Vortex mine, the E dike is only a few centimeters wide; but along the 30-m section of dike currently exposed by mining at the 61-m level, the dike is about 0.5 m wide, strikes S45°W, and is highly weathered to a reddish brown color. According to core drilling, unaltered dike material exists at a depth below 100 m (total proven depth is 110 m). Currently, all Vortex mine production is derived from the E dike and associated breccia zones.

F Dike. In 1993, core drilling by Vortex Mining revealed this new dike. Although underground tunneling has not yet reached the F dike, drilling indicates that it is approximately 1 m wide and strikes S60°W, on an intersect angle with the E dike to the southwest. Like the E dike, F has been proved to exist as deep as 110 m.

Secondary Deposits. Erosion of the dike system has created minor secondary sapphire deposits. Colluvial deposits on hillsides below the English mine and English Cut were quickly mined out at the turn of the century by the New Mine Sapphire Syndicate (Voynick, 1987a). In addition, Yogo Creek cuts through the A dike at the American mine, and has scattered sapphires as far as 4 km downstream. However, the sapphire-bearing gravels within Yogo Creek have never been commercially mined (L. Perry, pers. comm., 1994). Because the secondary occurrences are so limited, Intergem believed that the primary deposit had only recently been exposed by erosion (Voynick, 1987a).

is much thinner (15 cm) than the A dike (an average of 2.4 m wide). However, the American Sapphire Company recovered some sapphires from a small, 6-m-long, adit that was driven into it in 1902 (P. Ecker, pers. comm., 1994). There is no current production from this dike. Nor has any mineralogic or geologic description of the dike ever been published, although the author has observed that the dike material has been significantly altered by CO_2-rich ground water to yellow clay minerals.

D Dike. The D dike is located on the north rim of Kelly Coulee, at the west end of the Yogo deposit. Its orientation is slightly different—due east-west—from that of the other dikes described here (which are slightly inclined to the south; Voynick, 1987b). Vortex mined this dike in the mid-1980s. They

Figure 13. This photo clearly illustrates the effect weathering has had on Yogo sapphire-bearing rock. The greenish-gray sample of unweathered A-dike lamprophyre (from underground workings of the English mine) is composed of mica, pyroxene, analcime, and carbonates. The large circular feature is a carbonate-filled, pyroxene-rimmed vesicle; these vesicles were "bubbles" of an immiscible liquid within the Yogo magma. The reddish brown specimen is highly weathered material from the E dike within the Vortex mine; it consists of clays, carbonates, and some chlorite. After significant exposure to CO_2-rich ground water, the greenish-gray specimen would eventually look like the reddish sample. Because it is much easier to process weathered dike material, Yogo sapphire miners still (as they did 70 years ago) expose large piles of hard, unweathered Yogo dike ore to rain, snow, and frost to accelerate the decomposition process. Photo by Maha DeMaggio.

Mineralogy of the Dike Material. Mineralogic studies have shown that unweathered A-dike rock consists of phenocrysts of phlogopite and clinopyroxenes (augite) in a groundmass of analcime and various carbonates. Lesser amounts of titaniferous magnetite, ilmenite, apatite, zeolites, spinel, serpentine, and chlorite are also present, as are accessory sapphire, kyanite, garnet, and quartz (Clabaugh, 1952; Meyer and Mitchell, 1988; Brownlow and Komorowski, 1988; Dahy, 1988, 1991). For the most part, dike material from the Vortex mine has been altered to clay minerals by CO_2-rich surface and ground water. Analyses revealed that the weathered lamprophyre contained carbonates, clays

(montmorillonite and kaolinite; both identified by X-ray diffraction analysis), biotite, chlorite, magnetite, goethite/hematite pseudomorphs after pyrite, and minor apatite, quartz, pyroxene, rutile, and feldspar, as well as accessory sapphire and kyanite (Mychaluk, 1992). Meyer and Mitchell (1988) classified the unweathered rock as an ultramafic lamprophyre, variety ouachitite (figure 13). Lamprophyres, like kimberlites and lamproites, are thought to have been generated at great depths. Accordingly, Dahy (1991) believed that the Yogo magma formed at 125 km depth (i.e., in the upper mantle), but the lamprophyre did not begin to crystallize until it approached the Earth's surface (Meyer and Mitchell, 1988).

Although field evidence only indicates an age younger than about 320 million years (My), the dike system itself is generally assumed to be approximately 50 My old and is a member of the central Montana alkaline igneous province (Meyer and Mitchell, 1988; Brownlow and Komorowski, 1988). The geologic province hosts a suite of alkaline (typically Si deficient and high in Mg and K), upper-mantle-derived rocks. These include kimberlites, lamprophyres, lamproites, shonkonites, and carbonatites, which comprise several major igneous centers and mountain ranges in central Montana (Baker and Berg, 1991).

Ore-Grade Variability. Although Clabaugh (1952) stated that the grade of the A dike is 20–50 carats per ton (ct/t), more recent mining activity has shown that the grade is even more variable and sporadic. In fact, within the Vortex mine alone the grade may range from zero to as high as 70 carats per ton (Mychaluk, 1992). Dahy (1988) believed that multiple episodes of magma intrusion occurred along the A dike, producing a dilution effect whereby sapphire-bearing dike rock is diluted with sapphire-barren dike rock. Evidence included brecciated (broken and re-formed) samples of A-dike rock that contain two mineralogically distinct lamprophyres, one having brecciated and incorporated fragments of the first. Textural and mineralogically distinct samples of lamprophyre are common in the A dike.

Furthermore, the development of karst may have influenced Yogo ore grade. Work by Dahy (1988) led to the conclusion that karst features were present prior to the emplacement of the dike system and that karst continued to develop after dike emplacement. Sinkholes and small natural caves are common in and around the current mine work-

ings. Brecciated rock within these karst features may or may not contain sapphires, depending on a complex set of conditions, including whether the breccia was formed before or after dike emplacement.

There are at least six main brecciated zones within the Yogo sapphire deposit; four are located along the A dike, including the Kelly breccia (the letter "K" in figure 4). Although sapphires have been mined from the Kelly breccia, underground workings within breccias of the American mine produced little or no sapphire (Voynick, 1987a). Breccias are also quite common within the Vortex mine, mainly between the E and F dikes. These breccias are sapphire-bearing, with grades as high as 5 ct/t. The sixth breccia zone occurs on the west end of the D dike, on the ridge overlooking Kelly Coulee. These breccias have never been exploited, so it is not known whether they contain sapphires. Originally, the Kelly and Vortex mine breccias were interpreted to be volcanic breccias related to diatreme activity (Dahy, 1988, 1991; Mychaluk, 1992), although Baker (1994) suggests that they may simply be karst features such as collapsed sinkholes.

ORIGIN OF THE YOGO SAPPHIRES

The origin of sapphires in the Yogo dike system has generated much discussion and debate over the past century. Many of the first geologists to study the deposit concluded that the sapphires must have been formed directly from the Yogo magma as phenocrysts (Pirsson, 1900). These early workers envisioned the silica-deficient Yogo magma incorporating large amounts of Al-rich shales as it rose toward the surface. The magma consumed the aluminum and subsequently crystallized corundum directly from it. Later researchers, notably Clabaugh (1952), suggested that the Yogo magma incorporated fragments of a kyanite-bearing gneiss, instead of shales. The kyanite, a source of aluminum, was then consumed by the magma and later crystallized as corundum. Baker (1994) agrees with this latter phenocryst model and argues that inclusions he observed within Yogo sapphires, such as CO_2 gas and analcime, could only have been formed directly from the Yogo magma.

However, it is also possible that the sapphires were incorporated as inclusions in the Yogo magma (i.e., are xenocrysts). A detailed model describing this theory is presented by Dahy (1988). He envisioned that metamorphic rocks (e.g., gneiss) below the Yogo area already contained corundum, as they do in other parts of Montana (Clabaugh, 1952). The

Yogo magma, as it rose toward the surface, captured fragments of the corundum-bearing gneiss and transported it upward as xenoliths. The corundum crystals were eventually released into the magma as foreign fragments (i.e., xenocrysts). Dahy further hypothesized that magmatic heat naturally "heat treated" the corundum into uniform blue, gem-quality sapphire. Much of the corundum was later resorbed into the magma as it rose to the surface, creating the spinel reaction rims seen around some sapphires and rounding, pitting, and etching others. Evidence to support this theory includes the discovery of a xenolith—containing corundum, feldspar, augite, and spinel—which Dahy (1988) interpreted as a metamorphosed clay or bauxite. Another possibility is that the sapphires crystallized in an earlier magma and were subsequently borne upward; they would still be called xenocrysts because they did not crystallize in the transporting magma. Meyer and Mitchell (1988) also presumed that Yogo sapphires were xenocrystic.

New evidence supporting the xenocrystic origin of the Yogo corundum crystals comes from thermodynamic modeling of the crystallization sequence of the Yogo magma, which is now represented by the rock ouachitite. Such models can be calculated today with computer programs that use thermodynamic data for multicomponent (SiO_2, Al_2O_3, FeO, and other chemical constituents) silicate liquids (magmas). Computer simulations of the crystallization of the Yogo magma by J. Nicholls, University of Calgary, using the program described by Ghiorso and Sack (1995) suggest that corundum could not have crystallized directly from the Yogo magma. There are, however, some caveats to the conclusions drawn to date; additional research is needed to resolve this question.

MINING AND PRODUCTION

Mining and Processing. Gem-quality Yogo sapphires are extracted directly from their host rock. CO_2-rich surface and ground water has weathered portions of the lamprophyric dike rock to a soft, friable material that disintegrates in water (owing to its content of montmorillonite and other clay minerals). Unweathered dike rock, on the other hand, is in a hard, competent state, so mining requires careful blasting. To extract the gems from the rock, early sapphire miners exposed both types of material to rain, snow, and frost on large wooden "weathering floors" (Clabaugh, 1952). Within six to 12 months, the dike rock would decompose, at which point the sapphires could be recovered by simple

Figure 14. At the Vortex mine processing plant, ore is loaded into the yellow hopper, which feeds into the large rotating trommel. Heavy chains in the trommel help break down sapphire-bearing ore, which is then fed into a jig behind the bulldozer. Final clean-up of the sluice tray in the jig is done by hand. Photo by the author.

gravity methods such as sluicing. Today, small processing plants with rotating trommels break down the sapphire-bearing ore and trap the sapphires in modified jigs and sluices that are usually used in placer gold recovery (figure 14). Both steam and dilute HCl acid have been used experimentally to decrease ore-processing time, although neither method has been fully implemented (P. Ecker, pers. comm., 1994). Large amounts of goethite/hematite (limonite) cubes are also recovered in the processing jigs. The cubes may be heated to change the limonite to a magnetic phase for easier removal from the jig concentrates, a technique used by the New Mine Sapphire Syndicate at the turn of the century (Voynick, 1987a). Final sorting of the concentrate for sapphires is done by hand.

Production. Most of the Yogo sapphires recovered to date have come from six locations in the deposit: English Cut, English mine, Middle mine, American mine, Intergem Cut, and Vortex mine. Initially, sapphires were extracted by the New Mine Sapphire Syndicate from surface exposures of the A dike—and the colluvial gravels weathered from them—by means of hydraulic mining. This initial mining (roughly 1895–1901) occurred mainly at the English Cut, where early miners had to construct a 15-km-long flume to bring in the water needed for processing. Clabaugh (1952) reported production figures ranging from 296,862 carats in 1898 to 777,550 carats in 1901.

The next phase of mining at Yogo, which was also by the New Mine Sapphire Syndicate, occurred underground at the English and Middle mines.

Between 1902 and 1929, 200,000 tons of ore were extracted from the English mine, with a grade of 20–50 carats of rough per ton (Clabaugh, 1952). At 8–15 m below the surface, the Middle mine connects with the English mine (figure 7 in Clabaugh, 1952); the English mine was worked to a maximum depth of 76 m. Neither mine has been commercially operated since 1929, although the old Middle mine workings were the site of a 1993 Cyprus-AMAX bulk sample (the results of which have not been made public).

Between 1901 and 1914, first the American Sapphire Co. and then the Yogo American Sapphire Co. extracted a total of 3 million carats of sapphire rough from the American mine, which was worked to a depth of 91 m. The mine was not operated again until the early 1970s: Between 1970 and 1973, Sapphire International Corp. produced 300,000 carats of rough, of which 15%—or 45,000 carats—was gem quality (Dahy, 1988). In 1974, a further 250,000 carats of rough was produced (Sinkankas, 1976). Therefore, a total of at least 3.55 million carats of rough have been recovered from the American mine.

The three underground mines and hydraulic operations on the English Cut produced an estimated 16 million carats of rough sapphires between 1895 and 1929, according to Clabaugh (1952), who compiled detailed production statistics for this period. Fourteen percent, or about 2.25 million carats, of these stones were gem quality.

Intergem undertook a large-scale strip-mining operation along the east end of the A dike (now referred to as the Intergem Cut). Between 1980 and

1986, Intergem produced an estimated one million carats of rough sapphires from this cut (Dahy, 1988). Because, as discussed above, the sapphire content can vary greatly from one part of a dike to another, ore grades ranging from 5 to 50 carats of rough per ton have been reported (Voynick, 1987a). Cyprus-AMAX also took a bulk sample from the Intergem Cut in 1993, but little other development work has occurred there since 1986.

Currently, the Vortex mine is the only fully operating underground mine at Yogo, albeit relatively small compared to past operations. As of January 1995, the mine was 61m deep with one 50-m-long tunnel at the 61-m level, three 91-m-long tunnels at the 18-m level, and one 12-m-long adit at ground level (L. Perry, pers. comm., 1995). Although first opened in 1987, the Vortex mine only recently began full-time ore extraction. Allen (1991) stated that the Vortex mine is capable of producing 400 carats of rough sapphires a day, of which half are suitable for cutting. The mine produced 5,000 and 12,000 carats, respectively, of gem-quality sapphires in 1992 and 1994. There was no 1993 production because of a core-drilling and mine-development program (L. Perry, pers. comm., 1995). As noted earlier, the ore grade at the Vortex mine also varies greatly, from 0 to 70 carats of rough per ton.

Roncor, the current owner of the English, Middle, and American mines and the English and Intergem Cuts, has not undertaken any underground or hydraulic mining. Rather, most of Roncor's production is derived from reprocessing old mine tailings and left-over ore from the Intergem era. With this technique, Roncor has produced a reported 30,000 to 50,000 carats of rough sapphires annually (Verbin, 1993).

Total production for the deposit's 100-year operating period has been estimated by the author, by updating Clabaugh's figures, to be approximately 18.2 million carats of rough sapphires, of which 14%—or about 2.55 million carats—were of gem quality. Assuming an average cutting retention of 20%, the Yogo deposit has probably produced 510,000 carats of cut sapphires.

The geology of the deposit indicates that the depth of the A dike is considerably greater than the 91 m reached thus far. Given that the specific gravity of the sapphires is higher than that of the host rock, there may be even more sapphires at lower levels. One can conclude, therefore, that the reserves are significant, perhaps twice what has already been recovered, although the cost of recovery may be prohibitive.

SUMMARY AND CONCLUSION

Over 100 years of intermittent operation, the Yogo sapphire deposit has produced an estimated 18.2 million carats of rough sapphires, of which about 2.55 million were gem quality. More than a half million carats of cut sapphires have entered the marketplace from this locality. Approximately 97% of these gems are "cornflower" blue, whereas 3% are various shades of violet; there is no commercial heat treatment of this material. Yogo sapphires also contain fewer inclusions and fractures than sapphires from most other localities, although only about 10% of rough Yogo sapphires exceed one carat—their main drawback as a gemstone. Cutting retention of these typically flat-shaped crystals average 20%, producing many stones in the 0.10- to 0.50-ct range. Marketing high-quality sapphires of this size has been difficult for past and present producers. Profitability is further hampered by the extra costs associated with underground mining and subsequent ore processing, which are not incurred with alluvial sapphire deposits.

Geologic investigations have revealed that the deposit consists of at least six subparallel ultramafic lamprophyre dikes—not just one as is popularly recorded. Sapphires have been discovered in all the dikes except the B, or "barren," dike. The deposit has been influenced by the development of karst and by pre-existing faults and fractures in the host limestone, as well as by multiple magma intrusions. There is great variability in grade within the dike: Some areas produce little or nothing, and others produce as much as 70 carats of rough sapphire per ton of ore.

There is considerable disagreement in the literature as to whether the sapphires originated in the magma (as phenocrysts) or were part of "foreign" rocks transported to the surface by the magma (xenocrysts). Recent thermodynamic computer modeling lends some support to the theory that the Yogo sapphire crystals were xenocrysts. However, the original source of the Yogo sapphires, if truly xenocrysts, remains a mystery.

Sapphire reserves at Yogo appear to be considerable. On the basis of reports in the literature and his experience, the author estimates that they probably—if not practicably—exceed twice what has already been produced. Because of greater activity by groups such as Vortex, Roncor, and Cyprus-AMAX, the author suspects that production will gradually increase during the next decade, yielding many more of the now-legendary Yogo sapphires.

REFERENCES

Allen R.M. (1991) The Yogo Sapphire Deposit—New discoveries create more interest in America's finest gemstone. *Gemological Digest*, Vol. 3, No. 2, pp. 9–16.

Baker D.W. (1994) Montana sapphires–The value of color. *Northwest Geology*, Vol. 23, pp. 61–75.

Baker D.W., Berg R.B., Eds. (1991) *Guidebook of the Central Montana Alkalic Province: Geology, Ore Deposits and Origin.* Montana Bureau of Mines and Geology special publication 100, Missoula, MT.

Brownlow A.H., Komorowski J.C. (1988) Geology and origin of the Yogo sapphire deposit, Montana. *Economic Geology*, Vol. 83, No. 4, pp. 875–880.

Clabaugh S.E. (1952) *Corundum Deposits of Montana.* United States Geological Survey Bulletin 983, USGS, Washington, DC.

Dahy J.P. (1988) *The Geology and Igneous Rocks of the Yogo Sapphire Deposit and the Surrounding Area, Little Belt Mountains, Judith Basin County Montana.* Montana College of Mineral Science and Technology, Butte, Montana, M.S. thesis.

Dahy J.P. (1991) Geology and igneous rocks of the Yogo sapphire deposit, Little Belt Mountains, Montana. In D.W. Bake and, R.B. Berg, Eds., *Guidebook of the Central Montana Alkalic Province: Geology, Ore Deposits and Origin.* Montana Bureau of Mines and Geology Special Publication 100, Missoula, MT, pp. 45–54.

DelRe N. (1994) Gem Trade Lab Notes: Sapphires from Yogo Gulch, Montana. *Gems & Gemology*, Vol. 30, No. 2, p. 120.

Dunn P. (1976) Gem notes. *Gems & Gemology*, Vol. 15, No. 7, p. 200.

Ghiorso M.S., Sack R.O. (1995) Chemical mass transfer in magmatic process IV. A revised and internally consistent thermodynamic model for the interpolation and extrapolation of liquid-solid equilibria in magmatic systems at elevated temperature and pressures. *Contributions to Mineralogy and Petrology*, Vol. 119, No. 2, pp. 197–212.

Gübelin E.J., Koivula J.I. (1986) *Photoatlas of Inclusions in Gemstones.* ABC Edition, Zurich, pp. 345–347.

Hughes R.W. (1990) *Corundum.* Butterworths Gem Books, London, pp. 301–307.

Meyer H.O.A., Mitchell R.H. (1988) Sapphire-bearing ultramafic lamprophyre from Yogo, Montana: A ouachitite. *Canadian Mineralogist*, Vol. 26, Part 1, pp. 81–88.

Mychaluk K.A. (1992) *Geology of the Vortex sapphire mine, Utica, Montana.* B.S. thesis, University of Calgary, Calgary, Alberta, Canada.

Pirsson L.V. (1900) A report on the petrography of the igneous rocks of the district. In W. H. Weed, Geology of the Little Belt Mountains, Montana, with notes on the mineral deposits of the Neihart, Barker, Yogo, and other districts. In *Extracts from the 20th Annual Report, United States Geological Survey, 1898-99, Part 3, Precious Metal Mining Districts*, USGS, Washington, DC. pp. 463–581.

Sinkankas J. (1976) *Gemstones of North America in Two Volumes: Volume 2.* Van Nostrand Reinhold, New York.

Verbin E. (1993) AMAX breaks ground for U.S. gems. *Colored Stone*, Vol. 6, No. 4, pp. 1, 19–22.

Voynick S.M. (1987a) *Yogo: The Great American Sapphire.* Mountain Press Publishing, Missoula, MT.

Voynick S.M. (1987b) New Yogo sapphires—A new section of the gem-laden dike is now being mined. *Rock & Gem*, August, pp. 25–29.

Weed W.H. (1899) *United States Geological Survey Atlas, Little Belt Mountains Folio No. 56*, USGS, Washington, DC.

Zeihen L.G. (1987) The sapphire deposits of Montana. In D.C. Lawson, Ed., *Directory of Montana Mining Enterprises for 1986*, Montana Bureau of Mines and Geology Bulletin 126, Great Falls, MT, pp.29–40.

MEERSCHAUM FROM ESKISEHIR PROVINCE, TURKEY

By Kadir Sariiz and Iskender Isik

This study presents a model for the origin of the Eskisehir, Turkey, sepiolite deposits. Known as "meerschaum" in the gem trade when it occurs as compact masses (especially nodules), sepiolite is mined by local farmers using basic implements and traditional tunneling methods. The best nodules are carved into objects such as pipe bowls, bracelets, and necklaces. The sepiolite nodules occur in the Pliocene-age Imisehir conglomerates, associated with dolomite, magnesite, opal-CT, and lizardite. Fibrous in morphology, they probably formed in relatively shallow water under alkaline conditions, as a result of the replacement of magnesite gravels that were subjected to pore waters with high SiO_2 concentrations.

Sepiolite, $Mg_4Si_6O_{15}(OH)_2 \cdot 6H_2O$, is a clay mineral that has many industrial uses. One of the earliest was soap, because the compact material has a greasy texture and lathers when first recovered. White, compact, massive sepiolite is called meerschaum (from the German *meer* [sea] and *schaum* [foam]); it has a very low specific gravity (dry, it can float on water) and low hardness. Because it is easily carved and polished, meerschaum historically

has been a popular ornamental gem material. It is best known as a carving material for pipe bowls (figure 1), but it has also been used for objects such as cameos and jewelry.

Although meerschaum may have been used as early as the days of the Roman Empire (Ball, 1950; Ece and Coban, 1994), its use as a carving material has been documented since the late 1600s, when it was mined for the manufacture of pipe bowls, cigarette holders, and building material from the sepiolite deposit in Vallecas, Spain (Galan and Castillo, 1984). At present, the Spanish sepiolite deposits, the largest in the world, are mined for industrial uses only; there are no recent reports of gem-quality (nodular) material from Spain. Relatively new occurrences of sepiolite, some of which contain material classified as meerschaum, have been reported in the United States (California, Nevada), Spain, Kenya, Japan, Russia, and China (Singer and Galan, 1984; Jones and Galan, 1988), but the published reports on these areas do not mention material suitable for carving.

Within Turkey, virtually all meerschaum produced is from Eskisehir Province. Although another deposit of meerschaum nodules has been identified in Yunak Township, Konya Province (150 km [93

miles] southeast of the city of Eskisehir; Yeniyol and Oztunali, 1985), to date there is no known commercial production from that area. In the vicinity of Eskisehir (the provincial capital), there are three major and two minor sepiolite districts (figure 2). Turkmentokat-Gokceoglu is the most important meerschaum-producing district in Eskisehir, because of the superior whiteness, purity, and ease of carving of the material. With regard to the two other important sepiolite deposits in the region, Sepetci and Nemli, some meerschaum has been extracted from the former, whereas both meerschaum and industrial-grade sepiolite have been mined from the latter.

The Eskisehir sepiolite deposits are known to have been exploited since the 18th century. For much of this time, the district's meerschaum was exported to Vienna, Austria, as preforms, as well as to Budapest (Hungary) and throughout Germany, primarily for carving into *objets d'art* (figure 3) and articles for smokers (figure 4). Historically, meerschaum was known as "Vienna stone" in the European market (Uzkesici, 1988); even today, European pipe makers will use this term to refer to the finest quality meerschaum (Necdet Altinay, pers. comm., 1995).

At present, meerschaum products carved by Eskisehir artisans are supplied directly from Turkey to the world market. Meerschaum (sometimes called "Eskisehir stone") articles have been exported primarily to the United States, Australia, and Canada, as well as to England, Germany, Norway, Denmark, and other European countries.

Sepiolite usually occurs in sedimentary rocks, in forms ranging from massive to earthy, as thin layers, disseminated, and as concretions. Although
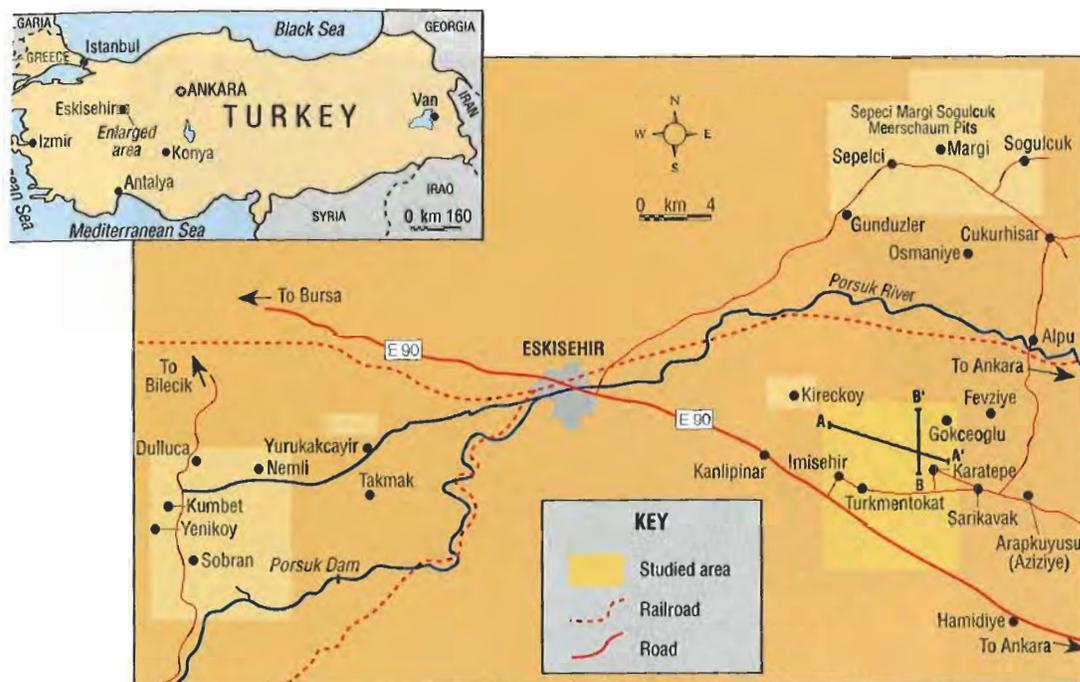
Figure 2. This map of the Eskisehir region of Turkey shows the location of the five main sepiolite districts identified to date in this historic meerschaum-producing area. The yellow area surrounding the villages of Turkmentokat and Gokceoglu—shown here in dark yellow—was studied extensively by the authors (see Sariiz, 1990). Lines marked "A" and "B" refer to cross-sections in figure 5.

the Eskisehir sedimentary sepiolite deposits have been exploited for more than 200 years, their geologic origin has not been studied in detail. The objective of this study was to develop a genetic model for the geologic origin of the deposits at Turkmentokat-Gokceoglu. In the course of this research, we also studied current mining practices, the gemological properties of meerschaum, and the fashioning and distribution of this ornamental gem material.

LOCATION AND ACCESS

The meerschaum is mined from shafts (or holes) in an area between the villages of Turkmentokat and Gokceoglu, approximately 20 km (12.5 miles) east of the city of Eskisehir (again, see figure 2). This region is about 1,000 m (3,280 feet) above sea level; vegetation is subtropical. The mean temperature is 11.3°C (about 52°F). The mean rainfall in the region is 250 to 300 mm (10 inches to 1 foot), with cool summers and cold winters (rainy and snowy). The city of Eskisehir is located about 250 km west of Ankara, the capital of Turkey, and 360 km southeast of Istanbul by road. Access to the mining area is possible by car via Highway E90 from Eskisehir to the center of the villages, and then by horse or by foot (and, in some cases, by car) via dirt trails for about another 1–2 km.

Eskisehir was founded in the first millennium before Christ by the Phrygions, as they settled on the banks of Porsuk River. It has an active artistic and cultural life, with world-class performances of the ballet, theater, opera, and folk dancing. The city is especially well known both for meerschaum (for

which it has hosted several international festivals) and for traditional folk dancing. The main industries of Eskisehir Province are farming, mining, carving, clothing, brick, and tile manufacture.

Figure 3. During the 19th century, meerschaum was also used for cameos, as illustrated by this 37.5 × 33.5 cm carving of Emperor Franz Joseph I of Austria. Courtesy of the Natural History Museum of Vienna.

Figure 4. Carved in 18th-century Vienna, these meerschaum cigar holders depict mythological, hunting, and historic scenes. Note the change in color caused by nicotine staining. Courtesy of the Austrian Tobacco Museum, Vienna; photo by Thomas Reinagl.

MATERIALS AND METHODS

Detailed geologic mapping of the study area was completed during the summer of 1990 (Sariiz, 1990). Descriptions and study of about 100 samples from the conglomerates in which the meerschaum deposits occur provided the primary data for this study.

Polarizing microscopy, X-ray diffraction (XRD) analysis, and scanning electron microscopy (SEM) were used to identify, study, and characterize meerschaum and other minerals within the deposit. XRD analysis was done at the Department of Geological Engineering of Istanbul Technical University using a Philips Model 1140 X-ray powder diffractometer. SEM analysis was done at the Department of Metallurgy of the University of Texas at El Paso with a dual-stage scanning electron microscope (Model ISI-DS 130).

Carved meerschaum articles provided by the meerschaum company Koncak and from the authors' personal collections were used for gemo-logical testing (i.e., determination of optical and physical properties).

GEOLOGY AND OCCURRENCE

Geology of the Eskisehir District. The oldest rocks in the district belong to the Upper Paleozoic Karatepe group, which is composed of deep marine (oceanic trench) rocks that have undergone metamorphism (high pressure and low temperature) as a result of subduction. The group is divided into three units: the Sarikavakcali marble, the Karakaya metamorphics (calc schist and quartz schist), and the Gokceoglu formation (quartz-bearing muscovite schist, glauconite schist, marble, "schisty" diabase, and phyllite). This group is overlain by the Turkmentokat ophiolites (mafic and ultramafic igneous rocks associated with a geosyncline), which are probably Triassic in age and are composed of dunite, serpentinite, and gabbro. The Turkmentokat ophiolites are overlain by the Jurassic Yildiztepe formation (a succession of fine-grained sandstones) and
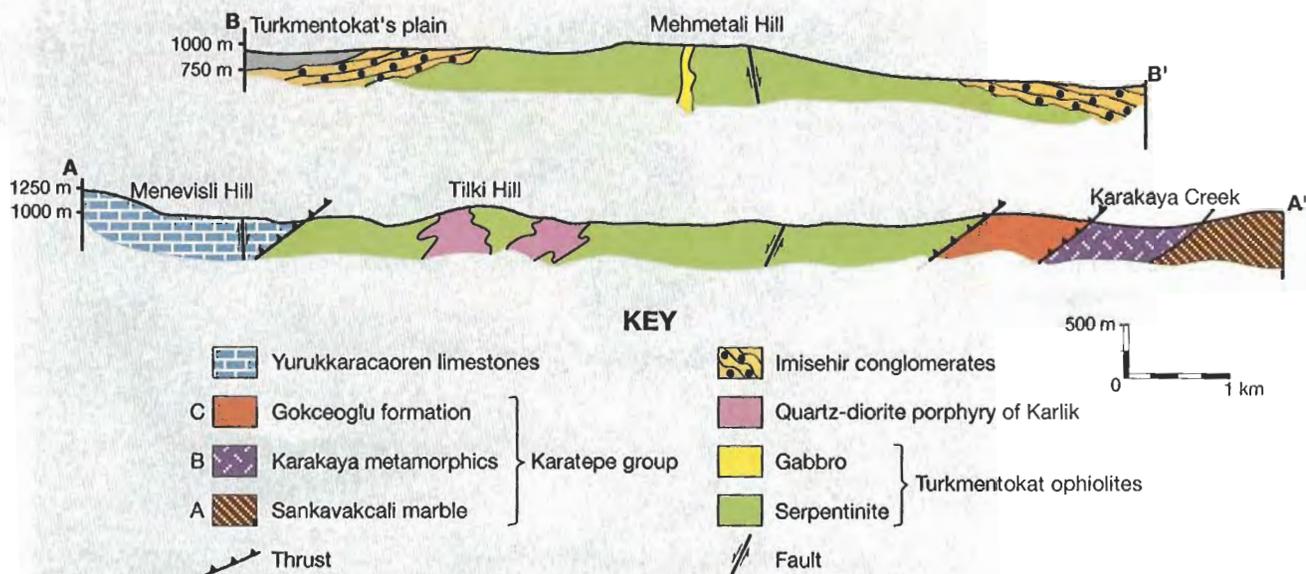
Figure 5. These cross-sections from the Turkmentokat-Gokceoglu district show the location of the stratigraphic sequence of rocks (see text for details) and the sepiolite (meerschaum) deposits. Locations of cross-sections are labeled "A" and "B" in figure 2.

the Yorukkaracaoren limestones (mostly massive and partly recrystallized). These, in turn, are overlain unconformably by the Pliocene-age Imisehir conglomerates and Koyunyatagi limestones; the former contain the economically important sepiolite nodules as well as peridotite, diabase, magnesite, and serpentinite gravels and sand-size grains of quartz, feldspar, and biotite, all of which are cemented by dolomite. The conglomerates are 35–40 m (about 115–130 feet) thick; the gravels (as distinct from the larger nodules) range up to 4 cm (about 1.5 inches) in diameter. The Turkmentokat ophiolites and the Jurassic rocks are cut by dikes and stocks of Paleocene-age Karlik quartz diorite porphyry (figure 5).

The present geologic structures (e.g., grabens) of the study area formed during a major deformational (tectonic) stage in the complex geologic history of the Aegean region during lower Miocene time. This was a result of the Arabian platform being pushed toward the Anatolian (Asia Minor) plate (Sengor, 1980).

The Sepiolite Nodules. At Eskisehir, sepiolite nodules occur in the Imisehir conglomerates (figure 6). Typically, the nodules are 8–10 cm in diameter, but some are as large as 25 cm. In natural form, they are gray to white, compact, and soft as some soaps. Some sepiolite nodules, when broken, display a magnesite core (figure 7), indicating a genetic relationship between the two minerals—in this case,

that the magnesite formed first and later was replaced by sepiolite. In addition, we observed that magnesite gravels, like the sepiolite nodules that form from them, are randomly distributed in different levels of the Imisehir conglomerates, which suggests that the gravels were transported from the magnesite deposits in the region.

Although bedded sepiolite is found in some parts of the Eskisehir district, this material is typically an undesirable gray color, is contaminated by

Figure 6. This view of the extracted Imisehir conglomerates shows the white meerschaum nodules and fragments, the dark gray serpentinite, light gray silica, and the brown dolomitic cements that bind the minerals.

Figure 7. Magnesite (Mg) cores and rims are visible in these two sepiolite (Se) nodules: left = 10 cm wide, right = 8 cm wide.
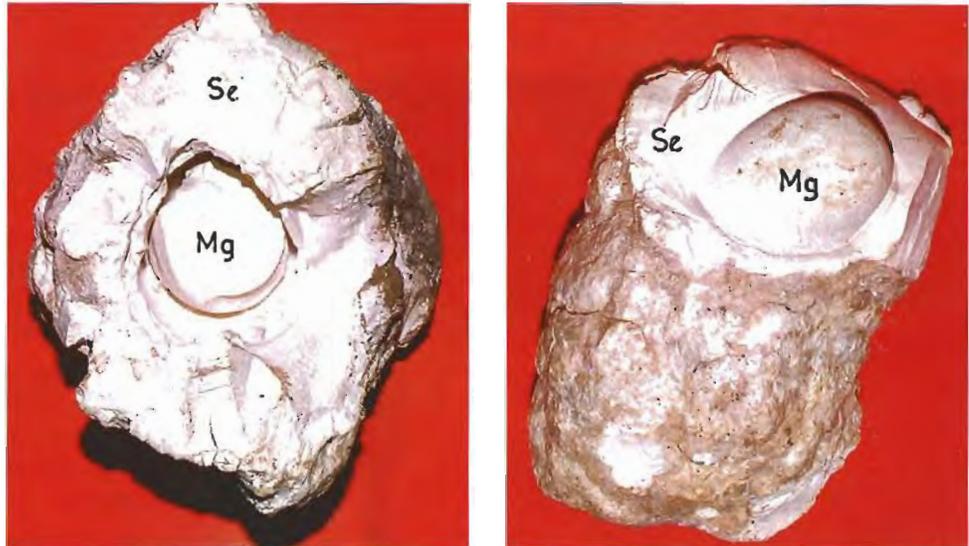
clay and other materials, has a relatively high specific gravity, and is subject to multiple cracking as it dries. Some has been used for carving, but the product is of very low quality. Gem-quality meerschaum occurs only in the sepiolite nodules.

On the basis of microscopic studies, we identified quartz and dolomite grains up to 30 μm in the sepiolite nodules. XRD patterns recorded the presence of dolomite, magnesite, and minor amounts of opal-CT (opal-cristobalite) and lizardite (a member of the kaolinite-serpentine group) in the nodules. The cement of the conglomerates contains dolomite and minor amounts of opal-CT and serpentinite.

Sepiolite shows a fibrous morphology in the scanning electron micrograph (figure 8), with fibers as wide as 0.5 μm and up to 35 μm long. The fibers

Figure 8. This scanning electron photomicrograph of a sepiolite nodule shows the fibrous texture typical of this material. Scale bar = 2.00 μm.

are intimately intergrown, and terminations are rare. The ends of the fibers are bent slightly.

Occurrence of Sepiolite. Singer and Galan (1984) and Jones and Galan (1988) made the most recent and authoritative compilations on all aspects (history, crystal structure, chemistry, synthesis, physical properties, geologic and geographic occurrences, industrial applications) of sepiolite, $Mg_4Si_6O_{15}(OH)_2 \cdot 6H_2O$. They show that it is closely related to palygorskite (varietal names for which include "mountain leather" and "mountain wood"), $(Mg,Al)_2Si_4O_{10}(OH) \cdot 4H_2O$, with which it frequently occurs.

Both minerals have been found in a number of geologic environments. These include: (a) marine environments (sediments) ranging from deep seas to shallow lagoons; (b) continental environments ranging from soils, calcretes (caliche), and alluvium (all characteristically alkaline and in arid or semi-arid regions); (c) continental saline and alkaline lake sediments; and (d) associated with igneous rocks as veins and alteration products, some of which may be related to hydrothermal alteration of Mg-rich (ultramafic) rocks (Singer and Galan, 1984; Jones and Galan, 1988). In addition, Ece and Coban (1994) discuss the diagenetic replacement of magnesite cobbles and pebbles by sepiolite with specific reference to these (Eskisehir) deposits. Because sepiolite may form in many environments, it is not surprising that this mineral is found in several physical states, ranging from compact (meerschaum) to earthy (as in soils).

The random distribution of sepiolite nodules within the Imisehir conglomerates can be related to ground-water fluctuations over time as well as to
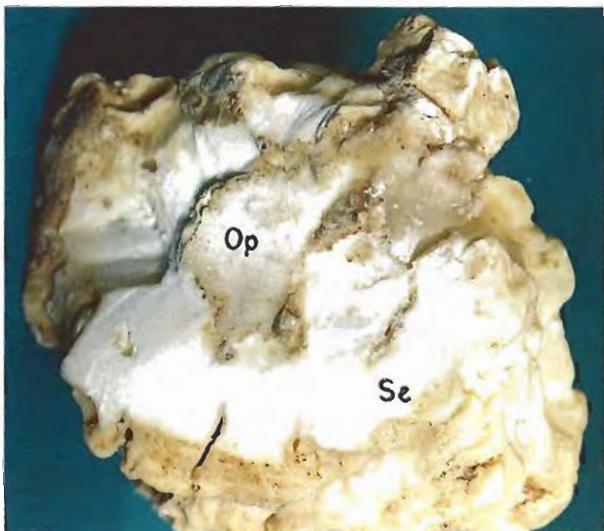
Figure 9. Areas of opal-CT (Op) were found to be associated with sepiolite (Se) in the nodules (here, 13 cm wide).

the proximity of the conglomerates to fault systems that enhance the flow of fluids. Also, clay layers may have influenced sepiolite distribution, because they affect the ability of pore water (subsurface water in the voids of the rock) to penetrate the formation. On the basis of the field investigations and on chemical, mineralogic, and petrographic analyses performed on sepiolite nodules (taking into consideration the stability diagram of Wollast et al. [1968]), we determined three main points about the physico-chemical behavior of the $Mg^{+2}+SiO_2(aq)+H_2O$-

Figure 10. A "spinning wheel" (rope and pulley) system is used to remove buckets of sepiolite nodules and waste materials from one of many mining "holes" operating in the Eskisehir district.

bearing solutions from which the Eskisehir sepiolite deposits formed:

1. Under alkaline conditions (pH = 8–8.5), when the SiO_2 concentration of the pore waters in the magnesite gravels reached saturation, sepiolite formed *in situ* as a replacement of the magnesite gravels. (Sepiolite does not form when the SiO_2 concentrations in pore waters are low.)

2. When pore waters were supersaturated with respect to SiO_2, both sepiolite and opal-CT formed together, as evidenced by the presence of opal-CT areas associated with sepiolite in the nodules (figure 9).

3. As no talc was detected in our samples, it can be assumed that dolomite—unlike magnesite—in the nodules did not react with the SiO_2-saturated pore waters. If such a reaction had taken place, talc would have been produced (Mueller and Saxena, 1977).

MINING

The Turkmentokat-Gokceoglu district contains hundreds of shafts that are believed to have been worked intermittently for sepiolite. Traditional methods for mining meerschaum, using simple hand tools, still appear to be the most economic. Specifically, shafts about 1 m in diameter and anywhere from 10 to 75 m deep are dug into the ground to reach the sepiolite-containing beds. When miners reach a layer that may have economic amounts of sepiolite, they drive a production gallery (horizontal "drift" or opening), approximately 120 cm (about 1.5 yards) high and 150 cm wide, in the direction that the sepiolite nodules appear to occur. Because the conglomerates bearing the sepiolite nodules are strongly cemented by the dolomitic material, miners can operate in the gallery without adding any structural supports.

To extract the sepiolite, miners use the traditional room-and-pillars style of digging. Both waste materials and sepiolite nodules are raised to the surface in buckets by a simple "spinning wheel" (rope and pulley system) at the top of the shaft (figure 10). Common extraction tools include picks, shovels, and wedges to pry the sepiolite from the conglomerate. Because wet sepiolite is very soft, miners must be extremely careful not to damage the nodules during extraction. Explosives are not used.

In the Eskisehir district, meerschaum is mined by small companies and groups (2–5 people, figure 11). Because most of the miners are farmers, the deposits are worked most intensively after the

Figure 11. A group of miners return to Karatepe village (visible in the background) at the end of a workday. Note the mining tools: a wedge, a shovel, and a carbide lamp.

farming season, in late fall through early spring (November through April). In addition, the relatively shallow depth of the water table in some areas means that flooding of the tunnels can be a major problem, especially in the spring.

PRODUCTION

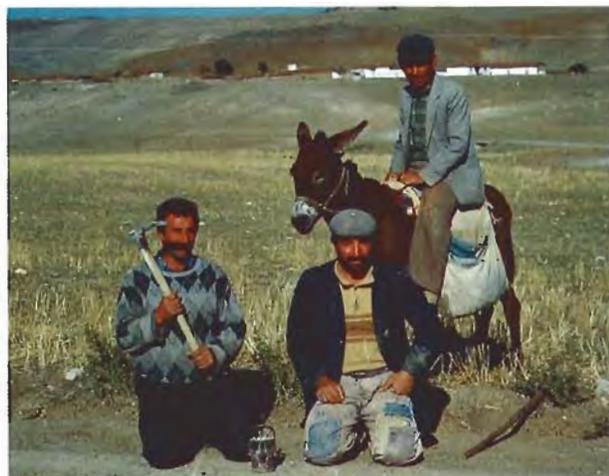Meerschaum is believed to have been exploited in the region since the time of the Roman Empire. From the end of the 18th century until the beginning of the 20th, meerschaum was mined extensively in Eskisehir, and the rough was exported to Europe and the United States. According to the State Institute of Statistics, Prime Ministry, Republic of Turkey (1990 and 1992), Eskisehir production at that time averaged an estimated 12,000 cases a year (one case = 12 kg). Between 1913 and 1952, sepiolite production fell to a total of 6,600 kg, while a total of 176,856 kg was produced from 1954 to 1973. To support the local carving industry, the Turkish government has banned the exportation of rough meerschaum since 1972. Production reported for the period since then peaked at about 525 cases in 1975 and dropped to a low of 40 cases in 1992. (Note that these figures represent production recorded by government sources. Because much of the meerschaum is extracted outside of government supervision, actual production is undoubtedly much greater.) About half of this reported production is believed to be mined from the Turkmentokat-Gokceoglu region (Necdet Altinay, pers. comm., March 1995). On the basis of information

provided by the State Organization of Planning (Prime Ministry, Republic of Turkey), we estimate that meerschaum reserves in the district exceed six million kilograms.

THE GEMOLOGICAL PROPERTIES OF MEERSCHAUM

The Turkmentokat-Gokceoglu meerschaum nodules have distinctive mineralogic and physical properties (table 1), as well as size, shape, and texture—that make them particularly suitable for carving decorative objects such as pipe bowls (figure 12), *objets d'art*, and jewelry (figure 13).

Properties such as sorption, chemical composition, the white color, high porosity, and low specific gravity, make meerschaum ideal for use in pipe bowls. Although some manufacturers produce sepiolite articles in tourist venues elsewhere in Turkey, Eskisehir Province is the center of sepiolite manufacture.

CARVING MEERSCHAUM

The first step in making a sepiolite carving is to pick the right nodule. Only by careful selection can defects such as cracks, color irregularities, and inclusions of other minerals be avoided in the final product. Sepiolite can be easily carved as long as it is somewhat moist. Because the nodules typically lose some of their natural moisture during the often lengthy carving process, they usually have to be soaked in water periodically to maintain sufficient softness. Eskisehir carvers use as many as 40 types

TABLE 1. Physical appearance and gemological properties of gem-quality sepiolite (meerschaum) from Eskisehir, Turkey.

Color	White (rarely, cream)
Refractive indices[a]	$n_g = 1.525–1.529$, $n_p = 1.506–1.520$ with a birefringence of 0.009 to 0.019
Specific gravity	2.0 (on compact material)[b]
Fluorescence	Inert to both long- and short-wave UV radiation
Internal characteristics	Quartz, dolomite, and magnesite inclusions (all identified by X-ray diffraction)
Hardness (Mohs scale)	2–2.5[c]
Other	Floats on water and adheres to tongue in its raw state

[a]*Microscopic observation with immersion as reported by Sagiroglu and Cogulu (1972, p. 871).*
[b]*Meerschaum floats on water when dry. Porous material has a specific gravity of 0.508–0.894.*
[c]*When heated, meerschaum loses its moisture and hardens further.*

Figure 12. The beautiful meerschaum bowl on this 40-cm long pipe was carved in Eskisehir. From the collection of Mr. Sedat Koncak.

of knives and other tools, which they usually manufacture themselves.

Once a nodule has been selected, the carver must choose a design that best fits the natural shape of that nodule and minimizes waste. From this point on, the single most important point in deciding on a design is the carver's vision and imagination. With talent, experience, and patience, the artisan can produce a variety of intricate designs.

After the nodule has been given the desired or requested form, it is partially dried slowly in the sun. Subsequently, the piece is carefully hand carved. Once the meerschaum carving is completed, it is dried in an oven at 110°C for two hours. Next, it is polished with a very fine abrasive and then immersed in heated, liquid beeswax for a few minutes; last, it is polished with a very soft cloth. This waxing and polishing treatment gives the fin-

Figure 13. In Eskisehir, meerschaum is also carved into jewelry, like this suite featuring a necklace, bracelet, and earrings. The meerschaum in the bracelet is 14.5 × 0.50 mm.

ished meerschaum article a creamy white color and shiny appearance. Meerschaum turns a progressively darker yellow when used as a pipe bowl because it absorbs nicotine from the tobacco.

DISTRIBUTION

In Eskisehir and nearby villages, all meerschaum products are manufactured by independent artisans at their workshops or homes. Currently, there are about 150 meerschaum carvers in Eskisehir Province. There are no large-scale, mechanized carving operations in Turkey. To educate meerschaum carvers and miners, and to raise future carvers, the local government established a meerschaum school in Eskisehir in 1989. However, it is not currently in operation.

To purchase meerschaum objects, one can contact either the Chamber of Trade of Eskisehir, as they publish requests in their journal, or any one of the several companies operating out of Eskisehir (e.g., Oztas, Altinay, Altintas, or Koncak). Meerschaum articles from Eskisehir artists reportedly have sold at high prices. For example, one by noted pipe-maker Ismail Ozel was auctioned for $18,000 five years ago (Necdet Altinay, pers. comm., 1995). According to Mr. Altinay, the owner of Altinay Co., collectors of meerschaum carvings consider three main factors: the date of manufacture (the older, the better), the carver (the more famous the better), and the artistry of the piece itself.

CONCLUSIONS

On the basis of a geologic map of the Turkmentokat-Gokceoglu district completed by the senior author, study of the local stratigraphy, and field observations, as well as X-ray diffraction, scanning electron microscopy, and petrographic analyses, the authors have concluded that the sepiolite (meerschaum) nodules probably formed at

shallow depths and in alkaline conditions, in the vicinity of paleo-shorelines of a lacustrine basin (large, inland lake). They are the result of replacement of transported magnesite gravels when these gravels were subjected to pore waters with high SiO_2 concentrations. Sepiolite's properties make it especially suitable for carving and polishing when it occurs in a compact, massive form, as meerschaum.

Although significant quantities of meerschaum were mined and exported from the 18th through the early 20th centuries, production appears to have declined greatly in recent decades. Since 1972, government regulations have limited export to only fashioned meerschaum. However, there are a num-ber of expert carvers in Turkey, especially in Eskisehir Province. Some of their works of art have been sold at auction for significant sums.

The worldwide decline in the popularity of smoking has undoubtedly affected the demand for meerschaum pipes. However, sepiolite has many other industrial uses, which suggests that mining is likely to continue. One potential use for meerschaum could be as an alternative to ivory, which is banned in many countries. Both have a similar color, take a high polish, and are easy to carve and cut. It must be noted, however, that ivory is harder than meerschaum and—unlike meerschaum—bends without breaking.

REFERENCES

Ball S.H. (1950) *A Roman Book on Precious Stones.* Gemological Institute of America, Los Angeles, CA.

Ece O.I., Coban F. (1994) Geology, occurrence, and genesis of Eskisehir sepiolites, Turkey. *Clays and Clay Minerals*, Vol. 42, No. 1, pp. 81–92.

Galan E., Castillo A. (1984). Sepiolite-palygorskite in Spanish Tertiary basins: Genetical patterns in continental environments. In A. Singer and E. Galan, Eds., *Palygorskite-Sepiolite. Occurrences, Genesis, and Uses*, Developments in Sedimentology 37, Elsevier, Amsterdam, pp. 87–124.

Jones B.F., Galan E. (1988) Sepiolite and palygorskite. In S.W. Bailey, Ed., *Hydrous Phyllosilicates (Exclusive of Micas)*, Reviews in Mineralogy, Mineralogical Society of America, Washington, DC, Vol. 19, Chap. 16, pp. 631–674.

Mueller R.F., Saxena S.K. (1977) *Chemical Petrology*. Springer-Verlag, New York.

Sagiroglu G., Cogulu E. (1972). *The Determination of Minerals with the Polarizing Microscope* (in Turkish). Technical University, Istanbul, Gumussuyu, Istanbul.

Sariiz K. (1990) The occurrence of magnesite deposits at Turkmentokat-Karatepe (Eskisehir) (in Turkish). *Bulletin of the Mineral Research and Exploration Institute* [Ankara], Vol. 110, pp. 77–96.

Sengor A.M.C. (1980) *The Fundamentals of the Neotectonics of Turkey* (in Turkish). A bulletin of the Geological Society of Turkey, 40 pp.

Singer A., Galan E., Eds. (1984) *Palygorskite-Sepiolite: Occurrences, Genesis, and Uses*, Developments in Sedimentology 37, Elsevier, Amsterdam.

Uzkesici T. (1988) *The State of the Meerschaum Industry* (in Turkish). First International Meerschaum Festival of Eskisehir, pp. 21–22.

Wollast R., Mackenzie F.T., Bricker O.P. (1968) Experimental precipitation and genesis of sepiolite at earth-surface conditions. *American Mineralogist*, Vol. 53, Nos. 9–10, pp. 1645–1662.

Yeniyol M., Oztunali O. (1985) The mineralogy and the genesis of the Yunak sepiolite (in Turkish). In *Proceedings of the 2nd National Clay Symposium*, Hacettepe University, Ankara, pp. 171–186.

ALEXANDRITE, with Pleochroic Twinned Growth Zones

A 1.21-ct faceted stone, with a green-to-purple color change, was sent to the West Coast laboratory for identification. We found the optical properties to be typical for alexandrite—biaxial optic character, with refractive indices of 1.743 to 1.750. The presence of fluid (including two-phase) inclusions was consistent with natural origin. Also characteristic of many natural alexandrites were the pronounced growth zoning and twinning.

Chrysoberyl, especially alexandrite, is strongly pleochroic, typically displaying red, orange, and green when viewed in different orientations. We have seen twinned synthetic crystals where one twin appeared red, while the other looked green because of the different orientations of the individual crystals.

Most of this natural stone was of one twin orientation, with only a small region near the culet belonging to the other twin. Although many-layer (polysynthetic) twinning in alexandrite (from the Elahera gem field in Sri Lanka) has been described before in *Gems & Gemology* (Gunawardene and Rupasinghe, Summer 1986, pp. 80–95), the twinned areas in this stone were unusual in that they were brightly colored and irregularly shaped, with a vermiform, or worm-like, appearance when observed through a microscope with an attached polarizer. We concluded that this feature was due to twinning and not to color zoning, because the regions traded colors as the polarizer was rotated (figure 1, left and right).   *MLJ*

DIAMOND

Untreated or Fracture-Filled?

Because the GIA Gem Trade Laboratory has a policy of not issuing grading reports on fracture-filled diamonds, any diamond submitted for grading that we determine to be so treated is instead issued an identification report. Therefore, once staff gemologists in the diamond-grading lab detect signs of treatment, they bring the suspect stone to the Identification and Research lab for further examination and the issuance of the report. Although some stones exhibit clear evidence of filling, the breaks in other diamonds have ambiguous features and thus require additional investigation. Graders also routinely show us stones that are not filled, but might be confused with ones that are, so that we can document them for research and education purposes.

Last Fall, the West Coast lab received for grading a 0.57-ct marquise-cut diamond that had a most unusual fracture. The break exhibited both thin-film iridescence and orangy brown natural staining (figure 2), two features that might be confused with flash effects in filled diamonds. (For more on such features, see the section on "Techniques to Identify Fracture Filling," pp. 169–173, in the article "Update on Filled Diamonds: Identification and Durability," *Gems & Gemology*, Fall 1994.) This is the first diamond we have examined that contained two such potentially confusing features in a single unfilled break. However, this separation also shows a "feathery" appearance, a feature typical of an unfilled break and one that we have not seen to date in a filled break.

RCK

Figure 1. With a polarizer, the twin planes in this 1.21-ct alexandrite look like brightly colored "worms" that change colors as the polarizer rotates from one orientation (left) to another (right).
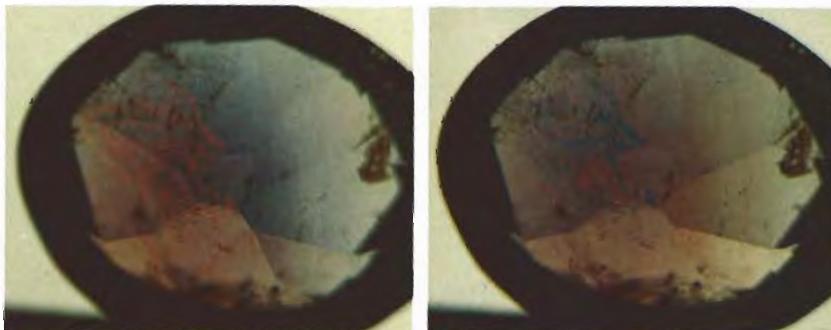
Figure 2. Both the thin-film iridescence and the natural color staining in this unfilled fracture in a diamond might be confused individually with the flash effects typically associated with a filled fracture. Magnified 25×.

Treated Old-Mine Cut

Just as a particular saturation and tone do not guarantee that the color of a diamond is natural (Winter 1994 Lab Notes, p. 264), neither does an old-style cut. In a Fall 1994 lab note (p. 185), we reported on an old-European-cut diamond with a green color that was due to irradiation by Americium. That stone raised our suspicions because of uneven surface features. More recently, we examined a 0.54-ct, old-mine brilliant-cut diamond with a natural-looking green-yellow color that also revealed some suspicious characteristics.

The stone showed a strong, slightly chalky, blue-and-yellow zoned fluorescence to long-wave ultraviolet radiation. There was moderate-to-strong yellow fluorescence (with one slightly blue zone) to short-wave UV, and no phosphorescence to either wavelength. Although these responses were consistent with natural color in a diamond, microscopic examination failed to reveal features that we expect to see associated with such a color. For instance, there were no irradiation stains, although we did find four unusually glassy "melted-looking" naturals on the girdle. When we examined the stone with fiber-optic lighting, the yellow graining appeared to be overprinted with a weak green graining. Although this is not unusual, the saturation of the green graining was not sufficient to

explain the depth of the stone's body color.

Spectroscopic examination provided strong hints that the color had been artificially enhanced. We saw a strong 415-nm line, but not the rest of the Cape spectrum—that is, no lines at 435, 453, 466, and 478 nm. The pair of lines at 496/503 nm were visible (with the 496-nm line being the stronger of the two), but there was no 595-nm line. These features are consistent with treated color in a diamond, but they still do not constitute proof of treatment.

Infrared spectroscopy, however, was conclusive. Weak, but definite, H1b and H1c peaks in the infrared spectrum of this type-Ia stone led us to conclude that the color was not natural. It probably resulted from just a light "kiss" of laboratory radiation.

MLJ, Dino DeGhionno, and Patricia Maddison

Triangular Inclusions in Diamond

Considering the thousands of diamonds that have been graded by GIA GTL, it is rare to see anything new in the way of inclusions. Still, it happens occasionally. In recent years, however, we have seen a number of triangular inclusions, all apparently due to distinct causes. For example, the Spring 1990 Lab Notes section (p. 95) described triangular inclusions in diamond that had possibly resulted from dissolution along a cleavage

Figure 3. The triangular growth features in this diamond form a plane associated with the octahedral face of an enclosed phantom diamond crystal. Magnified 30×.

plane. Then there was a triangular inclusion that was thought to have originated as lonsdaleite that reverted to graphite (Fall 1994 Lab Notes, pp. 185–186). Now, the West Coast staff has observed yet another type of triangular inclusion, this one in a 1.74-ct marquise diamond.

A diamond grader who saw the stone remarked that the reflective triangular features were reminiscent of platinum platelets seen in some synthetic gems. However, platinum platelets are opaque; these inclusons were not. Further, we are not aware of any synthetic diamonds that were grown in platinum crucibles, so there is no reason why they would contain platinum platelets. Synthetic diamonds may contain a nickel-iron flux, but we have yet to see such inclusions in triangular form.

When viewed through the table of the diamond, the feature appeared to be a triangular plane that in turn contained numerous transparent, flat, reflective, triangular inclusions (figure 3). An isolated inclusion of this type seemed unusual, but it was easily explained when we looked at it through the pavilion of the stone. From this angle, a phantom diamond crystal was visible in the host. The triangular plane corresponded to one of the octahedral faces of the phantom crystal. The smaller triangular inclusions contained within—and parallel to—this plane were representative of natural trigon growth (or dissolution) features on the octahedral face of the phantom crystal. The high relief of these trigons is attributed to gas that was trapped in triangular voids that formed at the interface of the enclosed octahedral face and the host diamond. *Cheryl Y. Wentzell*

SYNTHETIC DIAMOND,

Treated-Color Red

The Fall 1993 *Gems & Gemology* contains an article on two treated-color, synthetic red diamonds that had been submitted to the East Coast lab for standard origin-of-color reports (T. Moses et al., "Two Treated-Color Synthetic Red Diamonds Seen in the Trade," pp. 182–190).

Figure 4. The dark red color of this 0.14-ct (about 3.23–3.27 × 2.07 mm) synthetic diamond is the result of treatment.

In late October 1994, another dark red, 0.14-ct round brilliant (figure 4) was submitted to the West Coast lab for determination of color origin. Our suspicions were immediately aroused because red is exceptionally rare in natural diamonds, even as a treated color. We quickly confirmed these suspicions when a hand magnet picked up the specimen—a reaction typical for synthetic diamonds that contain large metallic flux inclusions (again, see the above-referenced Fall 1993 report).

Magnification revealed a large metallic-appearing inclusion under the crown facets and clouds of pinpoint inclusions confined to wedge-shaped areas. These latter zones were further defined by their green, hazy appearance; there was also a fairly distinct greenish zone in the center of the round brilliant. When this synthetic diamond was examined perpendicular to the table (face up) with both long- and short-wave UV radiation, we noted a cross-shaped area with moderate green fluorescence; the remainder was inert to long-wave UV, but fluoresced a faint orange to short-wave UV. These characteristics are all typical of synthetic diamonds (with the fluorescence colors consistent with treated-color red synthetic diamonds seen to date).

Examination with a desk-model prism spectroscope revealed several absorption lines between 500 and 660 nm—including lines at about 595 and 635 nm, and an emission line at about 580 nm. Such a spectrum is typical of treated pink to red color in both natural and synthetic diamonds.

On the basis of these test results, we identified the round brilliant as a synthetic diamond, treated color.

RCK and SFM

EMERALD, with Unusual Flash-Effect Colors

The Spring 1990 Lab Notes section reported on an emerald that exhibited orange and blue "flash effects" from large filled fractures (pp. 95–96). Since then, both East and West Coast labs have seen this pair of flash-effect colors in a number of clarity-enhanced emeralds.

Last year, the West Coast lab observed some "new" flash effects in an emerald submitted for identification. A series of fractures extended the length of this emerald-cut stone. When we examined them across the stone's width, they displayed an orange-to-pinkish purple flash effect (figure 5). However, when we viewed these same fractures down the length of the stone, the flash effect was blue and orange.

One possible explanation for this unusual behavior relates to the fact that emerald (beryl) is uniaxial, with two distinct refractive indices for light polarized in different directions. When a noncrystalline material (such as an oil, resin, or glass) and a crystalline solid have crossing dispersion curves—refractive indices that match at only one wavelength of light (i.e., at one color)—we see flashes of the color at which the indices match in brightfield illumination and flashes of its spectral-complementary color in darkfield illumination. (For a discussion of flash-effect optics, see Box B, pp. 156–157, in Kammerling et al., "An Update on Filled Diamonds: Identification and Durability," Gems & Gemology, Fall 1994.) Because emerald has two distinct refractive indices, however, blue (brightfield) and complementary orange (darkfield) form one pair of flash colors, seen in one optic orientation, whereas orange-to-pinkish purple (darkfield) is seen in the other orientation. The expected brightfield color, green to blue-green, is probably masked by the emerald's body color.

In this stone, we also noted some irregular, highly reflective bubbles—as well as some white, cloudy areas—in the filler; both of these features have been seen in other filled emeralds.

RCK, Patricia Maddison, and MLJ

Figure 5. Filled fractures viewed across the width of this clarity-enhanced emerald produce a clearly visible orange-to-pinkish purple flash effect in darkfield illumination. Different flash colors were seen when the same breaks were examined down the length of the stone. Magnified 15×.

Figure 6. In reflected light, the bottom of this polymer-impregnated jadeite cabochon shows strong evidence of selective grain etching. Magnified 25×.

JADEITE

Bleached and Impregnated, with Distinctive Surface Texture

The West Coast laboratory received for identification a 6.78-ct translucent, mottled-green cabochon that revealed properties typical for jadeite jade, with an R.I. of 1.66 (by the spot method) and an S.G. of 3.34. Chromium lines, seen with a spectroscope, proved that the green color was natural. The stone was inert to short-wave UV radiation, but some areas fluoresced a faint green to long-wave UV.

The gemstone had an unusual, etched appearance in reflected light (figure 6): The aggregate structure of the cabochon appeared to be made up of many interlocking grains in various orientations, with certain grains preferentially eroded. Because of this surface texture, we suspected that the stone had been bleached and polymer impregnated. Infrared spectroscopy confirmed this treatment by revealing several peaks between 2800 and 3200 cm^{-1}; the relative positions and intensities of these peaks matched those of "polymer 5" in ICA (International Colored Gemstone Association) Laboratory Alert No. 75, 1993, issued by S. McClure and E. Fritsch. Therefore, we identified the stone as impregnated jadeite jade, natural green color, sometimes known in the trade as "B jade." Interestingly, the S.G. of this stone was higher than that of most poly-

mer-treated jadeites we have encountered thus far.

MLJ and Dino DeGhionno

Treated and Untreated Beads in One Necklace

A comprehensive report on bleached and impregnated jadeite in the Fall 1992 *Gems & Gemology* (Fritsch et al., pp. 176–187) described features diagnostic of this treatment. The Lab Notes section has also reported on jade objects treated in this fashion, including entries on necklaces constructed of treated beads (see, e.g., Fall 1994, p. 187). Until recently, however, our testing had shown that all of the beads in these necklaces were treated.

In November 1994, the West Coast lab was asked to identify a double-strand necklace with 69 beads (7.88–5.08 mm) on one strand and 74 beads (8.18–5.49 mm) on the other. Standard gemological testing proved that the translucent to semi-translucent, mottled green-and-white beads were jadeite jade. A desk-model prism spectroscope showed chrome lines, proving that the green color was natural. One unusual feature was noted during testing: Some of the beads on both strands fluoresced a weak-to-moderate, mottled yellow to long-wave UV radiation, while others were inert.

Most polymer-impregnated jadeite fluoresces. However, some untreated material may also fluoresce a weak yellow to long-wave UV. In our experience, we usually do not get such varied reactions from beads on one necklace. Further testing, using infrared spectroscopy, proved that there were treated (impregnated) and untreated beads in both strands. This was our first encounter with such mixed strands. *RCK*

Dyed Green NEPHRITE

Of the two jades (jadeite and nephrite), jadeite is much more commonly color enhanced (usually dyed green). Nevertheless, we occasionally find evidence of green dye in nephrite submitted for identification (see, e.g.,

Spring and Summer 1984 Gem Trade Lab Notes, pp. 48 and 108, respectively).

In December 1994, the West Coast lab was asked to identify five oval, translucent, mottled-green cabochons, which ranged from 6.38 to 7.12 ct. All had an appearance similar to that of good-quality jadeite. However, standard gemological testing—including a 1.61 spot R.I. and an S.G. of 2.95 or 2.96—identified the five stones as nephrite. Magnification revealed dye concentrations (figure 7) like those seen in dyed jadeite and other similarly treated gem materials. The absorption spectrum observed with a desk-model prism spectroscope revealed a broad dye band in the red region, much like that seen in dyed-green jadeite and quartzite. In these stones, the diagnostic absorption band was centered at about 660 nm. All five specimens were therefore identified as dyed nephrite. *RCK*

Blister PEARL Attached to Shell

Pearls submitted for identification frequently pose testing challenges. Usually it is a mounting that interferes with a complete examination, but occasionally it is something different. One such challenge was presented to the West Coast lab in the form of a shell with an attached gray baroque pearl (figure 8). Our client stated that the item came from the

Figure 7. At 15× magnification, concentrations of green dye are easily seen in this nephrite jade cabochon.

Figure 8. The gray baroque pearl attached to this shell measures 12.1 × 11.5 mm.

Gulf of California, near La Paz, Mexico, on the east coast of Baja California. The client wished to know: (1) if the pearl was natural or cultured, (2) if its color was natural, and (3) if it was assembled or naturally attached to the shell.

Examination with low-power magnification answered the last question first. The pearl's nacre formed a continuous bridge to the mother-of-pearl layer on the shell, proving natural attachment.

Natural or cultured origin of the pearl was determined by X-radiography; a slightly longer than usual film-exposure time was required in order to compensate for the extra thickness of the shell. The X-radiograph showed no bead nucleus, but rather a series of concentric rings near the center of the pearl, proving natural origin (figure 9).

Origin of color was determined using long-wave UV radiation. The mottled, weak, chalky reddish brown fluorescence of the pearl closely matched that of the grayish lip of the attached shell (again, see figure 8). Together with the physical appearance and the absence of any evidence of dye when examined with magnification, this verified the natural color of the pearl. Our final report stated that the pearl was a natural solid blister pearl, with natural color.

Of further interest, especially since we had not previously seen any used in this context, were a series of CAT scan (Computerized Axial Tomography) images of the pearl and shell provided by the client (see, e.g., figure 10). Although we know of no data regarding CAT scan analyses of pearls, we do know that axial tomography uses X-rays to make a different type of image than that obtained by conventional X-radiography. Consequently, an attempt to interpret a CAT scan by conventional X-radiographic analysis could well lead to an erroneous conclusion. For instance, the CAT scan in figure 10 displays what appears to be a roughly spherical "core" surrounded by an outer layer, giving the illusion that this natural pearl is bead nucleated. Just as dental X-radiographs are inadequate for resolving the fine detail necessary for pearl identification, CAT scans cannot be used interchangeably with specialized pearl-testing X-radiography.

Cheryl Y. Wentzell

Figure 9. Concentric rings seen near the center of the pearl in this X-radiograph show that it is natural.

Figure 10. Although this CAT scan image clearly shows the point of attachment of the pearl to the shell, the circular white area could easily be misinterpreted as the bead nucleus of a cultured pearl.

SAPPHIRE, with Diffusion-Induced Color and Star

Recent reports in Bangkok jewelry publications indicate that corundum with diffusion-induced stars is now appearing in the trade, with a large quantity soon to be released on the world market. For example, the laboratory of the Asian Institute of Gemological Sciences (AIGS) in

Figure 11. Laboratory testing proved that the star in this 23.26-ct purple sapphire was induced by diffusion treatment.

Figure 12. When the stone in figure 11 is immersed in methylene iodide, there appears to be a "red" color confined to the surface.

Bangkok described two such stones with stars that appear to have the same basic characteristic as the first synthetic stars introduced in the 1940s; that is, the wispy silk causing the asterism is located at, or just beneath, the surface (see "AIGS Finds More Stars," *Jewellery News Asia*, June 1994, p. 74). Unlike most natural asterism, the individual needles in the induced-star sapphires usually cannot be detected at lower magnifications.

The East Coast Gem Trade Laboratory has also examined a slightly different diffusion-treated star corundum. The 23.26-ct purple stone in figure 11 illustrates the cloudy appearance of the induced star. Routine examination revealed that the starting material was natural. On close examination with the stone immersed in methylene iodide, we noted a thin layer of red that appeared to be confined to the surface of the stone (figure 12). On the dome of the cabochon, near the center of the star, we also noticed a number of red spots and a red "cloud" (figure 13). All of these observations strongly suggest that the stone was originally intended to be a diffusion-treated "ruby."

One possible explanation for the less-than-satisfactory end result is that impurities in the original cabochon may have "contaminated" the color, so the operators decided to create a star stone by diffusing titanium into the surface. Another scenario is that the red color and asterism were simultaneously diffused, but again the iron present in the cabochon reacted with the titanium in the diffusion process, resulting in a blue component that ultimately produced the purple hue.   GRC

SYNTHETIC STAR SAPPHIRE with an Unusual Color

In our experience, green is an uncommon color for gem sapphires. Those we do encounter are almost invariably iron-rich stones, such as the ones from Australia, that have been

Figure 13. These red spots and "cloud" seen on the dome of the stone in figure 11 at 45× magnification provide proof that the red surface color, like the asterism, was diffusion induced.

fashioned with the table facet essentially parallel to the optic axis. This results in their displaying the strong green dichroic color face up. Because of their significant iron component, such stones typically reveal heavy absorption bands in the 450–470 nm range when examined with a spectroscope.

Green star sapphires are even less common. One such natural stone was reported in the Spring 1989 Gem Trade Lab Notes section (p. 39). It was thus with interest that, in late Fall 1994, the West Coast lab examined a ring set with the translucent, asteriated oval cabochon shown in figure 14. The stone had a spot R.I. of 1.76, and a uniaxial optic figure was easily resolved in the polariscope. Examination with a desk-model spectroscope failed to reveal iron-related features, although we did detect an absorption line at 670 nm, which we attributed to cobalt (see below). Magnification revealed that the asterism-causing inclusions were not evenly distributed. Rather, they were confined to a thin, mottled, cloudy area just below the surface of the cabochon's dome. This distribution of star-producing silk is similar to what we have seen in several synthetic star corundums (for an extreme example, see the Summer 1994 entry on a pinkish orange synthetic star sapphire, pp. 119–120).

For further documentation, GIA Research performed chemical analysis using energy-dispersive X-ray fluorescence (EDXRF) spectroscopy. This revealed cobalt (Co) as the probable coloring agent. Using detailed UV-visible absorption spectroscopy, we had previously documented cobalt (as Co^{3+}) as the sole coloring agent in a rarely encountered non-phenomenal green synthetic sapphire produced in Switzerland. The non-phenomenal green synthetic sapphires produced in the U.S. that GIA Research and the GIA Gem Trade Laboratory have studied are colored by a combination of cobalt (Co^{3+}) and vanadium (V^{3+}). To date, we have not documented cobalt as a coloring agent in natural sapphires.

On the basis of these tests, we identified this cabochon as a synthetic star sapphire.

RCK and Emmanuel Fritsch

Figure 14. The unusual color in this synthetic star sapphire (about 14 × 12 × 5.90 mm) is probably due to Co^{3+}.

Figure 15. This dendrite in a 1.37-ct natural spinel could be confused with a flux inclusion in a synthetic spinel. Magnified 20×.

SPINEL, Natural with a Dendritic Inclusion

Frequently, identification of spinel requires advanced testing techniques. Many spinels do not contain characteristic inclusions that could be used to distinguish natural stones from their synthetic counterparts, especially from flux synthetics. In these cases, EDXRF spectroscopy is needed to make the separation (see, e.g., Muhlmeister et al., "Flux-Grown Synthetic Red and Blue Spinels from Russia," *Gems & Gemology*, Summer 1993, pp. 81–98).

A 1.37-ct orangy red oval mixed-cut spinel, which arrived in the West Coast laboratory in December 1994, presented a slightly different identification challenge. It contained several inclusions: octahedral crystals (possibly negative crystals) scattered throughout the stone, as well as large feathers, some with brown iron staining. Among the latter was a prominent dendritic iron stain (figure 15) that could be mistaken by an unwary gemologist for the yellowish white to yellowish brown flux seen in some synthetic spinels. The stain probably resulted from iron-rich fluids penetrating a secondary fracture that formed after the crystal grew. In addition, according to the Muhlmeister et al. article cited above, some flux-grown synthetic spinels contain "pyramid-shaped phantoms in near-perfect alignment with the external faces and edges of the octahedra." These could also be confused at first glance with the octahedral-crystal inclusions in this stone.

MLJ

ROBERT C. KAMMERLING, JOHN I. KOIVULA, AND EMMANUEL FRITSCH, EDITORS
MARY L. JOHNSON AND DINO G. DEGHIONNO, CONTRIBUTING EDITORS

TUCSON '95

In what has become an eagerly awaited annual pilgrimage, Gem News editors traveled to Tucson, Arizona, again this February to attend the many overlapping trade shows in this Southwestern desert community. In doing so, they joined thousands of others—including gemologists, retail jewelers, gem and mineral dealers and collectors—in what is often referred to as the "Tucson experience."

This experience has something for anyone with an interest in minerals and the gem materials that are fashioned from them. The large gem shows, such as the American Gem Trade Association (AGTA) show at the Tucson Convention Center, draw many retailers from all over the world. When that show closes, the Tucson Gem and Mineral Society takes over the same venue for what was historically the main show, the nucleus around which the others have grown. This show draws mineral collectors and enthusiasts, as well as dealers. Then there are shows that cater primarily to fossil dealers and collectors, not to mention the "mom-and-pop" roadside shows where everything from the chic to the cheap is offered in an atmosphere

more reminiscent of swap meets than sophisticated jewelry industry events. And, throughout the almost two-week experience, there are classes and lectures for those who wish to combine formal education with buying.

Helping the editors and regular contributors with this Gem News section were Dr. Sang-Ho Lee, Shane F. McClure, Thomas M. Moses, and Cheryl Wentzell, of the GIA Gem Trade Laboratory; and Dr. James E. Shigley, Dr. Ilene Reinitz, Sam Muhlmeister, and Yan Liu, of GIA Research. Because of the scope the 1995 Tucson shows, this report will continue in the Summer issue.

DIAMONDS

New diamond cuts. Two new trademarked faceting styles for diamonds, produced in cooperation with world-famous gem designer Bernd Munsteiner, were debuted in Tucson by Figg Inc., of Fairfield, Iowa. Company president Guido Figdor loaned the editors one sample of each cut (figure 1) for examination.

The "Context Cut," a square faceted octahedron, has four crown and four pavilion facets and a faceted girdle; there is no culet and no table facet. Although not mentioned in their accompanying promotional brochure, this cut is reminiscent of the earliest fashioned diamond, the point cut, which was reportedly first produced before the 14th century. On the sample provided, pavilion angles were 40° and the crown angles were 23°, 25°, 27°, and 25°. The various crown angles cause the pavilion apex to be slightly misregistered from the crown apex, producing the appearance of a four-pointed star within the stone. According to the manufacturer, each "Context Cut" diamond comes with documentation detailing where the stone was cut and the weight, size, color, "purity," designer of the cut, manufacturer, jeweler, owner of the finished piece, etc. Reportedly, only octahedral rough is used.

The "Spirit Sun" cut is a round modified brilliant. Both crown and pavilion are cut with 16 equal main facets, again without culet or table facets. On our sample, the crown angles were 20°, and the pavilion

Figure 1. The 1.02-ct round modified brilliant diamond illustrates the new "Spirit Sun" cut; the 0.51-ct diamond is a "Context Cut," a type of square faceted octahedron. Courtesy of Figg Inc.; photo by Shane F. McClure.

Figure 2. This 2.46-ct. cat's-eye emerald (7.38–7.89 × 5.61 mm) is from Santa Terezinha, Brazil. Courtesy of David Kaassamani; photo by Shane F. McClure.

Figure 3. Note the distinct "spokes" in this 59.04-ct elongated trapiche emerald crystal from Colombia. Courtesy of Guillermo Ortiz; photo © GIA and Tino Hammid.

angles were 42°, creating the illusion of a round disk, surrounded by bright rays, at the center of the stone. Michael Good Designs, of Rockport, Maine, has used these cuts in new jewelry designs, with a two- or three-point "Paragenesis" setting (similar to a tension setting).

COLORED STONES

Large apatites from Madagascar. For several years, highly saturated greenish blue to bluish green apatites from Madagascar have been available at the Tucson shows (see, e.g., Spring 1994 Gem News, pp. 50–51). Almost all the material the editors saw before this year's Tucson show had been fairly small, with cut stones typically no larger than about 2–3 ct.

This year, however, we saw some significantly larger faceted stones. For example, Neal Littman, of San Francisco, showed one of the editors a 40.25-ct. faceted bright greenish blue stone; Mark H. Smith, of Bangkok, Thailand, had a 47.62-ct stone; and the firm Jonte Berlon of Poway, California, had a few cat's-eye apatites in the 10-ct range, as well as three faceted stones in the 18–36 ct range and one of 153 ct. Thomas M. Schneider, of San Diego, California, explained that fairly large crystals have been mined for years from the deposit. However, as noted in the above-referenced item, this material was being heat treated as soon as it came out of the ground, on large circular steel plates placed over open fires. This treatment method caused the heat-sensitive apatite crystals to break into many fragments, the source of the

many small stones. Some time in 1994, however, dealers began purchasing untreated crystals at the deposit and having them heated outside Madagascar under more controlled conditions. (See additional entry on Madagascar gems, below.)

Diaspore from Turkey. A number of vendors featured the color-change diaspore from Turkey described in the Winter 1994 Gem News section (pp. 273–274). Mine Design, of Clarence, New York, had some 50 faceted stones, ranging from 1 to 8 ct. They also had a number of cabochons, the largest of which was a 22.72-ct flat, "bullet" shape. Two of the cabochons were chatoyant.

Stephen Kotlowski, of Golden Land Trading Company, Newburgh, New York, was marketing diaspore that he had fashioned. Stones ranged from 1.79 ct to over 20 ct; among the largest were a 26.06-ct "apex fan cut" and a 29.04-ct antique cushion cut. Commercially significant reserves of this material exist, according to Mr. Kotlowski.

Cat's-eye and trapiche emeralds. In both 1993 and 1994, we saw and subsequently reported on cat's-eye emeralds from the Santa Terezinha area of Brazil. This year, David Kaassamani, of South Lake Tahoe, California, had some attractive cat's-eye emeralds from this source (see, e.g., figure 2); the largest was a 9.47-ct stone from the Vienna mine. Also from that mine was a 5.93-ct emerald cabochon with a somewhat indistinct but complete six-rayed star. Colombian dealer Gonzalo Jara showed us a 3.23-ct light-toned emerald that also had weak chatoyancy, found in a parcel of nonphenomenal cabochons from Cosquez, Colombia.

Among the attractive trapiche emeralds seen were a matched pair of heart-shaped cabochons with a total weight of 24.71 ct, offered by Eminent Gems, of New York. We saw an exceptional 59.04-ct columnar trapiche emerald crystal (figure 3). It was interesting to note the great variation, along its length, in the concentrations of carbonaceous inclusions producing the "spokes."

Emerald necklaces fashioned in India. One of the more striking pieces of jewelry encountered was a necklace of 24 large emerald beads with a total weight of about 1,200 ct. Although the stones were somewhat light in tone, all were highly transparent and well cut. They were of Colombian origin and had been fashioned in India in 1994, according to a representative of Fine Emerald, New York. There was a smaller (294 ct total weight) rope-strung emerald necklace consisting of similar good-quality, well-made beads.

Garnets from Mali. The Winter 1994 Lab Notes section (pp. 265–266) contained an entry on a rough grossular-andradite garnet reportedly from the Republic of Mali in Western Africa. A number of dealers offered similar material at Tucson, also described as from Mali. Thomas M. Schneider had a dozen or so faceted stones that ranged from light greenish yellow to medium brown, and a 200-ct parcel of small "cobbed" rough that would produce finished stones of 1 ct or less. Mr. Schneider said that approximately 300 kg of these garnet crystals had just been received in Australia. Some 3 kg (15,000 ct) of very gemmy facet-grade material was quickly gleaned from this lot, and good cuttable material is still being recovered from the remaining lower-quality crystals. The firm Herman Lind II, of Idar-Oberstein, was also offering faceted material.

At various booths, we saw large, opaque, euhedral garnet crystals from this locality. One dealer, David Bunk Minerals, of Wheat Ridge, Colorado, also had a small collection of other mineral specimens from Mali: epidote, vesuvianite, and vesuvianite with prehnite; another, Azizaj Minerals of Ennepetal, Germany, had small quartz crystals (similar to "Herkimer diamonds") reportedly from a locality near the garnet deposit.

Fashioned natural glasses. Iridescent "rainbow" obsidian, which we first described in the Summer 1993 Gem News section (p. 133), was available from several dealers and in a variety of fashioned forms. Carvings included both geometric and representational shapes, an example of the latter being fish figurines sporting iridescent scales. Slightly domed tablets, free forms, and oval cabochons were among the pieces fashioned for jewelry. Some of the oval cabochons, offered by Gem Marketing International, of Rockville, Maryland, were fashioned to show the iridescence as a somewhat

diffused chatoyant band. We also saw carvings in non-phenomenal black obsidian and carvings exhibiting a golden sheen. One vendor had models of tetragonal crystals fashioned from obsidian, approximately 12.5 cm (5 inches) long.

Other types of natural glasses were seen in both rough and fashioned form. These included moldavite, a grayish green material from what is now the Czech Republic; and Libyan Desert glass, a pale yellow material that is reportedly nearly pure silica (see, e.g., Webster and Read, *Gems*, 5th ed., Butterworth and Heinemann, London, 1994, p. 293). The desert glass reportedly was collected by the vendor in western Egypt's Libyan Desert.

Fashioned "rainbow" hematite. When the Fall 1993 Gem News entry on iridescent "rainbow" hematite from Brazil (pp. 209–210) was written, most of the material seen by the editors was in rough form. Not anymore.

Bill Heher, of Trumbull, Connecticut, was offering fashioned material that included individual free-form tablets and matched pairs (see, e.g., figure 4). As

Figure 4. Iridescent "rainbow" hematite is now being used in jewelry. These pieces were fashioned by Bill Heher; courtesy of Zoltan David. Photo © GIA and Tino Hammid.

Figure 5. This 1.33-ct iolite (7.63–7.77 × 5.11 mm) was fashioned from material mined at a new locality, Ambovombe, in the far south of Madagascar. Photo by Maha DeMaggio.

the phenomenon displayed by this material is confined to the surface, the fashioned pieces, which measured about 2 to 2.5 mm thick, were backed with a similar thickness of agate for additional strength. In this backed form, according to Mr. Heher, the material appeared to be quite durable and had presented no problems during setting.

Rainbow hematite has drawn the attention of some respected jewelry designers. Zoltan David, of Austin, Texas, indicated that he was designing a line of jewelry incorporating it.

Iolite and other gems from Madagascar. One gem we saw for the first time this year was iolite from Madagascar. The material was only discovered in 1994, at a locality called Ambovombe in the far south of the island nation, according to a representative of Le Mineral Brut, Saint-Jean-le-Vieux, France. Although many crystals have been found, he reports, they are typically very highly included, greatly reducing the yield of facet-grade material. Nevertheless, the firm was offering faceted stones up to 2–3 ct as well as some interesting small (about 1 cm) cubes, fashioned to display the material's strong pleochroism.

One round brilliant (figure 5) was purchased for gemological characterization. Properties determined were: R.I. = 1.536–1.548; birefringence = 0.012; S.G. (determined hydrostatically) = 2.59; strong trichroism in colorless, light bluish violet, and medium violet; inert to both long- and short-wave UV radiation; and a weak absorption spectrum typical of iolite (see, e.g., R. T. Liddicoat's *Handbook of Gem Identification*, 12th ed., 1990, p. 146). All these properties were consistent with those reported in the literature, although

the birefringence was somewhat higher than the 0.008–0.009 that is typical for transparent iolite.

Another vendor, Saint-Roy Gems and Minerals, of Antananarivo, Madagascar, and Paris, France, was offering petrified wood from the Morondavo region. We also saw two feldspar gems—yellow orthoclase and phenomenal labradorite—as well as semitranslucent-to-opaque, well-formed hexagonal tabular crystals of ruby and transparent purple scapolite crystals.

Some blue sapphires of good color were available from Madagascar. A report on their gemological properties will appear in the Summer 1995 Gem News section.

Iolite and other Orissa gems. Last year's Tucson report mentioned at least eight gem materials from the Indian state of Orissa. Many of these were seen at the show again this year, including significant amounts of iolite, much of it calibre cut. We found that in the great majority of cases where the source of iolite was identified, that source was Orissa.

The Orissa area is actually producing an even greater variety of gems, according to Ashok Kaushik, president of Orissa Gems, Jaipur, India. Available at his booth were rubies, opaque blue sapphires, alexandrite (up to several carats, with a good color change), very nice cat's-eye chrysoberyl, aquamarine, small amounts of green and yellow beryl, emerald (including some crystals of good—but not exceptional—color), amethyst with good color, green tourmaline and indicolite, cat's-eye sillimanite, dark brown sphene, pink zircon, dark green apatite, and pink fluorite of very good color. Rhodolite and hessonite garnets were both available in large quantities. The hessonite was generally highly transparent, lacking the "roiled" appearance of Sri Lankan stones. Also seen was some irradiated blue topaz, the starting material for which reportedly came from Orissa.

Cat's-eye quartzes from Orissa were also available. According to Michael Randall, Gem Reflections of California, San Anselmo, his material came from an area that also produces the cat's-eye chrysoberyl. In general, cat's-eye chrysoberyl seen this year was of far better quality than that seen in past years. We also saw a few cat's-eye alexandrites, some with a fairly dark body color and prominent color change.

Temple Trading, of Encinitas, California, had cat's-eye diopsides from Orissa with a much purer and somewhat lighter color than what is typically seen. When illuminated from above, these stones exhibited a bright, medium-dark-green body color and a lighter, distinctly green chatoyant band. This material reminded the editors more of cat's-eye tourmaline with an atypically sharp eye than of the usual Indian cat's-eye diopside.

More meteorite products. In our 1993 Tucson report (pp. 55–56), we noted the availability of extraterrestri-

al materials. These included jewelry set with "Gibeon class" iron-nickel meteorite slices from Namibia and free-form "gems" fashioned from the large pallasitic meteor found in Esquel, Argentina. Both at the 1994 show and again this year, the editors saw these and several other meteorite materials being offered by the firm Robert Haag Meteorites, of Tucson. Among the specimens were pieces from the pallasitic meteorites that struck near Mount Vernon, Kentucky (in 1868), and near Brahin, Russia (discovered in 1810). Also offered were pieces of the nickel-iron meteorite that fell near Odessa, Texas, about 50,000 years ago; this material exhibits the same "Widmanstätten" lines that are seen in the Namibian material (see Summer 1992 Gem News, figure 6, p. 133). New "products" fashioned from nickel-iron meteorites include spheres, finger rings, guitar picks, and buttons.

This year, we also saw a material that superficially resembled pieces of a peridot-containing nickel-iron pallasitic meteorite. These specimens of peridot in basalt matrix from San Carlos, Arizona, had been coated with shellac. Although the purpose of the treatment was to keep the small, fragile peridot crystals from separating from the matrix, the coating gave the basalt a metallic appearance.

Miscellaneous notes on peridot. As is often the case, much of the larger high-quality peridot seen in Tucson was reportedly from Myanmar. Gem Tech, of New York City, showed off three attractive stones—weighing 45.87, 49.47, and 61.16 ct. Andrew Sarosi, of Los Angeles, had a nicely cut rectangular cushion weighing 57.82 ct. Direct Gems, of New York, had a 47.25-ct cushion cut and three other stones in the 20+-ct range.

Peridot from a new source, Pakistan (Fall and Winter 1994 Gem News, pp. 196 and 275, respectively), was seen for the first time at the Tucson shows this year. Dealers included John Bachman, of Boulder, Colorado, who had two well-cut 27-ct stones; Jonte Berlon Gems, which had about a dozen stones in the 3–8 ct range; and Shades of the Earth, of Phoenix, Arizona, which provided information for the previously cited Gem News entries and had a large selection of this material. Pala International, of Fallbrook, California, had a nice selection of about 50 stones. The largest weighed 74.5 ct. "Peridot from Pakistan," a report in the January 1995 Gem Spectrum, the firm's newsletter, said that the material is similar to peridot from Myanmar and Egypt (Zabargad Island) because it forms in pockets in high-temperature veins. This mode of formation explains why the new Pakistani material often occurs in large, transparent, euhedral crystals—in contrast to peridot from localities such as San Carlos, Arizona, where the material forms as xenocrysts in basalts. The largest faceted peridot we have seen to date from this locality was offered at

Tucson by the firm Gebr. Henn, of Idar-Oberstein, Germany. This exceptional cushion-cut Pakistani gem weighed 309.90 ct. Gebr. Henn also had another cushion cut of 108.37 ct and a 125.25-ct round brilliant cut.

Many crystal specimens of Pakistani peridot were available at the mineral show. We noted that some had very large, acicular inclusions (see, e.g., Winter 1994 Gems & Gemology, p. 275).

"Strawberry" quartz and other Russian gems. Natural and synthetic gem materials are coming from Russia and other republics of the former Soviet Union at what appears to be an ever-increasing rate (see also entries elsewhere this section). This trend was again evident at Tucson. The drusy uvarovite garnet described in our Tucson '94 report (Spring 1994 Gems & Gemology, pp. 53–54) was available in both rough and tablet form (including matched pairs for use in earrings) from several dealers. Interestingly, some dealers were marketing this material by the square centimeter.

One Russian gem seen at Tucson for the first time was "strawberry" quartz. Short crystals with polished faces (figure 6) were offered by Judith Whitehead, of San Francisco. The color-causing inclusions in this material seemed to be a lighter and more saturated color than that seen in similar material from Mexico. With magnification, however, the inclusions appeared to be goethite and lepidocrocite, the same minerals found in the Mexican material.

Also encountered was Russian amazonite, as large tumbled pieces and steep-angled pyramids (fig

Figure 7. This amazonite pyramid is from an unspecified locality in Russia; the skarn cabochon and slab (10.3 × 5.0 × 0.5 cm) are from the Primorye region of Siberia. Photo by Maha DeMaggio.

ure 7). This rough material appeared to have a stronger "pure" green component than most amazonite, which is typically green-blue to bluish green. According to the vendor, Marco Schreier of Renningen, Germany, the material will be marketed as cabochons.

Yet another ornamental material being sold this year was skarn from the Primorye region of Irkutsk in Siberia. This opaque material has a light tan background with gray to green markings. Depending on the orientation in cutting, these markings appear either as concentric circles or as stripes (again, see figure 7). According to promotional material provided by the vendor—White Nights Company of Anchorage, Alaska—the skarn is formed by metasomatic action on limestone and contains the minerals wollastonite, apatite, and hedenbergite as major constituents.

Another new material from Russia, marketed by the Russian Colored Stone Company, of Golden, Colorado, was aventurescent aquamarine from a locality near Krasnoyarsk, Lake Baikal, Siberia. This beryl contained iridescent "rain-like" inclusions. It is cut either as tablets, to emphasize the aventurescent effect, or as chatoyant cabochons.

Other Russian gem materials seen this year include moss agate, jasper, Siberian nephrite, some calcite-rich lapis lazuli, small quantities of jadeite, yellowish green serpentine, and charoite. We were also shown a few cabochons cut from Uralian emeralds in their feldspar matrix. These appeared to be very similar to emerald-in-matrix cabochons from North Carolina (Summer 1993 *Gems & Gemology*, p.

132; emerald-in-matrix from Brazil, fashioned as carvings and spheres, was also available). Faceted Russian gem materials included small quantities of demantoid garnet, alexandrite, and emerald.

Miscellaneous notes on sapphires. Malhotra Corp., of New York City, had an interesting 1.38-ct emerald-cut bicolored sapphire that was about two-thirds blue and one-third light yellowish brown. The border between the two colors was distinct. The House of Williams, Loveland, Colorado, had a small quantity of blue sapphire rough containing yellow cores. This rough material reportedly came from Burundi about three years ago. Apparently, the unsettled political climate (especially in neighboring Rwanda) is limiting development of the deposit.

Both ruby and sapphire from gem gravels in Sierra Leone, West Africa, were being marketed by Tideswell Dale Rock Shop, of Derbyshire, United Kingdom. The material was translucent to nearly opaque and probably best suited for cutting cabochons and beads. According to Don Edwards, of Tideswell Dale, a significant percentage of the material yields asteriated stones (several of the samples displayed the characteristic sheen when viewed perpendicular to the basal plane). Mr. Edwards said that this alluvial material from Sierra Leone was first marketed some 10–12 years ago.

NCE Enterprises, of Chicago, Illinois, had about 60 faceted sapphires from Cambodia that exhibited a color change: areas that were blue and yellow in (incandescent) halogen light appeared greenish blue in diffused daylight. Because all the stones were quite color zoned, however, it was somewhat difficult to see the color change under "field" conditions.

Sapphires from Tanzania. Sapphires in a range of colors were available from a new deposit in the far southwest of Tanzania. The source is in the Mbinga District of the Ruvuma Region, according to Abe Suleman, of Tuckman International, Bellevue, Washington. The closest village to the deposit is Amanimakoro.

The editors saw a wide range of pastel-colored sapphires from the region, including light pink, purple, and blue. Mr. Suleman reported that dark green, "magenta," and dark red sapphires, seen at the show, are also found in the region. Michael Couch, of Cumming, Iowa, offered a few dozen very dark purple-red stones that were reportedly from this new area. They did not appear to be quite in the ruby color range; he described them as a "wine" or "burgundy" color.

A small percentage of stones from this region exhibit a color change, ranging from weak to distinct. In general, the change was from grayish bluish green to reddish brown. This is more reminiscent of the color change displayed by vanadium-doped synthetic

Figure 8. These five sapphires, ranging from 1.32 to 2.14 ct, show different colors in incandescent (left) and fluorescent (right) light. They are all reportedly from a new deposit in southern Tanzania. Courtesy of DW Enterprises; photo © GIA and Tino Hammid.

color-change sapphires and some alexandrites, rather than the violet-to-purple effect shown by some sapphires from other sources—Sri Lanka and Montana, for example.

Bill Marcue, of DW Enterprises, Boulder, Colorado, subsequently loaned the editors 11 sapphires (1.06–2.16 ct) from southern Tanzania. The stones all showed some color change between incandescent and daylight-equivalent fluorescent light (see, e.g., figure 8). With incandescent light, colors ranged from pink-brown through brownish pink and purple; under fluorescent light, colors included yellowish brown, grayish violet, and grayish greenish blue. Documentation of both the faceup colors and color change was complicated by strong color zoning. For instance, among the distinct colors noted with magnification (in incandescent light) were yellow, green-blue, blue, purple-pink, and brownish pink. Other features seen with magnification include dark red-brown crystals (possibly rutile), exsolution needles (also most likely rutile; some showed twinning), pinkish orange crystals that looked like garnet, and light brown crystals similar in appearance to clinozoisite crystals found in Montana sapphires from Dry Cottonwood Creek.

Gemological properties for these stones were: R.I. of o = 1.770 to 1.771, ε = 1.761 to 1.762, and birefringence = 0.008 to 0.009; S.G., determined by hydrostatic weighing, of 4.00–4.03. All the stones appeared red through the Chelsea color filter, were inert to both long- and short-wave UV radiation, and showed an absorption spectrum combining absorption features typical of ruby and pink sapphire with iron-related lines at about 450, 460, and 470 nm. Energy-dispersive X-ray fluorescence analysis confirmed the presence of both chromium and iron.

Faceted sphalerite and other collector stones from Canada. Tucson is the place where collectors of rare gems congregate in search of the new and unusual. We saw a number of new gem materials that we had not documented before, as well as some exceptional examples of already known species.

One of the editors (EF) was shown an interesting collection of gems from Quebec and elsewhere in Canada by Montreal collectors Guy Langelier and Gilles Haineault. Many of these gems were from Mt. St. Hilaire, outside Montreal; several of these are noted below because of their quality or rarity.

Faceted *sphalerite*, ZnS, from Mt. St. Hilaire is not new, but the 3.98-ct hexagonal cut in figure 9 is the first we have seen in this saturated, medium bluish green, devoid of any yellow overtones. The nicest green color previously seen was a medium-dark yellowish green. (Other colors include yellow, brown, red, orange, and black; it also may be colorless.) The R.I. of this particular stone was over the limits of the gemological refractometer. S.G. was measured at 4.10, typical for low-iron sphalerite. We observed a weak orange fluorescence to long-wave UV radiation only. In the hand-held spectroscope, we saw weak, moderately broad bands at about 480, 500, and 560 nm—and a stronger one at 590 nm. There was total absorption above 620 nm. EDXRF analysis revealed that the gem was almost a pure zinc sulfide (which confirmed the identity of the stone). There was a small peak for calcium, and traces of manganese and iron.

Origin of color was established by UV-visible spectroscopy, which showed small absorption bands at 475, 491, 564, and 591 nm, with total absorption between 660 and 740 nm. These features come from Co^{2+}. None of the iron-related absorptions known to cause a yellow-to-brown color component were

Figure 9. Rare stones from Mt. St. Hilaire include (clockwise from upper left) remondite-(Ce) (1.70 ct), sugilite (4.14 ct), sphalerite (3.98 ct), manganotychite (0.28 ct), shortite (0.23 ct), and serandite (0.79 ct).

observed, as one would expect since only a trace of iron was found. It is not surprising that EDXRF did not detect cobalt, although we believe cobalt—a very strong absorber of light in even minute amounts—to be the cause of color. A few parts per million Co^{2+}, which is below the detection limit of our instrument, is sufficient to cause this intensity of coloration. Finally, the trace of Mn^{2+} present may explain the orange luminescence.

Serandite, $Na(Mn^{2+},Ca)_2Si_3O_8(OH)$, is one of the best-known minerals found at Mt. St. Hilaire. It usually crystallizes as blade-like, opaque, slightly pinkish orange ("salmon") crystals. Very rarely, parts of these crystals are gem quality. Most faceted serandites are very small, or not totally transparent. The 0.79-ct stone we studied recently is unusual for its size, remarkable transparency, and very bright orange color (again, see figure 9). Its indices of refraction are approximately $\alpha = 1.679$, $\beta = 1.680$ to 1.681, and $\gamma = 1.711$. S.G., measured hydrostatically, was 3.47. The stone was inert to UV radiation. In the hand-held spectroscope, it showed total absorption up to about 420 nm, and a strong, broad band centered at about 520 nm. UV-visible absorption spectroscopy confirmed this and showed absorption decreasing from the ultraviolet to about 600 nm, sharp peaks at 343 and 408 nm, a shoulder at about 420 nm, and a moderately broad band centered at 520 nm. These features are typical of Mn^{2+} absorption. EDXRF analysis demonstrated that silicon and manganese were major components (sodium cannot be detected with our instrument at the expected concentration), with minor calcium and zinc. The predominance of manganese over calcium in the composition is typical of crystals from Mt. St. Hilaire.

Shortite is a rare sodium-calcium carbonate, $Na_2Ca_2(CO_3)_3$, which occurs very sparsely in the Mt. St. Hilaire deposit. Most crystals are less than a millimeter in longest dimension and yellow. However, some exceptionally large and transparent crystals have been found and faceted (the largest-known gem is a 3.52-ct yellow square cut). We examined a 0.23-ct, slightly greenish yellow, cut-corner rectangular mixed cut (again, see figure 9). Such stones are strictly collectors' items, as the crystals are water soluble. We noted a moderate pleochroism from very light yellow to greenish yellow and colorless. R.I.'s were $\alpha = 1.530$, and both β and γ very close to 1.568, for a birefringence of approximately 0.038. S.G. was measured hydrostatically (quickly and without damage to the stone) at 2.58. The stone was inert to UV radiation and did not show any spectral features in the hand-held spectroscope. With magnification, we noted several healed fractures with liquid or two-phase inclusions. We confirmed the identity of this gem by exploring its chemistry with EDXRF analysis. A peak for sodium established that this element was a major constituent; calcium was also present in large amounts. We did not detect any other element.

Manganotychite, $Na_6Mn_2(SO_4)(CO_3)_4$, is a very rare mineral in itself. Rarer still are large transparent crystals that can be faceted. This species also is water soluble, making faceting a real challenge. We studied a 0.28-ct emerald cut (again, see figure 9). The stone appeared brown, but on close examination that color was found to be due to a superficial coating, presumably resulting from alteration of the surface. We found no pleochroism, and the R.I. was 1.552. The specific gravity, measured hydrostatically (also quickly), was 2.83. The stone was inert to UV radiation; it showed a sharp band at about 414 nm in the hand-held spectroscope (presumably due to Mn^{2+}). Magnification revealed healed fractures and negative crystals. EDXRF analysis confirmed the presence of sodium, manganese, and sulfur as major components. However, it also revealed fairly large amounts of iron, although we would estimate the iron concentration to be significantly lower than the manganese concentration. This confirmed that the gemstone was manganotychite, but not a pure end member.

Sugilite, $KNa_2(Fe^{+2},Mn^{+2},Al)_2Li_3Si_{12}O_{30}$ (again, see figure 9), is a popular gem best known as a purple, polycrystalline, opaque material from the manganese deposits of Hotazel, South Africa. We were surprised to discover that large single crystals of light purple sugilite had been discovered in 1994 at Mt. St. Hilaire. We examined several dozen such crystals, which ranged from a few millimeters to over 2 cm. They exhibited a hexagonal pyramid habit, truncated at the top by a basal plane. Some crystals contained portions that were transparent and suitable for faceting. We borrowed one such crystal for further study.

Only a very weak pleochroism in slightly different intensities of purple was detected. In the hand-held spectroscope, the crystal showed a strong absorption at about 420 nm. It was inert to UV radiation. EDXRF analysis showed silicon, iron, and sodium to be major components; potassium as a minor constituent; and traces of zinc, rubidium, calcium, titanium, and zirconium.

We obtained polarized UV-visible absorption spectra of the crystal using a Hitachi 4001 spectrophotometer and calcite polarizers. The two spectra were very similar, with two intense doublets at 350–363 nm and 413–419 nm, and two weak, broad bands centered at approximately 555 and 770 nm. Such an absorption spectrum is typical of Fe^{3+} in octahedral coordination. Although the color was very similar to that of manganoan sugilite from South Africa, the cause of color was different. The band at 555 nm induced the purple color, while the doublet at 413–419 nm was the feature seen in the hand-held spectroscope. The 365-nm peak was stronger than the 350 peak in the $E \perp c$ direction compared to the $E \| c$ direction. We could not see any significant difference in the intensity of the 555-nm band between the two orientations, which explained the very weak pleochroism.

Leifite, $Na_2(Si,Al,Be)_7(O,OH,F)_{14}$, a rare alkali pegmatite mineral, is generally found as small acicular crystals unsuitable for faceting. We studied a light purplish pink, 2.30-ct modified fan-shape cut. The pleochroism was faint, from a slightly lighter to a slightly darker pink. The optical character was uniaxial positive. R.I.'s were $o = 1.517$ and $\varepsilon = 1.522$; S.G. was about 2.62. The stone was inert to both long- and short-wave UV radiation and did not show any noticeable absorption bands in the hand-held spectroscope. Numerous needles parallel to the optic axis (and perpendicular to the table) were seen with magnification, some arranged in a step-like growth pattern.

EDXRF confirmed the presence of the major components: sodium, aluminum, and silicon. Also detected were potassium, manganese, iron, zinc, gallium, rubidium, and cesium. UV-visible and near-infrared absorption spectroscopy showed a sharp band at about 375 nm (typical of Fe^{3+}), with a complex broad band—the cause of the color—centered at about 485 nm, and another broad band centered at about 1160 nm. We do not know the reason for the 485-nm broad band.

Again seen this year from Mt. St. Hilaire was the so-called burbankite, which has been shown to be actually *remondite-(Ce)*, $Na_3(Ce,La,Ca,Na,Sr)_3(CO_3)_5$ (also in figure 9). For more on this gem material, see the Winter 1992 Gem News, pp. 270–271.

Swarovski debuts machine-cut gems. A new line of calibrated, machine-cut natural-color natural gems, marketed under the "Swarogem" name, was intro-

Figure 10. Under its Swarogem brand name, D. Swarovski and Co. is manufacturing and marketing calibrated natural peridot, amethyst, citrine, and rhodolite in novel bubble-wrap packages. Photo ©'Harold & Erica Van Pelt.

duced at Tucson by an Austrian firm well known for its synthetic gems and cut-crystal products.

Applying its expertise in state-of-the art automated cutting, D. Swarovski and Co., of Wattens, Tyrol, is initially offering faceted peridot, rhodolite garnet (in "orchid," "pink rose," and "raspberry"), amethyst ("lilac" and "violet"), and citrine ("saffron" and "golden"). Each type will be available in 50 sizes and shapes, including round and "princess" cuts (2–4 mm), square step cuts (2–2.5 mm), ovals and pear shapes (5 × 3 mm and 6 × 4 mm), and marquise and baguette cuts (5 × 2.5 mm and 6 × 3 mm). According to a recent press release, all stones are cut to a maximum of 0.10-mm tolerance. The company experimented with larger sizes but found the yield too low given the quality standards, according to Swarogem Product Manager Stephen Kahler. Swarogem has the capacity to cut about 300,000 synthetic and natural gemstones a day, he said.

To meet promised consistency in color and quality, as much as possible Swarogem buys each gem material (in extremely large quantities) from a specific region: For example, the peridot is from Arizona, and the citrine is from South America. Initially they used rhodolite garnet from India, but thought the overtones too bluish gray. They switched to rough from an unnamed locality in Africa, according to Mr. Kahler.

Still, graders use master stone sets for each size and shape in order to match color intensity, Mr.

Figure 11. This 141.79-ct bicolored topaz was carved from material mined from the Wolodarsk pegmatite, in the Ukraine. Courtesy of Turmali & Herschede, Sanibel, Florida; photo by Shane F. McClure.

Kahler said. Clarity grading is more narrow. The company offers only one clarity grade: eye-clean in the faceup position.

Stones come in distinctive, sealed bubble-wrap packages, reminiscent of tamper-proof packaging for over-the-counter pills (figure 10). In the fall, Swarogem hopes to offer calibrated machine-cut ruby and sapphire in small rounds and squares.

Topaz and beryl from the Ukraine. In the Spring 1993 Gem News section, we reported on large greenish yellow to yellowish green beryls from a major pegmatite at Wolodarsk, Ukraine (pp. 54–55). A later entry (Summer 1994, p. 128) described topaz, some of it bicolored, from western Russia and the Ukraine.

At the 1995 Tucson show, we saw more topaz from these sources, including a carving fashioned from the 1,644-ct Ukrainian rough that was shown on page 129 of the Summer 1994 Gem News (figure 11). Tais International, of Miami, Florida, was marketing Ukrainian gem materials fashioned by members of a Moscow art group, Tais-Panin, including some very large, light orangy brown topazes. They showed us faceted triangular brilliants of 715, 780, and 975 ct; a 2,520-ct faceted free form; and a 4,128-ct faceted egg shape. Particularly interesting were large faceted

topazes with images—such as Abraham Lincoln and the Great Seal of the United States—carved intaglio-style into their table facets. The firm also had some sizable faceted aquamarines from this source, including a 108-ct stone. Tais-Panin also fashions copies of famous gems, according to a brochure from the firm.

Also exhibiting was gemologist Vladislav Iavorskii, from Kiev, Ukraine. Among materials that he offered were fashioned beryls and topazes from the Wolodarsk pegmatite, including a 105-ct faceted aquamarine egg, some bicolored topaz, and a 35.40-ct orangy brown egg faceted from topaz.

Miscellaneous notes on tourmaline. The bright tourmalines from Paraíba, Brazil, were scarce this year. What limited quantities we saw were primarily in the greenish blue to blue-green range and in melee sizes. In their absence, people looked for similarly colored tourmaline from other sources. Ron Ohm Exotic Stones, of Carmel, California, was offering material from Bahia, Brazil, with a color similar to, but less saturated than, that of Paraíba tourmaline. We also saw some fine-quality tourmaline with a color close to that of the greenish blue Paraíba stones. Reportedly it came from the Araçuaí area of Minas Gerais, Brazil. Good blue-to-greenish blue stones are also coming from the area of Itambacuri, a town about 35 km southwest of Teófilo Otoni, according to Jerry Manning, of MCM Gems, Middletown, Ohio. He said that about 300 ct of exceptional material was produced in late 1994. He loaned us a 30.17-ct oval modified

Figure 12. This 30.17-ct tourmaline (18.82 × 17.79 x 13.42 mm) was mined near the town of Itambacuri in Minas Gerais, Brazil. Courtesy of MCM Gems; photo by Shane F. McClure.

brilliant that was recovered from this area in November (figure 12). EDXRF analysis revealed that the stone contained no copper, which is the primary coloring agent responsible for the vivid blue-to-green colors of the Paraíba material.

As for other colors of tourmaline, Fernando Otavio da Silveira, of Braz-G-Can International Trading, Rio de Janeiro, had some interesting bicolored Brazilian tourmaline—matched pairs cut perpendicular to the crystal's c-axis, like watermelon tourmaline is typically cut. However, unlike watermelon tourmaline, this material had a medium green core surrounded by a light "mint" green outer layer.

INSTRUMENTATION

Inclusion-viewing system. Gemstone inclusions, which frequently provide diagnostic information for experienced gemologists, can also be fascinating to observers of any level of sophistication. Photomicrographs have even been used to market amber with insect "inclusions" (see, e.g., Summer 1994 Gem News, p. 124).

Recently, GIA GEM Instruments introduced a system for displaying the internal world of gemstones. The GEM MicroVision system consists of a CCD camera, which attaches to the eyepiece of a gemological microscope. The camera is connected to a high-resolution video monitor and a color printer (figure 13). The GEM MicroVision system can display just about anything that the microscope "sees" under various lighting methods (darkfield, brightfield, fiberoptic, polarized). Calibrated and proportion-indicating eyepieces can also be used. The system adjusts to mimic different color temperatures, allowing the operator to show true colors or to enhance contrast.

Such a remote-viewing technique has obvious advantages over a traditional microscope. For example, more than one person can watch, and individual features can be preserved for future reference as photographs or on videotape.

New magnet for gem testing. Until recently, magnetism was a property with little practical application in gem testing. By and large, magnetic minerals are few and far between. Even fewer are used in jewelry. Now, however, that has changed.

Testing for magnetism is being used to help identify gem-quality synthetic diamonds, as those examined to date have been grown in iron-nickel fluxes. Inclusions of such flux—sometimes so small that they are not resolvable with a standard gemological microscope—can cause the stones to be attracted to a strong magnet (see, e.g., "The Gemological Properties of Russian Gem-Quality Synthetic Yellow Diamonds," *Gems & Gemology*, Winter 1993, pp. 228–248).

Figure 13. The GEM MicroVision system includes a CCD camera that is attached to a microscope eyepiece, a high-resolution video monitor, and a color printer. Courtesy GIA GEM Instruments.

At Tucson, Scottish gemologist Alan Hodgkinson showed the editors a magnetic device developed to detect the magnetic properties of certain synthetic diamonds. Called the "Magnetic Wand," it consists of a small, powerful neodymium iron boron magnet about 5 mm in diameter that is mounted on a 60-mm-long wooden rod. According to literature provided to the editors with a sample magnet, neodymium iron boron alloy is the most compact magnetic material available. Experiments by Mr. Hodgkinson proved that the instrument is very effective in detecting magnetism in a range of synthetic diamonds. Preliminary testing by the editors on De Beers, Sumitomo, and Russian gem-quality synthetic diamonds supported Mr. Hodgkinson's findings.

In our test, seven synthetic diamonds were individually suspended from a thread. The magnet was then brought close to each stone to see if there would be an attraction. Five of the stones were clearly drawn to the magnet. An alternative method, suggested in the product literature, is to make a small "raft" of plastic foam and float the gem in a glass of water. The diamond is then checked—actually, drawn across the water—with the magnet.

Dr. William Hanneman, of Hanneman Gemological Instruments, Poulsbo, Washington, is marketing the product and offered some precautions about it. Do not carry the magnet in or near your wallet. This could result in erasing the magnetic strip on credit cards and magnetic door keys. For the same reason, keep the magnet away from computers and computer diskettes.

Figure 14. This 0.84-ct Kashan synthetic pink sapphire is an example of lighter-toned material offered at Tucson. Photo by Shane F. McClure.

SYNTHETICS AND SIMULANTS

Faceted Kashan synthetic rubies and sapphires. Ruyle Laboratories, of Dallas, Texas, was offering faceted Kashan flux-grown synthetic rubies and pink sapphires in four quality grades, based on their clarity, and in calibrated sizes in a variety of cutting styles. They were being sold as "Kashan Created Ruby," further described in the firm's marketing flier as "permissively grown stones." According to the company's president, Steve Ruyle, they are using this tag line to distinguish this solution-growth product from what he calls "forced-growth" melt synthetics.

Mr. Ruyle further informed us that although all their Tucson material was from old stock, new production has begun and the first commercial material is expected to be available later this year. Mr. Ruyle added that the new material will be grown in a furnace he designed, using essentially the same method and flux as that used by Kashan in the past.

We had not seen many of the higher-quality, lighter-toned Kashan products, so we purchased for examination a 0.84-ct round, mixed-cut synthetic sapphire (figure 14). We determined that the properties of this transparent purplish pink stone were consistent with those reported earlier for Kashan synthetic rubies (see, e.g., "Some Aspects of Identification of Kashan Synthetic Rubies," by U. Henn and H.-W. Schrader, *Journal of Gemmology*, Vol. 19, No. 6, 1985, pp. 469–478).

Trace-element chemistry was determined using EDXRF analysis. This revealed the presence of chromium, but less than is typical for ruby—as would be expected given the lighter color. Titanium was also detected, however, in a concentration proportionally much lower (relative to chromium) than that typical of Kashan synthetic rubies.

More Russian synthetics and simulants. A number of synthetic and imitation gem materials from Russia were available. A firm new to the show this year, the Morion Company, of Cambridge, Massachusetts, offered both rough and cabochon-cut synthetic opals produced at the VNIISIMS facility in Alexandrov, Russia (for more on this facility, see the Winter 1994 Gem News, pp. 279–280). This material was available in both black and white body colors; it showed great variation in both color and distribution of play-of-color, ranging from multicolored pinpoint patterns to broad flashes of a single hue.

Morion also offered rough Czochralski-pulled synthetic alexandrite, hydrothermal synthetic emerald, and flux synthetic spinel (both red and blue). The latter two materials were produced at the Institute of Monocrystals in Novosibirsk. Synthetic quartz and split boules of flame-fusion synthetic corundum were available in a broad range of colors as well.

Among the imitation gem materials (that is, those with no natural gem counterpart) being offered by Morion was cubic zirconia (CZ) in a wide range of colors, including a color-change type. Both the blue and various shades of green CZ were produced at the Physical Institute, Russian Academy of Sciences, according to Dr. Leonid Pride, a geologist and president of the firm. He said that the acronym in Russian for this institute is PHAIN, from which the Russian trade name "Phainite" was derived for CZ. Other manufactured materials offered by Morion included VNIISIMS-produced pink yttrium aluminum garnet (YAG) and gadolinium gallium garnet (GGG) in several colors.

Figure 15. These synthetic zincites (1.35–3.26 ct) are accidental by-products of an industrial kiln in Silesia, Poland. Photo by Maha DeMaggio.

"Recrystallized" synthetics. Just before the show, the editors learned that TrueGem, of Las Vegas, Nevada, was beginning to market what it called "recrystallized" Czochralski-pulled synthetic ruby and synthetic pink sapphire. These are being sold under the trademarked names of "TrueRuby" and "TrueSapphire." The rationale behind this nomenclature, according to Larry Kelley, TrueGem executive director, is his claim that the materials are produced by a process in which natural ruby or pink sapphire rough is melted, purified, and then regrown. This last step is said to be performed using the Czochralski method. (For more information, see D. A. Catalano: "New Created Gem Irks Veteran Growers," *National Jeweler*, February 1, 1995, pp. 1, 146 and "Gem Recrystallization to Fore," *National Jeweler*, March 16, 1995, pp. 3, 75.) This material was introduced in Tucson.

TrueGem was not the only firm offering synthetic ruby under the "recrystallized" moniker. Argos Scientific, of Temecula, California, was selling rough Czochralski-pulled "recrystallized" ruby. According to a company flier, they produce about 5–7 kg per month by taking Indian ruby, Montana sapphire, and "Cr+ for color, " melting it all, and then pulling crystals. "Chakravorty Ruby," reportedly produced in India, was marketed by Creative Gems, of Seagoville, Texas. This "recrystallized" material reportedly contains 15% natural ruby.

Yet another firm, A. G. Japan Ltd., was selling "Agee Emeralds," which a company-provided flier described as "refined and recrystallized." The flier said that they crush Colombian rough emerald into a fine powder, "purify" the powder with a laser process, and then recrystallize it hydrothermally.

The editors cannot comment at this time on the feasibility of any of these processes. However, with respect to nomenclature, we would gemologically classify all these materials as *synthetics*. In all three instances the end products have been crystallized—manufactured—artificially in the laboratory.

Synthetic zincite from Poland. The Winter 1985 Gem Trade Lab notes contained an entry on faceted yellow synthetic zincite (p. 237). The client who had submitted the stone for identification said that it was a by-product of an industrial process used in Poland. Also mentioned was that synthetic zincite has been produced experimentally by at least two methods: hydrothermal and vapor growth.

This year the editors encountered a considerable amount of this material. While most were single crystals up to 15 cm (6 inches) in length, and complex crystal aggregates, faceted stones were also being sold. The material ranged from a medium-toned yellow through orange and dark orangy red, with a few yellowish green crystals.

Danuta and Jacek Wachowiak, of Minerals and Gemstones, Krakow, Poland, shed more light on this material. Apparently, it was an accidental by-product of an industrial kiln in Silesia, Poland, that was used to produce zinc-based paint. The synthetic zincite formed spontaneously and randomly by vapor deposition in the air vents of the kiln's chimney due to some undetermined error in the commercial production process.

We purchased both rough and faceted samples for examination. Gemological properties, determined on three highly saturated modified round-brilliant cuts (figure 15) were: R.I. = over-the-limits (1.81+); optic character = doubly refractive (weak doubling noted with magnification); uniaxial; pleochroism = very weak, in slightly different tones of the body color; S.G. = 5.68–5.70 (determined hydrostatically); UV fluorescence = moderate to very weak yellow to yellow-orange to long-wave, and moderate yellow to orange or inert to short-wave, with the reaction slightly stronger to long-wave than to short-wave (the strength of the reactions was inversely proportional to the depth of the body color); absorption spectrum—a cut-off at about 430 nm and a weak band at about 500 nm for the lightest-colored specimen, with the other two showing cutoffs at about 510 or 530 nm; magnification—no inclusions noted.

This is not the first report of synthetic zincite crystallizing by accident. In "A Modern Miracle" (*Lapidary Journal*, 1983, Vol. 36, No. 12, pp. 1974–1979), author Marie Kennedy reported on some yellow and red-orange "amber"-colored crystals found at the Blackwell Zinc Smelter in Blackwell, Oklahoma, when an old furnace used to produce zinc ore concentrates was torn down.

New source of synthetic emeralds. The editors came across another firm that was marketing hydrothermal synthetic emerald as both rough crystals and fashioned gems. Sold as "Maystone, Siberian-Created Emeralds," the product was being offered by Russia-based Asia Ltd., of Novosibirsk. This material is produced at a facility other than that used by the Tairus joint venture, according to the firm's executive director, Oleg Yu.Yachny.

ENHANCEMENTS

Diffusion-treated sapphires. Although they seemed to receive little attention, small quantities of blue diffusion-treated sapphires were available from a few firms, including Budsol Merchandising, of Tacoma, Washington, and Super Shine Gems, of Nugegoda, Sri Lanka. The latter also had a 64-ct parcel of small diffusion-treated corundums in the pink-to-red-to-purple range. All these colors (plus orange) of diffusion-treated corundums were included in the firm's price list in both calibrated and noncalibrated sizes, in two color and two quality grades each.

THE GEMS & GEMOLOGY
MOST VALUABLE ARTICLE AWARD

Alice S. Keller, Editor

In choosing the Most Valuable Articles of 1994, our readers focused on the "how" side of gemology. By "how," I mean the nuts-and-bolts, hands-on type of practical information that a jeweler or appraiser, for example, can put to use immediately after digesting one of these articles, information that teaches gemologists "how" to avoid costly mistakes. Not surprisingly, first place went to an article in the Fall 1994 issue that deals with how to spot the most talked-about diamond treatment of this or any year: "An Update on Filled Diamonds: Identification and Durability," by Robert C. Kammerling, Shane F. McClure, Mary L. Johnson, John I. Koivula, Thomas M. Moses, Emmanuel Fritsch, and James E. Shigley. Second place goes to the first comprehensive article to explain how GIA color grades colored diamonds: "Color Grading of Colored Diamonds in the GIA Gem Trade Laboratory," by John M. King, Thomas M. Moses, James E. Shigley, and Yan Liu, which appeared in the Winter issue. Reiterating the importance of how to identify synthetics, readers selected for third place "Synthetic Rubies by Douros: A New Challenge for Gemologists," by Henry A. Hänni, Karl Schmetzer, and Heinz-Jürgen Bernhardt. The article appeared in the Summer 1994 issue.

The authors of these three articles will share cash prizes of $1,000, $500, and $300, respectively. Photographs and brief biographies of the winning authors appear below. Congratulations also to Janet S. Mayou, of Watsonville, California, whose ballot was randomly chosen from all those submitted to win the five-year subscription to *Gems & Gemology*.

Front from left, Mary L. Johnson, Shane F. McClure; rear from left, Robert C. Kammerling, Emmanuel Fritsch, and John I. Koivula

FIRST PLACE

ROBERT C. KAMMERLING
SHANE F. McCLURE • MARY L. JOHNSON • JOHN I. KOIVULA • THOMAS M. MOSES • EMMANUEL FRITSCH JAMES E. SHIGLEY

Vice president of research and development at the GIA Gem Trade Laboratory in Santa Monica, California, **Robert C. Kammerling** is an associate editor of *Gems & Gemology* and coeditor of the Gem Trade Lab Notes and Gem News sections, the latter along with Mr. Koivula and Dr. Fritsch. A regular contributor to gemological publications worldwide, Mr. Kammerling coauthored—with Dr. Cornelius Hurlbut—the book *Gemology*. He has a B.A. from the University of Illinois. **Shane F. McClure** is supervisor of identification services in the GIA Gem Trade Laboratory, Santa Monica. Mr. McClure has 17 years of experience in gemology. He is also an accomplished gem and jewelry photographer. **Mary L. Johnson** is a research scientist in the Department of Identification and Research at the GIA Gem Trade Laboratory in Santa Monica. She holds a Ph.D. in mineralogy and crystallography from Harvard University. **John I. Koivula**, GIA Gem Trade Laboratory's chief research gemologist, is world renowned for his expertise in inclusions and photomicrography. He is coauthor—with Dr. Eduard J. Gübelin—of the *Photoatlas of Inclusions in Gemstones*. Mr. Koivula holds bachelor's degrees in chemistry and mineralogy from Eastern Washington State University. **Thomas M. Moses**, with

Thomas M. Moses

James E. Shigley

19 years of trade and laboratory experience, is vice president of identification services at the GIA Gem Trade Laboratory in New York City. He attended Bowling Green University, Ohio, and is a contributing editor of Gem Trade Lab Notes. He specializes in pearl identification and origin-of-color determination for colored diamonds. Manager of GIA Research **Emmanuel Fritsch** specializes in the application of spectroscopy to gemology, the origin of color in gem materials, and treated and synthetic gems. A native of France, he has an advanced degree in geological engineering from the Geology School in Nancy, France, and his Ph.D. from the Sorbonne in Paris. **James E. Shigley,** who received his doctorate in geology from Stanford University, is director of GIA Research. He has written many articles on natural, treated, and synthetic gems, and directs research on all aspects of identifying and characterizing gem materials.

SECOND PLACE

### JOHN M. KING • THOMAS M. MOSES
JAMES E. SHIGLEY • YAN LIU

John M. King is laboratory projects officer at the GIA Gem Trade Laboratory, New York City. Mr. King holds an M.F.A. from Hunter College, City University of New York. With 17 years of laboratory experience, he frequently lectures on colored diamonds and various aspects of laboratory grading procedures. **Yan Liu,** a color researcher with GIA Research, has an M.S. in color science from the Rochester Institute of Technology, New York, and an M.S. in color optics from Shandong College of Textile Engineering, Qingdao, China. The photographs and biographies for James E. Shigley and Thomas M. Moses appear under the first-place section.

John M. King

Yan Liu

Henry A. Hänni

Karl Schmetzer
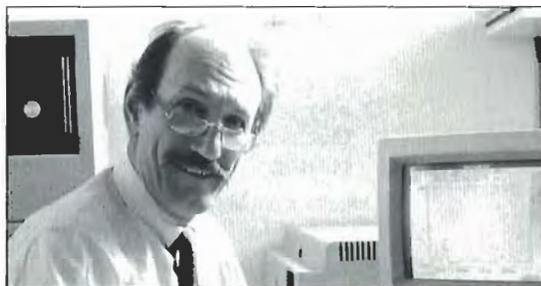
Heinz-Jürgen Bernhardt

THIRD PLACE

HENRY A. HÄNNI • KARL SCHMETZER
HEINZ-JÜRGEN BERNHARDT

Henry A. Hänni, who has a Ph.D. in mineralogy from Basel University, Switzerland, has worked at the SSEF Swiss Gemmological Institute, now in Basel, since 1980 and became its director in 1990. Also an associate professor of gemology at the Mineralogical Institute of Basel University, his specialties are applied gemology and modern analytical methods. **Karl Schmetzer** is an independent gemology researcher and consultant based in Petershausen, Germany, near Munich. He specializes in the identification of natural and synthetic gemstones, especially corundum and beryl. He has a Ph.D. in mineralogy and crystallography from the University of Heidelberg in Germany. **Heinz-Jürgen Bernhardt** also has a Ph.D. in mineralogy and crystallography from the University of Heidelberg. The German member of the commission on ore mineralogy of the International Mineralogy Association, he is head of the Ruhr University Electron Microprobe Laboratory, Bochum, Germany.

Gems & Gemology
C·H·A·L·L·E·N·G·E

Gems & Gemology articles over the past year spanned many topics about colored gems, from revealing gemological earmarks of a new synthetic ruby to dispelling myths about ametrine. Yet, it was diamond—arguably the industry staple—that seemed to be the center of attention. In particular, the presence of increasing numbers of fracture-filled diamonds in the trade prompted GIA to challenge some of the world's top gemologists to update ways of identifying this treatment. Now, once again, as part of GIA's continuing education program, we challenge you.

Based on information from the four 1994 issues of *Gems & Gemology*, the following 25 questions call on you to demonstrate your knowledge about developments in gemology. Refer to the feature articles and Notes and New Techniques in these issues to find the *single best answer* for each question, then mark your choice with the corresponding letter on the response card provided in this issue (sorry, no photocopies or facsimiles will be accepted). Mail the card so that we receive it no later than Friday, August 18, 1995. Be sure to include your name and address. All entries will be acknowledged with a letter and an answer key.

Score 75% or better, and you will receive a GIA Continuing Education Certificate. Earn a perfect score of 100%, and your name will also be featured in the Fall 1995 issue of *Gems & Gemology*.

Note: Questions are taken from only the four 1994 issues. Choose the single best answer for each question.

1. The bicoloration of ametrine crystals from the Anahí mine in Bolivia is the result of:
   A. natural color zoning.
   B. heat treatment of iron-bearing amethyst.
   C. irradiation of amethyst to produce color centers.
   D. heat treatment of colorless quartz.

2. The corundum deposits of Indaia, Brazil, have been found exclusively as:
   A Precambrian intrusive bodies.
   B. primary megacrysts in basalt.
   C. eluvial deposits associated with river gravels.
   D. alluvial or colluvial deposits.

3. Ametrine crystallizes as part of:
   A. hydrothermal brecciation.
   B. hydrothermal synthesis.
   C. volcanic activity.
   D. metamorphosis of silica sediments.

4. Noteworthy of the Indaia, Brazil, corundum deposits is:
   A. the high percentage of purple to pink sapphire.
   B. the high percentage of color-change sapphire.
   C. the sapphire's excellent reponse to heat treatment.
   D. their occurrence *in situ* in basalt.

5. "Fingerprint" patterns in Verneuil synthetic ruby are:
   A. found in all flame-fusion synthetic rubies.
   B. always different from those in natural rubies.
   C. induced by a flux-melt process to resemble those in natural rubies.
   D. a by-product of flux growth that is usually removed in cutting.

6. Douros synthetic rubies can be identified by:
   A. veil-like flux inclusions.
   B. typical chromium absorption features and penetration twinning.
   C. chemical analysis and growth patterns.
   D. no consistent combination of laboratory testing methods.

7. Douros synthetic rubies are grown by:
   A. hydrothermal synthesis.
   B. unseeded flux growth.
   C. the Czochralski method.
   D. flame fusion.

8. Synthetic forsterite can be separated from natural peridot:

A. by Cr features in the former's spectrum.
B. by the lower R.I. and S.G. of peridot.
C. on the basis of color.
D. All of the above.

9. The most common solid inclusion found in emeralds from Mananjary, Madagascar, is:

A. quartz.
B. mica.
C. feldspar.
D. apatite.

10. Fluid inclusions in emeralds from Mananjary, Madagascar:

A. resemble those of emeralds from Itabira/Nova Era, Brazil, and Zambia.
B. always distinguish Mananjary emeralds from those of African localities.
C. occur only very rarely.
D. Both A and B are correct.

11. Commercial mining of corundum in Vietnam:

A. has been accelerated at most major mines since 1992.
B. dropped off greatly in the Luc Yen district in 1994.
C. is carried out exclusively by the Vietnamese government.
D. is actively discouraged by the Vietnamese government.

12. The most useful instrument for identifying fracture filling in diamonds is:

A. a microprobe.
B. an infrared spectrometer.
C. a binocular gemological microscope.
D. an immersion cell.

13. The firm that fracture-filled a particular diamond can be identified conclusively by:

A. DXRF analysis.
B. microscopic features.
C. X-radiography.
D. None of the above.

14. The durability of fracture-filled diamonds:

A. is not of concern, because fracture filling is permanent.
B. is a major concern in the daily wear of diamond jewelry.
C. is subject to damage by prolonged or repeated exposure to typical jewelry cleaning methods.
D. is not affected by ultraviolet radiation.

15. Careful observation is required to distinguish flash effects in filled diamonds from:

A. opalescence.
B. adularescence.
C. thin-film iridescence.
D. color banding.

16. Copper inclusions in Paraíba tourmaline:

A. are proof of treatment.
B. are situated according to the trigonal symmetry of the host crystal.
C. are not found in other gems.
D. result from nucleation before growth of the host.

17. Gem corundum from the Ural Mountains of Russia :

A. is plentiful on the gem market.
B. is not currently mined commercially.
C. is mined primarily by hand.
D. is marketed through Thai dealers.

18. The GIA Gem Trade Laboratory has added these terms to its color grading terminology for colored diamonds:

A. *fancy vivid* and *fancy dark*.
B. *fancy deep* and *fancy intense*.
C. *fancy vivid* and *fancy light*.
D. *fancy deep* and *fancy vivid*.

19. When the GIA Gem Trade Laboratory grades a faceted fancy colored diamond, the stone is viewed:

A. face up.
B. through the pavilion.
C. edge up.
D. Both A and B are correct.

20. Color description includes the three attributes:

A. hue, density, and intensity.
B. tone, saturation, and hue.
C. hue, tone, and spectrum.
D. saturation, hue, and refraction.

21. Gem corundum from the Ural Mountains of Russia occurs in association with marble, as does corundum from:

A. Myanmar.
B. Montana, United States.
C. Thailand.
D. Australia.

22. Color grading of colored diamonds requires a controlled environment in which:

A. the ambient light contains no blue wavelengths.
B. ambient humidity is minimized.
C. reflection of incident light is prevented.
D. lighting is from a standard source.

23. Most gem corundum today comes from:

A. Mogok, Myanmar.
B. primarily marble-type deposits.
C. alluvial deposits in Sri Lanka.
D. secondary deposits in Southeast Asia and Australia.

24. The term that best describes corundum's relationship to alkali basalt magma is:

A. vug.
B. hololith.
C. xenocryst.
D. metamorph.

25. A new treated flame-fusion synthetic ruby is characterized by its:

A. included silk resembling that in natural ruby.
B. three-dimensional cellular network of flux-filled fractures.
C. fingerprint-like inclusions unlike those seen in natural ruby.
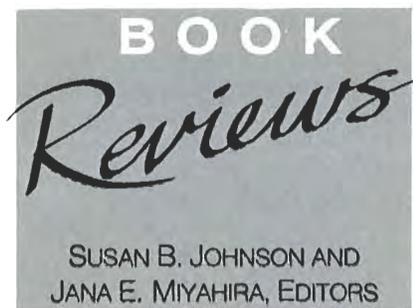D. Both B and C are correct.

GEMS, THEIR SOURCES, DESCRIPTIONS AND IDENTIFICATION 5TH EDITION
By Robert Webster

Rev. by Peter Read, 1,026 pp., illus., Butterworth-Heinemann, Oxford, England, 1994. US$120.00

This monumental gemology text, first published in 1962, went through three editions by the late Robert Webster, and then further revision in 1983 by the renowned Basil Anderson. With Mr. Anderson's death, Peter Read was asked to produce an updated edition. For this daunting task, he wisely called on several others whom he considered qualified in the various disciplines covered by this comprehensive volume. Enlisted were Grahame Brown, of Australia; C. R. Cavey, Roger Harding, Alan Jobbins, I. Mercer, Michael O'Donoghue, R. Sanderson, and C. R. Woodward, all of Great Britain; C. Dominy, of Canada; Ulrich Henn, of Germany; Richard Hughes, Robert C. Kammerling, John I. Koivula, and J. R. Rouse, of the United States; plus Kenneth Scarratt, now of Thailand.

In his original edition, Webster divided the publication into two separate volumes: The first described all the gem materials and their substitutes, and the second dealt with gem identification. Apparently, users complained that they wanted all of the information in one volume. As a result, from the second edition on, his work was consolidated into a single huge entity. (The downside to this convenience is that it makes for an unwieldy whole, and places great strain on the binding of a book that will undoubtedly be frequently used.)

This fifth edition maintains the "two part" organization of the first. As expected, there are relatively few changes in the chapters on properties. Exceptions are that the "Composite and Artificially Coloured Gemstones" and "Colour in Gemstones" chapters have been reorganized to "Composite Gemstones" and "Colour and Colour Enhancement." Throughout, various units of measurement have been converted to metric. The major changes are in the fields of new synthetics, substitutes, and enhancements.

In general, the additions have been handled very well, although it is easy to find relatively minor annoyances in almost any effort of this magnitude. For example, the diamond chapter pays too little attention to Russia, and especially Botswana, as sources. The map of southern Africa, unchanged from the fourth edition, shows neither Jwaneng, arguably the most important diamond mine in the world, nor the new Venetia mine. There are more serious problems as well. Fracture filling in diamonds is given only five lines, plus a before-and-after illustration, and the coverage of synthetic diamonds omits some recent developments, such as thin films. An illustration also carried over from earlier editions is the "correct" cut for a round brilliant, with a 39° pavilion angle and a 41° crown, angles little used for diamonds. Red beryl is almost dismissed under coverage of pink beryl.

Part of the problem may be that the newest revision has added only 10 pages to the basic text, plus 10 more to the appendices, over the fourth edition. (The Anderson revision added 75 pages.) Most illustrations are black and white, and there is a paucity of color plates. With such an important work, it would have been nice to see more full color and an easing of length restrictions.

Still, on the whole, this major update is a careful and competent revision. *Webster's Gems: Their Sources, Descriptions and Identification* remains, in its new fifth edition, an invaluable resource for every gemologist.

RICHARD T. LIDDICOAT
Chairman of the Board
Gemological Institute of America
Santa Monica, California

OTHER BOOKS RECEIVED

Hey's Mineral Index, 3rd Ed., *by A. M. Clark, 852 pp., Chapman & Hall, London, 1993, US$79.95*.* Hey's *An Index of Mineral Species* first appeared in 1950; since the second edition in 1974, the number of valid mineral species has increased to about 3,500 (with some 600 added in the last decade alone). This volume includes the names of valid species, as well as varieties, synonyms, misspellings, some meteorite and rock names (if they might be confused with minerals), and more—about 15,000 entries total.

The bulk of the book consists of an alphabetical listing of all the names, with the following given for valid species: chemical composition; original reference and type locality (except for minerals known in antiquity); crystallographic data; mineral group affiliation; synonyms; and a brief commentary, if warranted. In a separate part, minerals of similar chemical composition are grouped together—e.g., elements, sulfides, silicates.

Many gemological and varietal trade terms are included (e.g., copal, fabulite, maw-sit-sit, sunstone), unlike other excellent compilations that are not intended to be as comprehensive (e.g., Fleischer and Mandarino, *Glossary of Mineral Species;* and Nickel and Nichols, *Mineral Reference Manual).*

This book will be a welcome addition to the library of any gemologist interested in mineral nomenclature and chemistry. It contains a wealth of information that can be found elsewhere only with great difficulty.

A. A. LEVINSON
University of Calgary
Calgary, Alberta, Canada

---

*This book is available for purchase at the GIA Bookstore, 1660 Stewart Street, Santa Monica, CA 90404. Telephone (800) 421-7250, ext. 282.

BOOK Reviews

SUSAN B. JOHNSON AND JANA E. MIYAHIRA, EDITORS

GEMOLOGICAL ABSTRACTS

C. W. FRYER, EDITOR

COLORED STONES AND ORGANIC MATERIALS

FM-TGMS-MSA Symposium on topaz. *Mineralogical Record*, Vol. 26, No. 1, 1995, pp. 63–71.

Held in conjunction with the 41st annual (February 1995) Tucson Gem and Mineral Show, the Tucson Mineralogical Symposium on Topaz was sponsored by the Friends of Mineralogy, the Tucson Gem and Mineral Society, and the Mineralogical Society of America. *Mineralogical Record* published 13 abstracts of talks given at the symposium, all authored by the speakers themselves. Topics and authors include: "The Occurrence of Topaz in Northern New England Pegmatites," C. A. Francis and L. C. Pitman; "The Occurrence of Topaz in the Southeastern United States," R. B. Cook; "Colorado Topaz," P. J. Modreski and T. C.. Michalski; "Notes on the Occurrence of Topaz in Idaho," L. R. Ream; "Topaz from the Sawtooth Batholith, Idaho," M. A. Menzies; "Occurrences of Blue Topaz in the Pegmatites of the Peninsular Batholith, San Diego County, California," J. Fisher; "Pink Topaz from the Thomas Range, Juab County, Utah," E. E. Foord, W. Chirnside, F. E. Lichte, and P. H. Briggs; "Topaz Rhyolites in Arizona and the Southwest," D. M. Burt; "Topaz and Beryl-bearing Gem Pegmatites of the Alabashka-Mursinka-Adui district in the Ural Mountains, Russia," P. Lyckberg; "Geology and Occurrence of Well-Crystallized Topaz,"

M. A. Menzies; "Where's the Proton? Symmetry and Structure Variations in Topaz," P. H. Ribbe and S. C. Eriksson; "Topaz: Environments of Crystallization, Crystal Chemistry, and Infrared Spectra," E. E. Foord, L. L. Jackson, J. E. Taggart, J. G. Crock, and T. V. V. King; and "Items of North American Mineralogical and Gemological Note During 1994," M. Gray. Fifty-four crystal diagrams accompany the abstracts.   *LBL*

The mineralogy, geology and occurrence of Topaz. M. A. Menzies, *Mineralogical Record*, Vol. 26, No. 1, 1995, pp. 5–53.

This article addresses questions such as: How does topaz form? What are the conditions required for good crystals? How does the geologic environment influ-

---

ence topaz-crystal features and associations? Dr. Menzies tackles these questions by first discussing the tectonic regimes or settings that influence the parent magma from which topaz crystallizes. The text and accompanying diagrams explain orogenic (crustal compression) and anorogenic (crustal extension) processes, easing the lay reader into the complicated subject of deposit type and occurrence.

The deposit types are divided into three sections: volcanic (rhyolites), magmatic (granites, ongonites, and topazites), and late to post-magmatic (pegmatites). Each section discusses specific topaz localities. Two tables help the reader make quick and easy cross-references: One correlates different deposit types to localities, and the other lists locality, geology, and literature references. Because about 80% of topaz deposits are in pegmatites, and only 10% are in rhyolites, the author focuses on pegmatite deposits.

The section on crystal features covers morphology, color, size, composition, inclusions, and alteration and replacement. Table 3 relates geologic environment to composition, symmetry, size, habit, color, and quality. Table 4 compares geologic environment, locality, inclusions in topaz, and inclusion phases, with appropriate references. Numerous crystal diagrams and photographs illustrate the many habits of topaz.

The last section discusses the paragenetic sequence for cavity mineralization, mineral associations, geochemical environments, and formation processes. It also compares environments.

Topaz is a popular gemstone and is particularly intriguing to mineral collectors because it occurs in such a wide variety of sizes, colors, and crystal habits. Although there are volumes of literature about topaz (evidenced by the five pages of references), many questions remain.   *LBL*

On the morphology of malachite. O. V. Il'in, *World of Stones* (produced in Moscow in English), No. 4, 1994, pp. 3–9.

Malachite's popularity as a gem and ornamental stone results from its combination of rich green colors and variable textures and structures. This article illustrates, in 12 striking color plates, some of malachite's many different forms (e.g., radiating spherulite, hollow pseudostalactite, reniform). Seven of the specimens shown came from two classic localities in the Ural Mountains, the Gumeshevskii mine and the Mednorudyanskii mine. The author discusses the origin of the various forms, and concludes that many natural factors control the textural patterns in malachite. These factors include whether growth was restricted, the accumulation of impurities, and the rock type in which the copper-rich solutions precipitated.   *AAL*

Nanometre scale textures in agate and Beltane opal. T. Lu, X. Zhang, I. Sunagawa, and G. W. Groves, *Mineralogical Magazine*, Vol. 59, No. 1, 1995, pp. 103–109.

Optically observable fibers in concentrically banded agates of geode origin are composed of much finer fibers, in which quartz crystallites 8–100 nm long are stacked together parallel to <11$\bar{2}$0> or <1$\bar{1}$00>. Brazil-twin lamellae structures are frequently seen in grains longer than 30 nm. Uniformly spaced systematic striations consist of a cyclic alternation in quartz grain sizes, the smallest being 6 nm. Coarse quartz or amethyst represents the final stage of agate (lining type) formation.

The fine fibrous texture in opal from Beltane, California, is the result of cristobalite crystallites (8–20 nm) stacked together. They appear as the rims surrounding quartz crystals, and grow into regions with free space.   *RAH*

Topaz: A mineralogical review. M. A. Wise, *Rocks & Minerals*, Vol. 70, No. 1, 1995, pp. 16–25.

Dr. Wise effectively synthesizes the extensive literature on topaz into a compact, mineralogically intensive, review. He covers etymology, crystal structure, crystallography, chemistry, physical and optical properties, topaz deposits, and noteworthy localities. In the section on topaz deposits, he discusses the many geologic environments in which topaz occurs on almost every continent. For the noteworthy localities, he provides brief descriptions of deposit type and associated minerals. A concise table correlates locality to deposit type, and several attractive photographs of specimens from the Smithsonian Institution augment the text.

LBL

DIAMONDS

Radiolucency of diamond and its simulants. R. Coates, *Australian Gemmologist*, Vol. 18, No. 11, 1994, pp. 348–351.

This article reports on the author's investigation into the comparative radiolucency (i.e., X-ray transparency) of diamond and its imitations when contained within the human body. The unusual investigation was prompted by an actual case in the Australian courts where a thief attempted to switch a diamond with an imitation in a jewelry store by swallowing the diamond. The diamond was subsequently located in the thief's body by means of X-radiography. During the trial, questions about the differences in X-ray opacity of diamond and its imitations were often raised.

The author's experiments used diamond and a number of imitations, including colorless quartz, topaz, synthetic spinel, synthetic sapphire, lead glass, CZ, YAG, synthetic rutile, and strontium titanate. Procedures and equipment are described in detail. The stones were X-radiographed in the stomach, bowel, and bony pelvis of a "Pixy whole-body phantom," essentially a medical mannequin with "internal organs" manufactured to radiologically simulate those of a 30-year-old female.

The data showed that the radiopacity of the study samples was inversely related to the atomic weight of their principal elemental constituents: the lower the atomic weight of the principal atoms, the higher the radiolucency of the sample. Most of the materials fell into two distinct groups: a relatively radiolucent group (diamond, topaz, quartz, and synthetic spinel) and a radiopaque group (synthetic rutile, CZ, YAG, and strontium titanate). It was especially difficult to locate the materials with low atomic weights (such as diamond) in the radiographs taken within the simulated abdomen. Furthermore, when X-ray tube voltage was increased above 70 kV, diamonds and simulants with low atomic weight became transparent to X-rays; the resulting images had no diagnostic value.

This article is well illustrated with X-radiographs and contains tables that present the data succinctly. It is a most interesting example of forensic gemology.

RCK

Story on the "Cross of Asia" fancy yellow radiant cut diamond. A. Szymanski, *Archiwiem Mineralogiczne,* Vol. 50, No. 1, 1994, pp. 8–10,

This brief article reports on the author's examination of the famous Cross of Asia yellow diamond in October 1993. Found in the Jagersfontein mine, South Africa, in 1902, the original piece of rough weighed 280 ct. It was cut first to 142 ct, and was later recut three more times. At the time the author examined it, the Radiant-cut diamond weighed 79.12 ct and measured 28.67 × 22.21 × 15.77 mm. The play of colors on the table facet create the outline of a Maltese cross.

RAH

Zircon from the mantle: A new way to date old diamonds. P. D. Kinny and H. O. A. Meyer, 1994, *Journal of Geology,* Vol. 102, pp. 475–481.

Age dating of diamonds has been performed in the past by measuring the isotopic contents of diamond inclusions, notably samarium (Sm) and neodymium (Nd) isotopes in garnet and clinopyroxene inclusions. However, because diamond inclusions are small, and rare-earth elements are uncommon in the minerals present, inclusions in many diamonds must be measured at the same time to get an average age date for a diamond region. In this article, the authors use a different technique, uranium-lead (U-Pb) age dating with an ion microprobe, to determine the age of a single zircon inclusion in a kimberlitic diamond from Mbuji Mayi, Zaire.

The analyzed zircon measured 0.14×0.10 mm and showed a zoned 0.02-mm rim with cathodoluminescence, which suggests that it originated from a melt. Three areas in the zircon core were measured twice for total uranium, total thorium, total lead, and the isotopes ^{235}U, ^{238}U, ^{206}Pb, and ^{207}Pb. The zircon had a high uranium content (350–650 ppm U). Six measurements gave an average age of 628 million years, with a 2-Σ error (95% confidence level) of ± 12 million years.

In general, age-dated diamonds have proved to be older than the pipes that brought them to the surface. Zircons associated with the Mbuji Mayi kimberlite, but not included within diamonds, have been age-dated at 70 million years old, consistent with other measurements of the age of the kimberlite pipe. The authors believe that the 628 million years represents the age of the host diamond, which makes it the youngest diamond age reported to date. Note that the use of the ion microprobe for U-Pb age-dating of individual diamonds is limited to diamonds that contain included zircon or other uranium-rich phases. *MLJ*

GEM LOCALITIES

Almandine garnets from Vietnam. R. C. Kammerling and J. I. Koivula, *Australian Gemmologist,* Vol. 18, No. 11, 1994, pp. 356–358.

The far north of Vietnam is a new locality for gem-quality almandine garnets. This article provides a detailed gemological study of garnets from this new deposit, describing microscopic features as well as the results of standard physical tests. Since pyrope garnets had been discovered in southern Vietnam, the authors wanted to determine exactly what type was coming from the north. Chemical analysis proved that the samples were essentially almandine, with minor pyrope, grossular and spessartine components. *JEC*

Brazil—a gemstone giant reawakens. R. Weldon, *Jewelers' Circular-Keystone,* Vol. 166, No. 2, February 1995, pp. 108–120.

Although national inflation, world recession, and local governments have conspired to stifle gem mining and sales in Brazil, recent market liberalization and political and social changes have opened up new and exciting opportunities for the country's mineral riches. A commercial-free zone is now being developed in Teófilo Otoni, in the gem-rich state of Minas Gerais, to help promote the gem, jewelry, and lapidary industries.

This informative article also describes the current mining and supply status of various gems indigenous to Brazil, including emerald, tourmaline, topaz, aquamarine, kunzite, chrysoberyl, and quartz. Copiously illustrated with wonderful photographs by the author, the article provides current insights that will be invaluable to anyone interested in Brazil and its cornucopia of mineral riches. *JEC*

A brief report on Indonesian opal. G. Lambert and G. Brown, *Australian Gemmologist,* Vol. 18, No. 11, 1994, pp. 359–361.

According to a fact sheet provided the authors by the Directorate of Mineral Resources in Bandung, Java, opal is found in at least three regions of Indonesia: The Labak District of West Java (including black, white, colorless, and brownish "tea" opal), the Bengkulu Province on the northwestern coast of Sumatra (predominantly white potch), and in southeast Sulawesi

Province (translucent-to-opaque greenish white potch).

The authors examined three cabochons of material from the first deposit, the only one currently being mined commercially. Two were of the "tea" type, while the third is described as black. Properties determined were: spot R.I.—1.385 to 1.395; S.G.—1.81 to 2.09; Chelsea filter reaction—green; long-wave and short-wave UV fluorescence reactions—various shades of green (except the black opal, which was inert to short-wave UV); and very slight phosphorescence only in the black specimen. All stones exhibited play-of-color, described and illustrated for each. There is also a photomicrograph of prominent flow structures seen in one of the tea opals.

RCK

A contribution to understanding the infrared spectra of rubies from Mong Hsu, Myanmar. C. P. Smith, *Journal of Gemmology*, Vol. 24, No. 5, 1994, pp. 321–335.

A study of 31 rubies from the new deposit at Mong Hsu, Myanmar, revealed infrared features distinctive of heat-treated as compared to non-heat-treated stones from this locality. Features were found in the mid-infrared range between 1900 and 3400 cm^{-1} in some (but not all) of the untreated specimens examined. These were related to the presence of diaspore and boehmite inclusions (including submicroscopic ones), although only the former has been confirmed by X-ray diffraction analysis. In some heat-treated specimens, strongly pleochroic features between 3100 and 3600 cm^{-1} were found. These were related to structural OH groups bonded within the corundum lattice. Other heat-treated samples showed no structural OH. The author concludes that the structural OH groups found in heat-treated Mong Hsu rubies were formed as the result of alteration and dehydration of diaspore particles in the host rubies during heat treatment. He suggests that the features observed may be useful to distinguish natural from heat-treated material. He warns, however, that infrared evidence of diaspore should not be used alone to identify locality.

CMS

Gemstone mineralization in southern Kerala, India. R. D. Menon, M. Santosh, and M. Toshida, *Journal of the Geological Society of India*, Vol. 44, No. 3, 1994, pp. 241–252.

Within a gem field that extends over an area 70×35 km^2 in south Kerala and the adjacent region of Tamil Nadu, many gem minerals occur, including chrysoberyl (cat's-eye and alexandrite), ruby, sapphire, emerald, topaz, zircon, and amethyst. The primary mineralization is in zoned, complex pegmatites of Pan-African age, emplaced in granulite-facies metapelites (khondalites), and variably weathered and laterized; secondary gem deposits are found in stream gravels and placers. Thermal decrepitation of fluid inclusions indicates the presence of variable amounts of CO_2 in quartz (72.7 ppm), garnet (141.2 ppm), and chrysoberyl (51.6 ppm). Gem localities in Kerala contain vast untapped potential. At present, though, most mining is done illegally. A map of gem occurrences is included, as are photographs and brief details of chrysoberyl, sapphire, ruby, topaz, and zircon.

RAH

Hsa-Taw green tourmaline. U Tin Hlaing, *Australian Gemmologist*, Vol. 18, No. 11, 1994, pp. 352–353.

Green tourmaline has been mined for about 25 years at two deposits in Myanmar's southeastern Kayah State. One site is located about 10 miles (16.5 km) north—and the other about 30 miles (50 km) south—of the town of Hsa-Taw. The deposits occur in a belt of Paleozoic metamorphic rocks. Crystals average about 5 ct; after cutting, the best-color stones average 1–2 ct. Common crystal forms include triagonal prisms terminated by rhombohedral and pyramidal faces, with and without a pinacoid. Short prismatic crystals are more common than long ones, and vertical striations on prism faces were absent in about 25% of the crystals examined by the author.

Gemological properties are reported to be typical for elbaite tourmalines (although specific values are not given). Surface-reaching breaks are typically filled with reddish brown iron oxides. Internal features noted include color zoning, trichites, mica, and solid black inclusions of undetermined identity.

The report includes color photographs of both rough and cut specimens, as well as a sketch map of Myanmar that shows the general location of the deposits.

RCK

The 1995 ICA World Gemstone Mining Report. I. Z. Eliezri and C. Kremkow, *ICA Gazette*, December 1994, pp. 1, 12–19.

This relatively optimistic report begins by stating that the greater liberalization of trade in many countries expanded the potential market for gemstone sales around the world, as well as the potential for gem mining. It then gives a brief overview of new mines and the current production status of the more important colored gems in selected countries. Highlights are as follows.

Ruby production—quality and size—is up in India and Myanmar; production is doing well in Cambodia (despite the sporadic supply caused by turmoil in the mining areas), and large quantities of lower-grade ruby are coming from Sierra Leone. Fewer Thai rubies are available due to heavy mining over the past few decades. Production is down in Vietnam as well, because too many buyers have been sold parcels salted with synthetics.

Demand for Australian sapphire rough was stronger over the last two years. New sapphire deposits have been found in Russia (Siberia), Myanmar, and

Laos. A large new deposit of very heat-treatable blue sapphire from southern Madagascar is causing excitement. There was a new find of pastel-colored sapphires in Tanzania and a new deposit of "white" sapphires in Sri Lanka.

Production is up for peridot, due to new finds in the United States (Arizona), Ethiopia, Pakistan, and Vietnam, as well as increased production in China.

Emerald production is up, with new deposits in South Africa, the Ural Mountains in Russia, China (first ever), Tanzania, Somalia, and Brazil. Zambia has reopened the famous Kamakanga mine (with reduced mining elsewhere in that country). Regular production continues in Colombia. Large amounts of greenish yellow beryl are coming from the Ukraine, with small amounts from Finland.

Fire-opal production is up in Canada, with large quantities being mined in Mexico. There was less opal from the south Australian fields, but Lightning Ridge took an upturn. The United States produced various types of opal from volcanic deposits in Oregon and Arizona. There is a new yellow dendritic opal from Zambia.

New finds of garnet occurred in Namibia, Mali, Ethiopia, and China. A new variety was found in the Sierra Madre Mountains of Mexico. Massive green grossularite is being mined in China.

As for amethyst, production of high-quality material increased in Zambia. Bolivia held its own in general production.

Madagascar and Nigeria continue to supply considerable amounts of aquamarine. Fine blue tourmaline is coming from Namibia. There was a major new find of tourmaline in Minas Gerais, Brazil (at Morro Redondo), plus a new variety of color-change tourmaline from India.

Tsavorite production continues in Kenya, with a new find reported about 1,000 km northwest of the previously known localities, in Lokirima.

The report also noted new finds of kornerupine, sillimanite, and epidote in India; of scapolite in China; of alexandrite in Brazil; and of rhodochrosite in the United States.   *CEA*

Pink topaz from the Thomas Range, Juab County, Utah. E. E. Foord, W. Chirnside, F. E. Lichte, and P. H. Briggs, *Mineralogical Record*, Vol. 26, No. 1, 1995, pp. 57–60.

Pink topaz was first reported in the Thomas Range in 1934. These gems are found only as float crystals and so have been exposed to sunlight. Although the crystals may be as long as 4 cm, transparent, gem-quality crystals with uniform pink to pinkish red color are usually less than 2 cm. Crystals from newly opened cavities are a yellow-orange "sherry" color and typically fade to colorless in a few days to weeks (depend-

ing on air temperature, and duration and intensity of light). Heating causes the color to fade rapidly. Some crystals do not fade completely to colorless, but reveal a colorless core and a distinctly pink to pinkish red outer rim. The initial yellow-orange "sherry" color masks the pinkish red zone, which is stable to light and heat.

Bulk chemical analysis by ICP-AES—using gem-quality, colorless crystals and color-zoned crystals—showed that the pink material contains more Mn (20 ppm) and Fe (0.08%) than the colorless material (<8 ppm and 0.05%, respectively); the colorless material contains more Cr (17 ppm) than the pink material (11 ppm). Cr is not believed to be a chromophore in this case. Chemical analysis by laser-ablation ICP-MS of individual spots on a color-zoned crystal showed Mn to be concentrated in the outer color zone; Cr and other possible chromophores were not detected. Trivalent Mn and Fe are likely substituting for the Al in the topaz crystal structure. This is believed to be the first documented occurrence of pink-red topaz that is colored by Mn ± Fe.   *LBL*

Remarkable finds of minerals of beryllium: From the Kola Peninsula to Primorie. I. V. Pekov, *World of Stones*, No. 4, 1994, pp. 10–26.

Beryllium is a relatively rare element in nature, yet 82 minerals (as of 1991) contain it as an essential component. Forty-five beryllium minerals are found in the CIS (Commonwealth of Independent States). There are classic localities for beryl and chrysoberyl (and their many gem varieties), but some of the more unusual beryllium species sought by gem collectors, such as phenacite and euclase, are also found there.

This article lists all 82 known beryllium minerals (with their chemical compositions). It also has a table containing the type locality (worldwide) and the first place each of the beryllium minerals known in the CIS was found there. A map shows 72 important locations (such as type specimens for new species) ranging from the Kola Peninsula (northwest Russia) to Primorie (in the Far East); genetic types of geologic formations (e.g., granitic pegmatite, greisen) in which the minerals occur are also indicated. Twelve museum-quality specimens (and one collage of cut beryls) are illustrated in color. Of 83 references, 80 are in Russian. Those interested in beryllium minerals will find this a worthwhile compilation.   *AAL*

Siberia and Far East: A brief mineralogical guide. A. A. Evseev, *World of Stones*, No. 4, 1994, pp. 42–54.

This article reports on various aspects of "notable" mineralogic occurrences in the vast reaches of Russia lying east of the Ural Mountains. As "notable" occurrences, the authors include those famous for museum-quality specimens, type localities of new species, and

first occurrences of mineral species in Russia, among others. The article is divided into four major parts.

The first part, "Mineral Localities," lists the 114 selected occurrences, which include individual mines (e.g., the Mir kimberlite pipe), massifs (e.g., Murun, the type locality for charoite), districts (e.g., Noril'sk, famous for metallic ore minerals), and even a volcano (Klyuchevskaya Sopka) in Kamchatka, noted for fumarole minerals. A map of the localities is included (note that the map key was not bound in the issue but appears on a separate sheet of paper). Minerals found at each locality are listed (58 for the Noril'sk district alone).

The second part, "Minerals," is essentially a cross-index that alphabetically lists 89 well-known minerals and gives their important localities (from the first part of the article, as described above). For some minerals, the author includes interesting bits of history or observations from the Russian perspective.

The third part, "Review of Mineralogical Finds," is a brief history of mineralogic discoveries in Russia starting about 11,000–12,000 B.C., when the prehistoric people of Kamchatka used such materials as chalcedony and amber. The final part, "Minerals from Siberia in Museums," lists about two dozen Russian museums and briefly describes their Siberian holdings. These collections range from a museum at "Tura Settlement," specializing in Iceland spar, to the Fersman Mineralogical Museum in Moscow, which has more than 20,000 specimens.

This encyclopedic paper is not specifically gemologically oriented, but it does contain a wealth of gemological information that—to my knowledge—is available nowhere else.   *AAL*

Smoky moonstone: A new moonstone variety. H. Harder, *Journal of Gemmology*, Vol. 24, No. 3, 1994, pp. 179–182.

Moonstones with a "smoky" body color have recently been coming from two localities in Sri Lanka—near Imbulpe in the Central Mountains and in the Balangoda region. Chemical composition revealed a higher iron content than is typical for colorless moonstone. Much of the material is heavily included, mostly with clay minerals. The blue adularescence shows up particularly well when the body color is dark. The author proposes the variety name "smoky moonstone" for this material.   *CMS*

Studies on kosmochlor, jadeite and associated minerals in jade of Myanmar. Win Htein and Aye Mye Naing, *Journal of Gemmology*, Vol. 24, No. 5, 1994, pp. 315–320.

In proper gemological usage, the term *jade* applies only to nephrite and jadeite. However, it is well known that individual specimens are rarely pure. In this discussion of jadeite from Myanmar, the authors meticulously use the terms *jadeite jade* or *pure jade* versus *impure jade* for polymineralic material. The most common admixture is jadeite and kosmochlor, with a continuous series from essentially pure jadeite to 85% kosmochlor. The latter mineral is well known to gemologists as a major constituent in Maw-sit-sit, also from Myanmar. The authors present an excellent overview of this complex topic, including chemical analyses and X-ray diffraction data that emphasize the difficulties that gemologists face in identifying jade and jade-like green specimens. Minerals found as components in the specimens studied include jadeite, kosmochlor (once known as ureyite), edenite, richterite, tremolite, chromite, magnesiochromite, and enstatite. This is an important paper that should be read carefully by gemologists involved in the trade and identification of jades.   *CMS*

INSTRUMENTS AND TECHNIQUES

ROS/GEM Optics Model RFA 322 Refractometer. A. Shields and B. Neville, *Australian Gemmologist*, Vol. 18, No. 11, 1994, pp. 354–355.

This Instrument Evaluation Committee report examines a U.S.–manufactured refractometer that is now being offered in Australia. The compact unit (118 × 64 × 32 mm) has a cast-metal body and removable hinged lid. It features a small (3.5 × 11 mm) high–R.I. glass prism; a screw mount to hold the eyepiece polarizer when not in use; a clip within the lid to hold a small bottle of R.I. liquid; a sliding filter holder at the light entry port, which is fitted with both diffused white and near sodium-equivalent filters, as well as a circular mount for a small penlight; a focusable push-pull eyepiece; and a scale calibrated at 0.005 intervals from 1.30 to 1.84.

The evaluators tested various gems with the instrument and found that it produced clear readings, with the high-quality scale in 0.005 intervals being particularly helpful in reading R.I.'s of stones with low birefringences. The narrow width of the hemicylinder was an advantage when testing prong-mounted stones (presumably because the prongs would clear the hemicylinder on either side).

Although there were some criticisms (for example, some light leaked between the plate housing, prism, and outer case), the evaluators felt that the instrument would appeal to many in the field.   *RCK*

JEWELRY RETAILING

The China market: Poised to take off. G. Holmes, *Jewelers' Circular-Keystone*, Vol. 166, No. 2, February 1995, pp. 124–131.

Are you an entrepreneur? Do you want to get in on the ground floor of an economy that is about to explode? Then consider China! The Chinese are not only ready

to take back Hong Kong, they are already working toward being number one in the world jewelry market by the 21st century.

With nearly 1.2 billion people, almost half between the ages of 15 and 39, China is more than just another market. One indication of how fast things are progressing there is De Beers's advertising outlay: from $100,000 in 1990 to over $3.4 million in 1994. Last year, China consumed 220 tons of gold. The World Gold Council predicts that if the consumption of gold reaches the level of their Taiwanese neighbors, China will soon be importing over 10,000 tons annually!

Mr. Holmes predicts that China will be the leader in both jewelry manufacturing and retailing, but the two ends of the business will be intertwined. Hundreds of new jewelry plants have opened in the past three to four years. Sixty diamond cutting firms are scattered around the country. Private businesses are doing well, with plenty of discretionary income being spent. Sales in Shanghai's leading department store were $230 million in 1993, up 45% from the preceding year.

But not all is wonderful. China is still struggling to provide decent housing, drinkable water, and working sewage systems in many areas. Bicycles remain the standard mode of transportation, banks are inefficient, and import duties are still as high as 90%.

However, the *Asian Wall Street Journal Weekly* reported that China is anxious to cut the red tape to encourage major retailers to set up shop. And with one-fifth of the world's population in one spot, you can bet the retailers will be coming. Today, gold jewelry is considered the third most important purchase in a Chinese household, after a color TV and a refrigerator. This makes the potential for gold sales phenomenal. De Beers hopes to convince Chinese consumers that diamond, not gold, is forever.   *GAR*

PRECIOUS METALS

Platinum apples of the asteroids. J. S. Lewis, *Nature*, Vol. 372, December 8, 1994, pp. 499–500.

In the *Journal of Geophysical Research* (Vol. 99, pp. 21129–21141, 1994), Jeffrey S. Kargel analyzed the economic potential of asteroids in Earth-crossing orbits. The average near-Earth asteroid contains abundant iron, nickel, and cobalt, carrying much higher concentrations of (dissolved) platinum metals than the richest known ore body on Earth. A kilometer-sized metal-bearing asteroid could be worth as much as"US$5 trillion ($5 \times 10^{12}$ US dollars) at present market prices," although its impact on the strategic metals market lowers this value to $320 billion. Rather than trying to divert metal-rich asteroids from impacts with Earth, Kargel suggests, we should go mine them. This short article is a good analysis of the policy aspects of Kargel's paper.   *MLJ*

World gold fabricators stage second half comeback. *Retail Jeweller*, Vol. 32, No. 838, January 12, 1995, p. 5.

Worldwide gold jewelry production recovered dramatically in the second half of 1994, rallying from an exceptionally subdued first half to end the year just 1.3% down from 1993.

According to a report from Gold Fields Mineral Services (GFMS), the United Kingdom and Switzerland were among the strongest performers in Europe; they, along with Italy, helped final figures for Europe show only a 1% decrease. Italy's jewelry manufacturing was fueled by an increase in exports in the second half while, in Switzerland, hallmarking figures for watch cases increased 16% over 1993. GFMS reported a 4.6% increase in U.K. jewelry consumption, based on hallmarking figures, imports faring slightly better than domestic fabrication. In comparison, however, France and Germany performed poorly. Jewelry production in Germany suffered from weak retail sales and increased competition from imports. Production in France declined by more than 17% in the first 10 months of 1994, which GFMS attributed to overproduction the preceding year.

GFMS estimated that jewelry consumption in the United States was up at least 5% for the first three quarters of the year. In Japan, increased confidence saw retailers restocking newer designs after an earlier reduction in inventory levels.   *MD*

SYNTHETICS AND SIMULANTS

Characteristics of natural and synthetic diamonds observed in cathode luminescence photographs (in Japanese). All Japan Gemology Association, *Four Seasons of Jewelry*, No. 116, August/September 1994, p. 37.

This brief item points to the possibility that synthetic diamonds will soon appear more frequently in the market, and it analyzes the usefulness of cathodoluminescence (CL) photographs to separate natural and synthetic diamonds. The CL photograph of a natural diamond displays a pattern of numerous concentric squares, indicating that it grew slowly. The CL photograph of a synthetic diamond is characterized by simple geometric patterns. The author concludes that this technique is one of the most effective ways to separate synthetic from natural diamonds.   *Himiko Naka*

Hydrothermal ruby (in Japanese). M. Shigeoka, *Gemmology*, Vol. 25, No. 300, September 1994, pp. 8–10,

This is an informative report on the appearance, gemological properties, and identifying characteristics of five faceted hydrothermal synthetic rubies (0.808–2.553 ct) that were purchased in Bangkok and reportedly manufactured in Russia.

As a whole, the rubies were dark red and had rather low transparency due to their wavy growth marks, which were very similar to those found in hydrothermal synthetic emeralds. The author believes that the relatively high R.I. readings were due to the stones' high iron content, which also explains their dark appearance. Their specific gravities ranged from 4.00 to 4.03, and most samples fluoresced a strong red to long-wave ultraviolet radiation, with moderate red fluorescence to short-wave UV.

The article is accompanied by three absorption spectra. Nine photographs (six photomicrographs and two laser tomographs) illustrate the stones' appearance, their growth marks, characteristic feather inclusions observed in one sample, and copper inclusions seen in another. *Himiko Naka*

A new type of synthetic ruby from Russia. U. Henn, *Australian Gemmologist*, Vol. 18, No. 11, 1994, pp. 362–364.

Beginning with a brief review of gemstone synthesis in Russia, the author proceeds to describe his examination of a single 138-ct "boule-like" synthetic ruby crystal, represented to him as having been grown hydrothermally in Novosibirsk, Siberia. The crystal had a small area with a metallic coating and displayed dark, eye-visible, dendritic inclusions. Other properties determined were: R.I.— ε = 1.762, ω = 1.770; birefringence—0.008; S.G.—4.00; long-wave UV fluorescence—strong red; short-wave UV—weak red. Magnification revealed that the dendritic flux was polycrystalline. Also noted were clouds of bubble-like flux residues in partially healed fractures.

Spectrophotometry revealed absorption features in the visible range due to Cr^{3+}. Chemical analysis revealed the expected aluminum and chromium oxides, while analysis of the metallic coating showed the presence of tungsten and molybdenum; these latter elements were also detected where dark dendritic inclusions in fractures reached the surface.

The author concludes that the synthetic ruby is a new type of flux-grown product. *RCK*

TREATMENTS

Heat treated corundums of Sri Lanka: Their heat treatment. T. G. Pemadasa and M. V. Danapala, *Australian Gemmologist*, Vol. 18, No. 11, 1994, pp. 346–347.

This report, by two employees of Sri Lanka's State Gem Corporation, begins with a brief history of that country's "gueda" sapphire [spelled *geuda* by this journal and other U.S. publications, such as Kurt Nassau's *Gemstone Enhancement*]. Until the 1970s, Sri Lankan miners often discarded this off-color material, unaware

that it could be heat treated. Thai buyers obtained large quantities at low prices. Today, there are more than 200 heat-treatment furnaces operating in Sri Lanka. The authors use a Sri Lankan–produced "Lakmini" furnace, fueled by a mixture of oxygen and butane.

The main focus of the report is a classification system for heat-treatable Sri Lankan corundums. Group 1 material is treated under reducing conditions to develop blue coloration. Within this group are two principal varieties, *"gueda"* and *ottu*. The former is further divided into four subvarieties: *silky* (which has a characteristic sheen), *milky* (slightly bluish in transmitted light), *waxy* (translucent with a waxy luster), and *dun* (colorless or slightly bluish and almost transparent). *Ottu* is transparent corundum with various patterns of blue-and-colorless zoning. It is divided into two basic types: *Ethul ottu* (which has patches of blue color within the stone and is further divided by the specific zoning distribution into *dot ottu*, *iri ottu*, and *normal ottu*) and *pita ottu* (blue color restricted to the stone's surface).

Group II corundum can be heat treated under oxidizing conditions to either eliminate blue or enhance yellow. This general category includes *bluish ruby* (which appears purple due to the presence of both blue and red chromophores), *red "gueda"* (pink to red corundum with characteristics such as a silky appearance), and *Kowangu yellow sapphire* (corundum that is slightly yellow in reflected light).

For each type of material described, the authors provide basic heating conditions, including temperature and length of heat treatment. This interesting report provides insight into the current state of knowledge in Sri Lanka about enhancing that country's corundum. *RCK*

MISCELLANEOUS

Microscopic examination of mineral grains in forensic soil analysis: Part 2. N. Petraco, *American Laboratory*, Vol. 26, No. 14, September 1994, pp. 33–36.

This article discusses further the identification, with a polarized-light microscope, of common mineral grains found in soil samples (part 1 appeared in the April 1994 issue of *American Laboratory* and was abstracted in the Winter 1994 issue of *Gems & Gemology*). The author uses the Michel-Levy interference chart to address the topic of interference colors observed between crossed polarizers. This short but informative article contains a dozen photomicrographs and several excellent references. With this information, readers can learn to identify microscopic minerals found in their own backyard. *CEA*

GUIDELINES FOR AUTHORS

Authors must use the following guidelines when submitting a manuscript to *Gems & Gemology*, or the paper may be returned unreviewed. Please contact the Editor's office if you have any questions about these guidelines or any other aspects of your topic.

APPROPRIATE TOPICS

Gems & Gemology publishes original articles concerning the study of gemstones and research in gemology and related fields. Appropriate topics include (but are not limited to) colored stones, diamonds, gemological instruments and identification techniques, gem localities, gem enhancements, gem substitutes (simulants and synthetics), gemstones for the collector, jewelry manufacturing arts, jewelry history, and contemporary trends in the trade. Remember that these are general guidelines only. Your best source of appropriate topics is *Gems & Gemology* itself. Read the journal to acquaint yourself with the breadth of material covered.

Manuscripts may be submitted as:

Feature Articles—full-length articles describing previously unpublished studies and laboratory or field research. Such articles should be no longer than 6,000 words (24 double-spaced, typed pages) plus tables, illustrations, and references.

Review Articles—comprehensive reviews of topics in the field. Length of text should not exceed 8,000 words (32 double-spaced, typed pages).

Notes & New Techniques—brief preliminary communications of recent discoveries or developments in gemology and related fields (e.g., new instruments or identification techniques, gem minerals for the collector, and lapidary techniques). Articles for this section should be approximately 1,000–3,000 words (4–12 double-spaced pages).

Gem News—very brief (100–500 words, one-half page to two double-spaced pages) items on current events in the field or unusual gem materials.

To be considered for publication, all contributions to *Gems & Gemology* must be original and not previously published in

English. We will consider articles already published in languages other than English only on a case-by-case basis and only if the author(s) inform us at the time of submittal when and where the article was first published. It is our policy not to publish feature articles, review articles, or Notes on single stones or research based on a single sample (unless of extraordinary historical importance, such as the Hope diamond). Authors may not publish the same material elsewhere for at least three months after the mail date of the issue in question, without express written permission from the Editor's office.

Gems & Gemology also includes these regular sections: *Gem Trade Lab Notes*—reports of interesting or unusual gemstones, inclusions, or jewelry encountered in the GIA Gem Trade Laboratory; *Book Reviews*—as solicited by the Book Reviews editor (publishers should send one copy of each book that they wish to have reviewed to the Editor's office); *Gemological Abstracts*—summaries of important articles recently published in the gemology literature.

MANUSCRIPT PREPARATION

All material (including tables, figure legends, and references) MUST be typed, double spaced (no exceptions), one side only, on 8.5 by 11 inch (21 by 28 cm) white paper (no colors) with 1.5-inch (3.8 cm) margins. Each page should be consecutively numbered—including the first and those containing figure legends, references, etc. Use a fresh typewriter or printer ribbon; one that prints black, not gray. Please avoid sending draft-quality dot-matrix printouts. It is *strongly* recommended that the article *also* be submitted on a floppy disk in: Microsoft Word 4 through 6 (DOS), Wordstar 3 through 5.5, Wordperfect 5+, Rich Text Format (RTF), Microsoft Word for Windows (2 or 6), Windows Write, Microsoft Word 4+ for Macintosh, or ASCII (DOS and Macintosh). Please indicate which format is used.

Identify the authors on the title page only, not in the body of the manuscript or figures, so that author anonymity can be maintained with reviewers (the title page is removed before the manuscript is sent

for review). The various components of the manuscript should be prepared and arranged as follows:

Title Page. Page 1 should include: (a) the article title; (b) the full name of each author; (c) each author's affiliation (the institution, city, and state or country where he/she was working when the article was prepared); and (d) acknowledgments of persons who helped perform the research, prepare the report, or do the photography, etc.

Abstract. Page 2 should repeat the title of the article, followed by an abstract. The abstract (no more than 150 words for a feature or review article, 75 words for a Note) should state the purpose of the article, what was done, and the main conclusions.

Text. Papers should follow a clear outline with appropriate headings. For example, for a research paper, the headings should be: Introduction, Previous Studies, Materials and Methods, Results, Discussion, and Conclusion. Use other heads and subheads as the subject matter warrants. Also, when writing your article, please avoid jargon, spell out the first mention of all abbreviations, and present your material as clearly and concisely as possible. For general style (grammar, etc.), see *The Chicago Manual of Style* (University of Chicago Press, Chicago).

Papers that describe original research must include a Materials and Methods section that contains, at a minimum, the numbers and descriptions of all samples examined, and the techniques and instrumentation used to obtain the data.

References. References should be used for any information that is taken directly from another publication, to document ideas and facts attributed to another writer, and to refer the reader to other sources for additional information on a particular subject. References must be cited in the body of the text (in parentheses), with the last name of the author(s) and the year of publication; add the appropriate page number when citing a direct quote or a specific illustration or set of numbers or data. An example would be: (Kammerling et al., 1990, p. 33). The list of references at the end of the paper should be typed

double spaced in alphabetical order by the last name of the senior author; if there is more than one paper by that author or same group of authors, list those papers in chronological order, starting with the oldest paper first. List only those references actually cited in the text (or in the tables or figures). A paper that lacks a reference section or is missing information in the reference section—publishers, dates, authors, etc.—may be returned unreviewed.

Include the following information, in the order given here, for each reference: (a) all author names (surnames followed by initials); (b) the year of publication, in parentheses; (c) for a journal, the full title of the article or, for a book, the full title of the book cited; and (d) for a journal, the full title of the journal plus volume number, issue number, and inclusive page numbers of the article cited or, for a book, the publisher of the book and the city of publication. Sample references are:

Kammerling R.C., Koivula J.I., Kane R.E. (1990) Gemstone enhancement and its detection in the 1980s. *Gems & Gemology*, Vol. 26, No. 1, pp. 32–49.

Armstrong J.T. (1988) Accurate quantitative analysis of oxygen and nitrogen with a Si/W multilayer crystal. In D.E. Newbury, Ed., *Microbeam Analysis*—1988, San Francisco Press, San Francisco, CA, pp. 301–304.

Liddicoat R.T. (1989) *Handbook of Gem Identification*, 12th ed., 2nd rev. printing. Gemological Institute of America, Santa Monica, CA.

Personal communications (for information obtained from someone with particular expertise) should be cited in the body of the text only, as follows—(G. Rossman, pers. comm., 1994). Permission must be obtained from the people cited to use their names for this purpose. Such resources should also be listed, with their affiliations, in the Acknowledgments section.

Tables. Tables can present a large amount of detail in a relatively small space. Consider using one whenever the bulk of information in a section threatens to overwhelm the text.

Type each table double spaced on a separate sheet. If the table must exceed one typed page, please duplicate all headings on the second sheet. Number tables in the order in which they are cited in the text. Every table should have a title; every column (including the left-hand column) should have a heading. Please make sure terms and figures used in the table are consistent with those used in the text.

Line Illustrations. We prefer that all line art (graphs, charts, etc.) be sent to us on computer disk, accompanied by hard copy. (Please contact us about acceptable formats.) If this is not possible, line art should be professionally drawn and the original sent to us.

Submit black-and-white photographs and photomicrographs in the final desired size if possible. Where appropriate, please use a bar or other scale marker on the photo, not outside it.

On the back of each illustration, affix a label with the appropriate figure number and the article title. Do not trim, mount, clip, or staple illustrations.

Color Photographs. For originals, 35-mm slides or 4- by 5-inch transparencies are ideal. For review purposes (see below) we need an *additional* three complete sets of color prints, slide dupes, or high-quality color Xeroxes submitted with the copies of the paper. We reserve the right to reject photographs that are not in keeping with the production standards of *Gems & Gemology*. Please contact the Editor's office if you need help finding appropriate photographers or specimens.

"Call Outs." Figures and tables must be called out at the appropriate place in the text. Figures and tables must be numbered consecutively, starting with the first mention in the text.

Figure Captions. Type figure captions double spaced on a separate page(s). Each caption should clearly explain, in complete sentences, the significance of the figure and any symbols, arrows, numbers, or abbreviations used therein; it should be consistent with the text. Where a magnification is appropriate, please include it in the caption. (For the purposes of this journal, the magnification for a photomicrograph should refer to the magnification at which the image was photographed.)

MANUSCRIPT SUBMISSION

Because your manuscript will be reviewed by at least three separate reviewers, we must have three *complete* copies of the paper and three *complete*, properly labeled sets of all illustrations. Color Xeroxes of the color illustrations are acceptable as long as they are of reasonable quality. We cannot consider any submission that does not include these three copies of the manuscript and figures.

Send all submissions to:

Alice S. Keller, Editor
Gems & Gemology
1660 Stewart Street
Santa Monica, CA 90404

No payment is made for articles published in *Gems & Gemology*. However, for each article the author(s) will receive 50 free copies of that issue.

REVIEW PROCESS

Manuscripts are examined by the editor, editor-in-chief, technical editor, and at least three reviewers. Authors will remain anonymous to the reviewers. Decisions of the editor are final. All material accepted for publication is subject to copy editing; authors will receive galley proofs for review and are held fully responsible for the content of their articles.